An Evaluation of the Approach Used by an Ergonomics Software Program to Predict Arm Strength Using Participant-Specific Elbow and Shoulder Strengths.

An Evaluation of the Approach Used by an Ergonomics Software Program to Predict Arm Strength Using Participant-Specific Elbow and Shoulder Strengths

By

Andrew David Hall, B.Sc.Kin

A Thesis

Submitted to the School of Graduate Studies

in Partial Fulfillment of the Requirements

for the Degree

Master of Science

McMaster University

MASTER OF SCIENCE (2014) McMaster University

(Kinesiology) Hamilton, Ontario

TITLE: An Evaluation of the Approach Used by Ergonomics Programs to Predict Arm Strength Using Participant-Specific Elbow and Shoulder Strengths

AUTHOR: Andrew David Hall (McMaster University)

SUPERVISOR: Dr. James Potvin

NUMBER OF PAGES: xiii, 108

Abstract

Ergonomics software programs often use an independent axis approach (IAA) to calculate resultant shoulder strength to predict manual arm strength (MAS). The IAA treats strength about each joint axis (joint axis strengths: JAS) in the arm as independent motors, which all combine to complete an exertion. However, this form of modeling is not a true physiological representation of how the shoulder/arm function. The weighted average approach (WAA) was proposed, which combines the axes by weighting each strength based on its relative contribution to the resultant moment vector. The primary purpose of this thesis was to test the IAA using participant-specific JAS values, such that it afforded the IAA the best opportunity to predict MAS accurately. The secondary purpose was to test the WAA, to determine if it was a viable replacement for the IAA. Fifteen university age females completed two data collections. One tested the eight different JASs for the shoulder and elbow, and the other tested participant's MASs in four hand locations and six exertion directions. The JAS force data, and postural kinematic data (from the MAS collection), were inputs into two models, which completed the MAS predictions. A 4 x 6 x 3 repeated measures ANOVA revealed a significant three-way interaction between hand location, exertion direction, and method of MAS estimation ($p<0.0001$) on MAS. The most important finding of the thesis was that both the IAA and WAA predictions were significantly different than the MAS values. The IAA and WAA explained only 17.9% & 19.1% of the variance with RMS errors of 74.5 N & 73.4 N, respectively. This indicated that ergonomics software programs, using the IAA, should not be used to make arm strength predictions by ergonomists, and that WAA was not a viable replacement for the IAA.

Dedication

This thesis is dedicated to my parents, Michael and Jayne Hall.

I am certainly proud of my accomplishments in life, but not as proud as I am to be your son. Thanks for always supporting me in everything I choose to do.

Acknowledgments

First and foremost, I would like to thank my thesis supervisor, Dr. Jim Potvin, for all the tireless help that he gave to help me finish this thesis on time. His guidance and support over the past 3+ years of my life have truly allowed me to push myself to reach some of my most eXtreme goals, some of which I did not even think were possible. I am blown away by his personal work ethic and knowledge base, and this is something that I hope that I can one day model my personal learning style around. I could not have asked for a better teacher, mentor and friend to learn from, and I am truly grateful for all of the unique opportunities he has given me. I would also like to thank my committee members, Dr. Peter Keir and Dr. Jim Lyons, for their valuable input and insight towards this project. Their thoughts and ideas greatly assisted in the completion of this thesis.

I would also like to thank my amazing lab mates for all their help and support over the past several years. Specifically, huge thanks to Nick La Delfa for all his help and support throughout my thesis, and various other projects. Working along side him over the past several years has taught me a lot, and I know he is destined for great things. Also, thanks to Dr. Joanne Hodder for always being there with the quick answer to my technical problems and occasional pat on the back to keep me going. I wish her all the best with her new career. To the rest of the BEST lab mates and friends anyone could ask for, I am truly blessed to have them, thanks for all their support and keeping it real at all times.

Finally, I would especially like to thank my parents, Michael and Jayne Hall, for all the love and support that they have given me to allow me to get to this point in my life. Ever since I was a young child, they have always encouraged me to do my very best in everything that I do, and they have given me every resource to reach each one of my goals. I cannot begin to express my gratitude to have such amazing parents like the two of them. Without them, I certainly could not have strived for, and reached, some of my proudest accomplishments

Table of Contents

List of Figures

List of Tables

Chapter 1 – Introduction

1.1 – Injuries in the Work Place

In the workplace, the mitigation of risk factors associated with the development of musculoskeletal injuries or disorders should be of the upmost importance. The upper extremity is one of the most injury prone sites associated with workplace tasks. In Ontario, according to the Workplace Safety & Insurance Board (WSIB), a total of 55,525 lost time claims due to injury were filed in 2012 (WSIB, 2012). Of these injuries 14,705 (26.48%) were in the upper extremity, which included injuries suffered to the fingers, hands, wrists, arms, and shoulder (WSIB, 2012). Although total injury benefit payments in Ontario actually decreased by 6.7% ($209 million), from 2011-2012, total injury benefit payments still amounted to approximately $2.9 billion (WSIB, 2012).

Common upper extremity injuries include: tendinitis, acromioclavicular syndrome, frozen shoulder, epicondylitis, sprains and strains, carpal tunnel syndrome, hand-arm vibration syndrome, bursitis, tenosynovitis, and nerve impingement (Putz-Anderson et al. 1997; Muggleton et al. 1999). All of these injuries can be further categorized collectively as musculoskeletal disorders (MSDs), and can be categorized as either acute or chronic in nature. In an acute sense, possible mechanisms of injury can include ballistic movements, a falling object, or unequal distribution of a load in the hands of the individual. Chronic MSDs of the upper extremity result from repetitive strain over a lengthy period of time, from day-in and day-out usage in the work place (Yassi, 2000).

The development of MSDs can alter the function of joints, muscles, tendons, ligaments, and nerves in the injured limb (Muggleton et al. 1999). This altered function can translate into a chronic condition for the employee, resulting in a reduction in workplace performance, potentially an inability to work, and reduction in the ability to perform activities of daily living (ADLs) (Van der Windt et al. 2000). This reduction in the ability to perform ADLs is often one of the more difficult aspects of an MSD for an individual to deal with, as now the MSD is affecting their personal life outside of the workplace. Following an injury, and the subsequent development of an MSD, the primary effect on employers are the direct and indirect costs that are incurred, which can include the costs: 1) to cover the insurance claim for the injury, 2) associated with a decrease in production due to the workers absence, and 3) to identify, train, and employ a new replacement employee.

A number of risk factors are present in a variety of workplace settings that can singlehandedly, or jointly, contribute to the development of the various types of MSDs that are associated with the upper extremity. As seen in the literature, tasks requiring the movement of a heavy physical load, positioning of an individual into an awkward posture (e.g. twisted postures, forward flexed trunk, or working with the arms above shoulder level), movement of a specific load a repeated number of times (e.g. an assembly line worker completing a highly repetitive task), prolonged tasks (e.g. driving or typing), tasks that produce vibration, and the duration of an individual's employment are all factors and contributing risk factors towards the development of a MSD (Anton et al. 2001; Das & Wang, 2004; Garg et. al, 2005; Grieve & Dickerson, 2008; Haslegrave et al. 1997; Muggleton et al. 1999; van der Windt et. al., 2000). Typically, moving a heavy physical load can result in acute injuries, such as breaks, sprains, and strains, whereas the other identified risk factors are more conducive to the development of chronic based MSDs, such as tendonitis, bursitis, thoracic outlet syndrome, and carpal tunnel syndrome. Often, with repetitive movements and awkward postures, the increased level of muscular activity, accompanied by a decreased number of periods of low muscular activity, can accumulate to cause the onset of pain, specifically at the shoulder, and the development of an MSD (Garg et. al, 2005; van der Windt et. al., 2000).

1.2 – Ergonomic Tools

Due to the occurrence of injuries in the work place, and the associated cost to businesses, it is essential that ergonomists play a key role in mitigating injuries by identifying and reducing risk factors in the workplace via the use of ergonomic tools. Specifically, tools that are designed to estimate muscle strength, based on specific task parameters, are a valuable resource to ergonomists. Commonly used ergonomic tools of this nature, that are specific to the prediction of strength for the upper extremity, include the Three-dimensional Static Strength Prediction Program (3DSSPP) (University of Michigan, Ann Arbor, MI) and Jack (Siemens, Ann Arbor, MI). Both of these software packages stem from strength data that were collected from only three published studies by Clarke (1966), Schanne (1972), and Stobbe (1982), with the majority of the strength data being contributed from the thesis completed by Stobbe in 1982. These tools can be used to estimate joint moments based on specific task inputs, to determine percent capable values within the population, and to ultimately determine task acceptability.

1.2.1 – Potential Issues with 3DSSPP

Software-based ergonomic tools, such as 3DSSPP & Jack, use inputs that include: the posture of the individual (in the form of a linked-segment model), the hand loads, sex, and their specific anthropometry, to predict joint moments using a biomechanical model developed specifically for these programs. Once the joint moment demands have been calculated, the percentage of the population (male or female) that would be capable of this demand can be determined. The biomechanical model uses a linked segment approach that is able to calculate joint moments correctly. However, the first issue that arises specifically with 3DSSPP is the population strength database, which this linked segment model uses to calculate the moments about the various joint axes. This issue has to do with the fact that the strength database may be somewhat limited. This is due to how this database was built, as the data collection occurred over the course of one study, completed by Stobbe (1982), that only tested two arm postures (strengths) for each joint axis (3 at the shoulder, and 1 at the elbow). In each axis, the two different strengths that were tested include: 1) horizontal flexion/extension (called forward/backward horizontal rotation in 3DSSPP), 2) medial/lateral humeral rotation, 3) adduction/abduction, and 4) elbow flexion/extension. 3DSSPP uses these joint axis strengths (JAS) as a series of strength anchor points within the program for each axis. Next, using strength equations developed by Schanne (1972), these eight Stobbe (1982) JAS were corrected for changes in joint angle, such that strength could be calculated along each axis, in a variety of positions. However, another issue arises, as 3DSSPP makes the same correction for a joint axis, regardless the angle of the other axes. For example, the joint angle corrections from Schanne (1972) are held constant for the forward flexion JAS, regardless of the adduction/abduction axis angle. The combination of a potentially limited strength database, and the issue of the constant joint angle corrections, ultimately leads to inaccurate strength predictions and percent capability estimations.

In addition to these two issues, the main issue that exists within 3DSSPP deals with how 3DSSPP computes multi-directional moment calculations about the shoulder. 3DSSPP treats each axis as an independent “motor” that all combine to produce a single required action about the shoulder. Essentially, 3DSSPP assumes that 1 motor drives the: 1) horizontal flexion/extension axis, 2) medial/lateral humeral rotation axis, and 3) abduction/adduction axis. This method ignores the fact that many of the same muscles are controlling different actions about the three separate axes. Typically, for actions

produced about a single axis, such as a maximal push in the anterior/posterior direction, there are no real issues when calculating the correct moment acting about the axis using 3DSSPP, as a singular "motor" is acting about an axis. However, when moments are required about 2 or 3 axes, this software program allows the moments acting about each axis to increase, independently, to the maximum magnitudes for each axis, as seen in Figure 1.1. These maximum magnitudes are based on the population strengths that have been collected by Stobbe (1982) and corrected by Schanne (1972) in each axis, and subsequently entered into 3DSSPP. Next, the overall moment that is required to complete a certain task is determined by the linked segment model, present in 3DSSPP. When calculating this overall moment about the shoulder, the model takes the resultant of the moments acting about each independent axis at the shoulder. Since this approach uses the moments acting about each independent axis to calculate the resultant moment, it has been termed the Independent Axis Approach (IAA). The use of this IAA method of calculation within 3DSSPP leads to the potential source of error in terms of multi-directional moment calculations.

This issue could ultimately result in an error in terms of calculating the acceptable joint strength for a task, as explained in the following example. It is known that the population strengths of the shoulder, while in a 90° abducted posture with 90° of elbow flexion and 0° of humeral rotation, about the forward/backward, adduction/abduction, and medial/lateral humeral rotation axes are: 1) 39.1 Nm for forward (anterior) flexion (called horizontal rotation in 3DSSPP), 2) 30.7 Nm for backward (posterior) extension (called horizontal rotation in 3DSSPP), 3) 34.9 Nm for adduction (down), 4) 37.0 Nm for abduction (up), 5) 21.4 Nm for medial humeral rotation, and 6) 37.2 Nm for the lateral humeral rotation (Figure 1.2). Next, it is known that a certain task, while in the same posture as above, requires a maximal load of 39.1 Nm of forward (anterior) flexion, 37.0 Nm of abduction (up), and 21.4 Nm of medial humeral rotation. Within the advanced hand load function (Figure 1.2), 3DSSPP uses the forces that have been entered and the weight of the segments of the arm to calculate the overall moment about the shoulder, which is required to complete the task. These forces can be entered such that, they assume, the moment created will be acceptable to a specific percentage of the population (e.g. 75%). For this example, 3DSSPP would determine the resultant moment, that would be acceptable to 50% of the female population, to be 57.93 Nm $[(39.1^2 + 37.0^2 + 21.4^2)^{½}]$, which is 148% (57.93/39.1) of the strongest axis (forward flexion) (Figure 1.2). This calculation is a result of 3DSSPP allowing the moments to

reach the maximal values about each axis ultimately calculating a resultant moment to be 48% greater than the highest possible independent axis. This example illustrates how this inherent source of error is built into 3DSSPP.

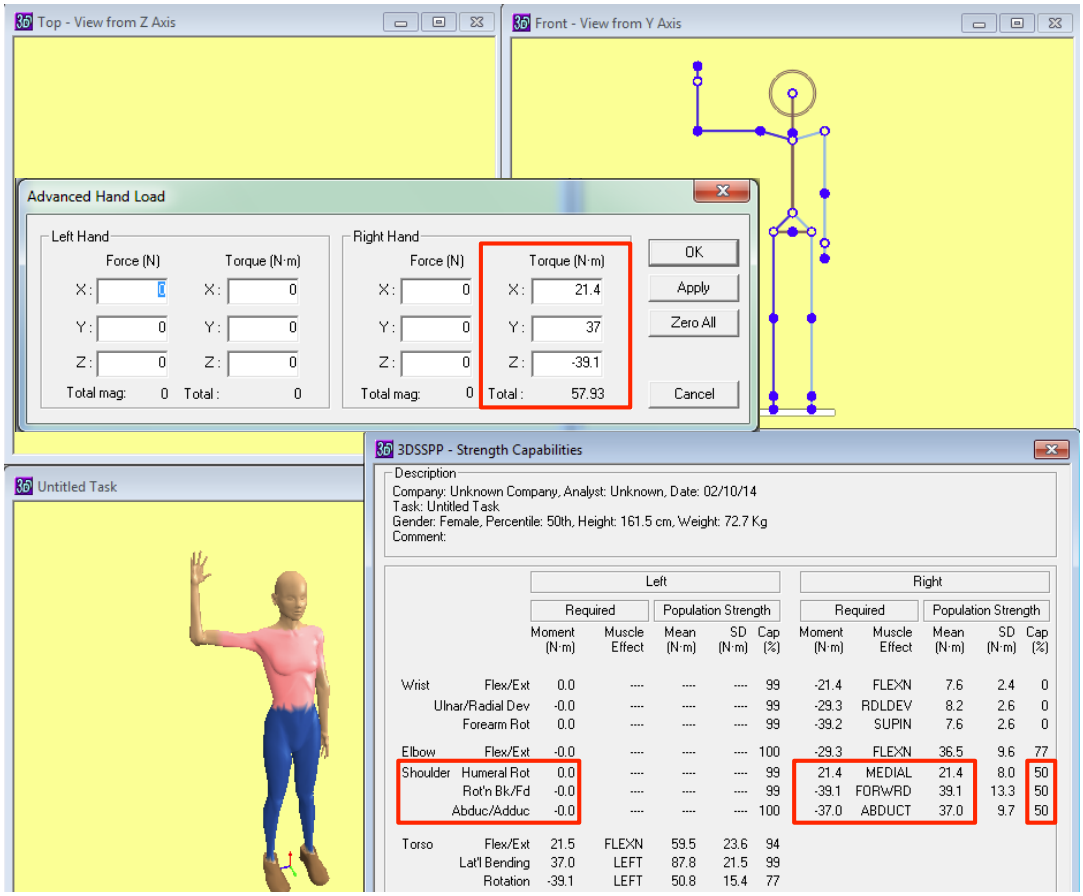

Figure 1.1: Maximum moments about each axis are possible in 3DSSPP. This diagram shows how 3DSSPP will allow the moment about each independent axis to increase until it reaches the maximum joint axis strength based on the collected population data for that axis. It can be seen in the advanced hand loads box that the moments identical to the population strength database have been entered for each axis. In the strength capabilities table the percent capabilities for each axis indicate that the moment about each of the three shoulder axes is the 50th percentile strength. This means that 3DSSPP has allowed each axis about the shoulder to ramp up to the maximal value, such that 50% of the population is able to generate those specific moments.

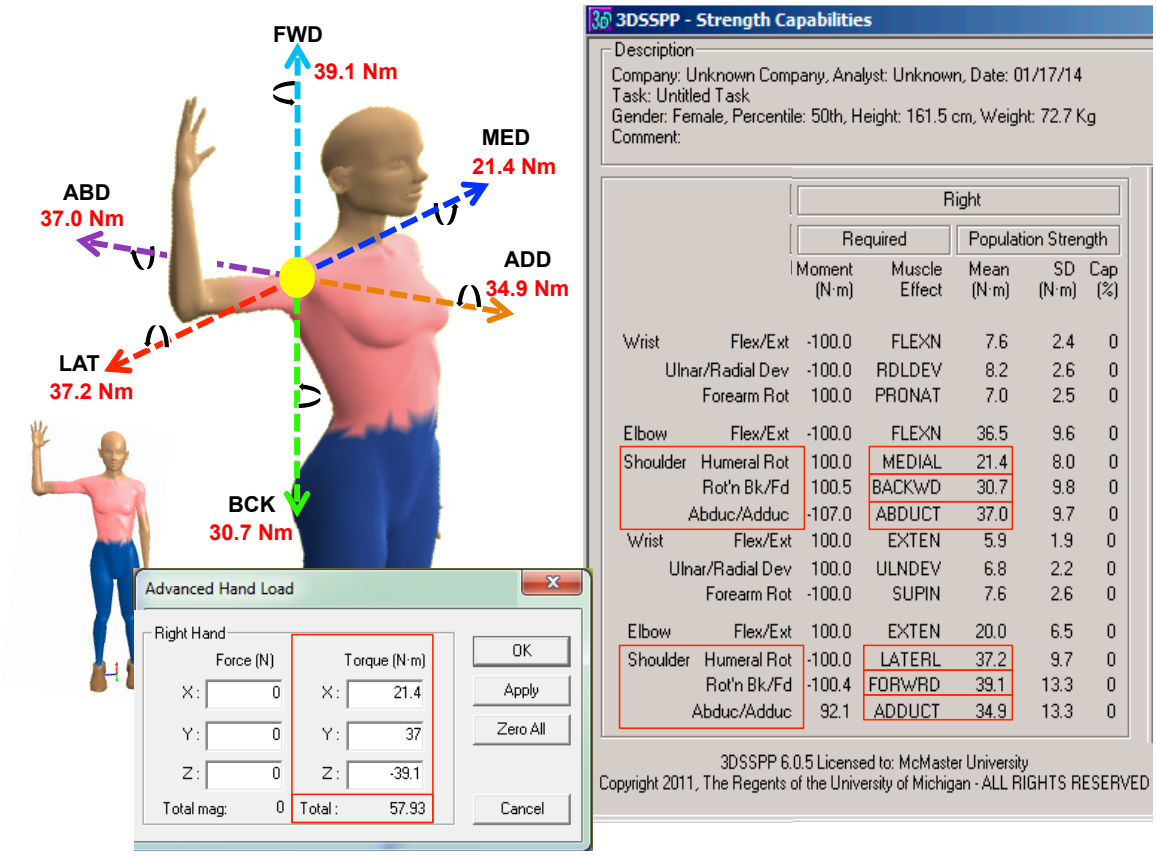

Figure 1.2: The independent axis approach, as present in 3DSSPP. This diagram depicts the known joint strengths about the forward/backward and adduction/abduction axes, as present in 3DSSPP.The light blue, green, orange, purple, dark blue, and red dashed arrows indicate the axis that each of the forward, backward, adduction, abduction, medial humeral rotation, and lateral humeral rotation moments act about, respectively. The black curves represent the direction each moment acts about each independent axis to create the desired movement about each axis. The 3DSSPP strength capabilities chart shows a condensed form of how this information would be displayed in 3DSSPP. The red rectangles highlight the population joint strengths about each shoulder axis. The Advanced Hand Load box shows that once 3DSSPP allows each axis to ramp up to its maximum force (Figure 1.1), the resultant moment is taken from each of the involved axes to produce a resultant of 57.93 Nm [(39.12 + 37.2 + 21.42)½]. This resultant moment is 148% of the strongest contributing strength axis (forward flexion: 39.1 Nm). The manikin in the bottom left-hand corner of the diagram are present to show how the human appears from both the frontal and sagittal view.

1.2.2 – The Weighted Average Approach (WAA)

Currently, our lab has hypothesized that the production of strength, about multiple axes, actually tends to follow more of a weighted average, treating the shoulder as 1 “motor”, opposed to 3 independent “motors”. We have termed this the weighted average approach (WAA). When comparing the WAA to the IAA, the WAA creates a curve that exists between the axes involved, while the IAA treats each axis as an independent motor, and takes the resultant of the involved axes at its most extreme. As previously mentioned, this WAA treats the shoulder as 1 singular “motor”, which functions simultaneously while completing singular, or multi-axial, exertions. In order to determine

the maximum resultant moment, the WAA uses the direction cosines between each of the involved axes based on the angle that each axis makes with its respective horizontal (Figure 1.3). For the above example, the task demands were 39.1 Nm of forward flexion about the forward/backward axis, 37 Nm of abduction (up) about the adduction/abduction axis, and 21.4 Nm of medial humeral rotation about the medial/lateral humeral rotation axis. If, for example, only 2 of these axes (forward/backward & abduction/adduction) were involved in producing the resultant moment, then the following comparison between the IAA and WAA methods of calculation will be conducted. The angle between the resultant and the horizontal, based on a load demand of 39.1 Nm of forward flexion, and 37 Nm of abduction, would be calculated to be 46.58° [$\tan^{-1}(39.1/37)$]. The calculated resultant, using the IAA, would be determined to be 53.83 Nm [$(39.1^2 + 37^2)^{½}$]. On the other hand, using the WAA, the calculated resultant moment at a 46.58°, between the forward flexion and the abduction (up) directions, would be determined to be 38.31 Nm [$37\cos(46.58)^2 + 39.1\sin(46.58)^2]^{½}$ (Figure 1.3). When comparing the IAA and WAA approaches, the IAA approach results in a moment that is 141% of the WAA moment.

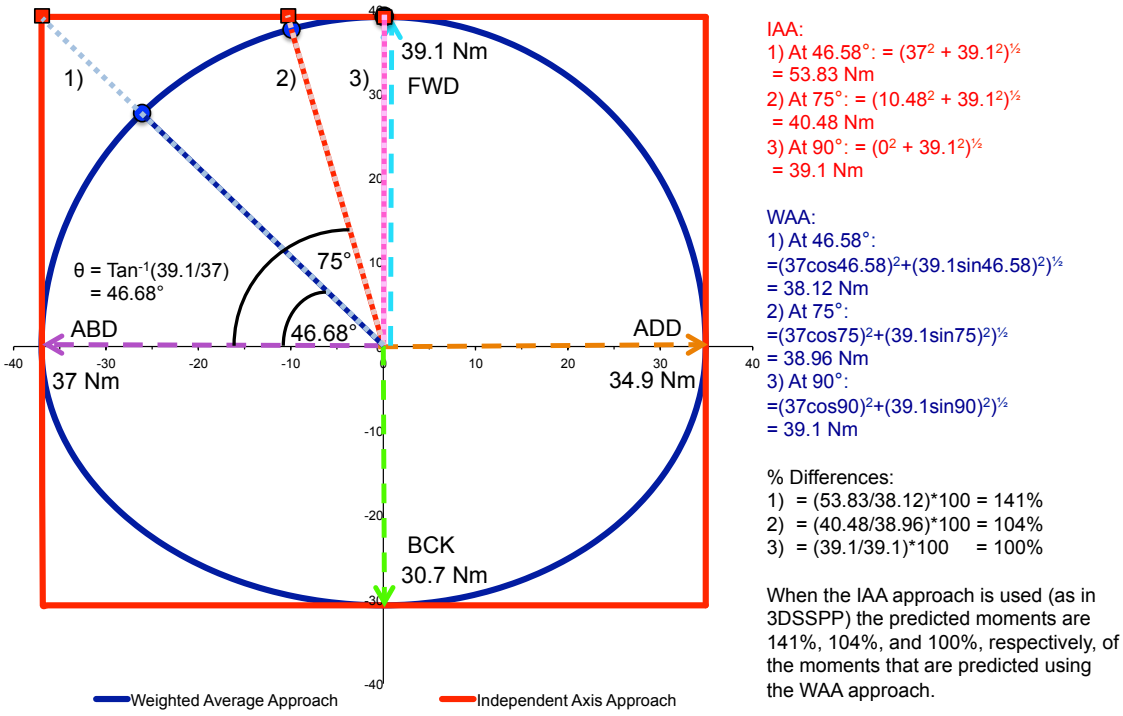

Figure 1.3: Comparison of the independent axis approach (IAA) and the weighted average approach (WAA). The two methods of calculation were compared in terms of how each predicts maximum moments about two axes. The IAA is currently used by 3DSSPP, and will allow moments to be as high as the resultant of the two or three contributing strength axes. The WAA is the hypothesized method of the resultant moments in 3DSSPP should be calculated, and uses the direction cosines of the angle that each strength axes makes with the horizontal. Both methods of calculation are shown in the text box on the figure. The red lines that form the rectangle indicate the strength calculation of the IAA, and the blue lines that form the oval indicate the strength calculation of the WAA. The light blue, green, orange, and purple dashed arrows indicate each of the strength axes, as presented in Figure 1.2. Examples are provided for load demands that had maximal moments in a combination of the forward and abduction directions at 46.68°, 75°, and 90° from the horizontal. The solid coloured blue, red, and pink lines, extending from the origin to different locations (highlighted by blue circle) on the blue curve generated by the WAA, indicate the combined moments that would be calculated for each of the required tasks (1, 2, & 3). The light coloured dashed blue, red, and pink lines extending from the origin to different locations (highlighted by a red square) on the red rectangle generated by the IAA, indicate the strengths that would be calculated for each of the required tasks (1, 2, & 3). The percentage differences in the calculations are provided in the text box to compare the results of the IAA and WAA.

Hodder and Potvin (2014) applied this WAA to actual physiological data from Makhsous et al. (1999) (Figure 1.4). In the study, a series of strength profiles about the scapular plane of the shoulder were developed using experimental strength data that were collected from seven male right hand dominant participants. Overall, two different arm postures were tested using a force transducer, measuring force at the distal end of the humerus, while participants completed maximal isometric exertions in 64 different directions within a plane intersecting the humerus perpendicularly (the humerus-

perpendicular plane). Exertion directions were chosen such that the whole range of the humerus-perpendicular plane was covered. After data collection, two circular strength profiles were created, one for each arm posture, for each participant, to depict how strength changes throughout the plane depending on the direction of exertion. The force profiles appear as a circular shaped graph about the origin (Figure 1.4). For each strength profile, the forces in each direction were presented as the force relative to the maximal force produced by participant throughout the testing period. Overall, mean strength profiles were determined by combing all 7 strength profiles onto 1 graph, for each of the 2 hand locations. To these mean strength profiles, Hodder and Potvin (2014) applied the WAA. Overall, the curve generated by the WAA follows the strength profiles fairly well, in comparison to the rectangle that is generated by the IAA. This result indicates that the WAA has some merit in regards to actual physiological data, and warrants further investigation of this method of calculation.

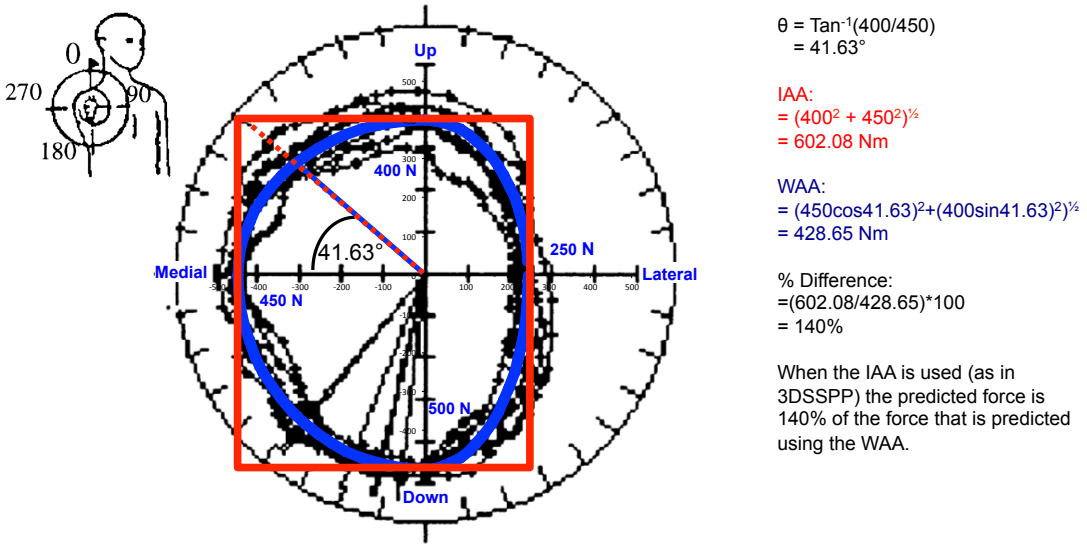

Figure 1.4: Independent axis approach (IAA) and weighted average approach (WAA) applied to the experimental shoulder strength profile, as created by Makhsous et al. (1999), for the case A arm posture by Hodder and Potvin (2014). The black circular lines represent the strength profile generated by each of the seven participants. The black lines extending from the origin to the circular black lines indicate each participant's max exertion trial within the total profile. The blue oval represents the predicted strength using the WAA, and the red rectangle represents the predicted strength using the IAA. To create these, Hodder and Potvin (2014) estimated the peak forces in each axes, and determined that average peak forces of 400 N, 500 N, 450 N, & 250 N existed for the up, down, medial, and lateral exertion directions, respectively. The calculations for the IAA and WAA have been applied using the same convention as completed in Figure 1.3. The strength profiles of Makhsous et al. (1999) follow fairly well with the WAA curve that was overlayed. In this example, the assumed task is a maximal exertion in a combination of the up and medial directions. The red dashed line, extending from the origin to the corner of the IAA rectangle, shows what the IAA would calculate the strength to be for this example, while the solid blue line represents what the WAA would calculate the strength to be. In this example, the IAA results in a predicted strength that is 40% greater than the WAA, at 41.63° from the horizontal.

1.3 – The Next Steps Required to Test 3DSSPP and the Weighted Average Approach

As previously discussed, the assumption that 3DSSPP treats each joint axis as an independent motor is the main issue of the program. This issue has been initially tested by La Delfa (2011), and will be discussed further in greater detail in the literature review. Essentially, La Delfa (2011) tested 17 female participants in a variety of arm postures and 1-Dimensional (1D) maximal exertion directions (up, down, medial, lateral, push anterior, & pull posterior). The forces that were collected at the hand were termed manual arm strength (MAS), as this was defined to be the strength of the whole arm when using the hand as the end effector. During the exertions, participants were fitted with a series of kinematic markers to measure arm posture throughout the various trials. The tested arm postures were based on the position of the hand, as defined by the horizontal (H), vertical (V), and lateral (L) position of the hand from the center of the glenohumeral joint of the shoulder. Participants completed exertions while grasping a vertically oriented handle that was fixed to a tri-axial load cell. La Delfa (2011) then conducted an analysis using 3DSSPP on the 17 participants he tested, as well as an additional 71 participants that were collected using similar methodologies from three other data collections. Next, using the posture prediction function within 3DSSPP, La Delfa (2011) used the mean hand location inputs of H, V, & L to predict how arm would be positioned in 3D space during each hand location and exertion direction. At this point he was able to determine what the average maximum forces were that 3DSSPP would predict for each arm posture and exertion direction. After all of the 3DSSPP predictions were determined, he was able to compare the 3DSSPP predictions to the mean MAS for each arm posture and exertion direction. However, during this comparison, he was only able to use 3DSSPP with the pre-programed population strength database and complete comparisons using the mean MAS data from the 88 participants. For an ideal comparison to occur, it would be best to know each participant's specific strength for each of the eight JAS, as measured by Stobbe (1982). Once these strengths are known, they could be used to determine what 3DSSPP (via the IAA) would estimate, in terms of the maximum MAS at various hand locations, using the same calculation methods that are present in 3DSSPP. A comparison could then be made between each participant's estimated MAS (via the IAA) and their empirically collected MAS data in a variety of hand locations and 1D exertion directions. This would allow for the "best case scenario" comparison to occur because it would be on an individual basis between the

participant's specific MAS and their predicted MAS levels based on their specific JAS. In terms of the hypothesized WAA, Hodder and Potvin (2014) has applied this method of calculation to data collected by Makhsous et al. (1999), and the results indicate that the WAA follows the true force production profile at the shoulder, opposed to the IAA method of calculation. The next steps to test this WAA theory will be to collect participant's actual strengths in each JAS, as measured by Stobbe (1982). Next, similar to the IAA comparison, the empirically collected MAS data at each hand location and exertion direction for each participant, can be compared to the estimated MAS, as produced by the WAA method of calculation. These comparisons should show which calculation method, WAA or IAA, predicts strength such that it follows the closest to the actual measured MAS for each participant.

1.4 – Purpose

The primary purpose of this thesis was to compare estimated maximum MASs from the 3DSSPP (IAA) method of estimation, for various hand locations and exertions directions, using individual participant JAS data, to actual MAS values. By collecting the individual strength data for each JAS, it allowed for the most direct evaluation of the strength prediction method used by 3DSSPP. As previously mentioned, La Delfa (2011) was only able to conduct a comparison using the population based strength data, and the mean participant MASs for each hand location. In this study, however, a direct comparison occurred between the participant's measured MAS and the 3DSSPP (IAA) prediction, using the participant's specific shoulder and elbow JAS. The secondary purpose of this study was to complete an additional comparison of the WAA method of calculation to the collected MAS values. By completing this analysis, evidence was provided as to if this hypothesized WAA calculation method held true when calculating MAS exertions that require moments about multiple shoulder axes. Figure 1.5 depicts how the study progressed to achieve the goals that were made for this study.

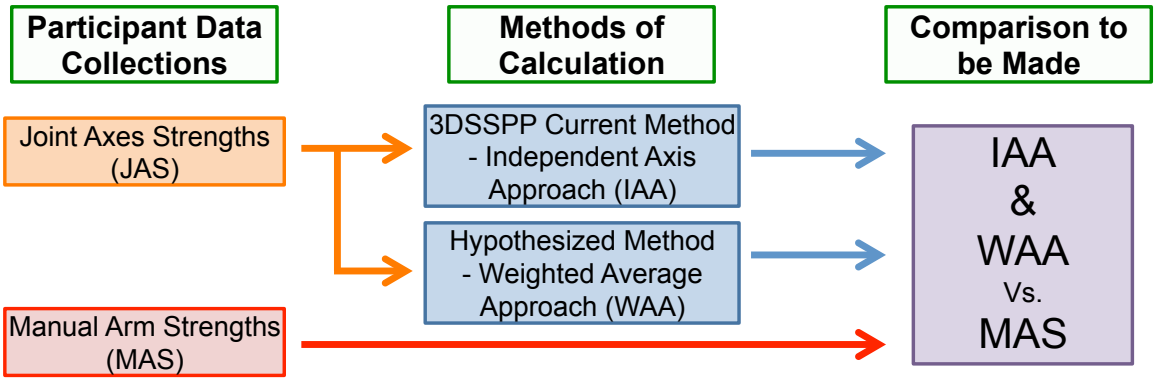

Figure 1.5: Flow chart depicting the progress of the study. There were three main components (highlighted in the green boxes) that need to be completed throughout the course of this study: 1) the collection of participant joint axis strength (JAS) data in the same postures used by Stobbe (1982), and the collection of manual arm strength (MAS) data in several hand locations, 2) the calculations that were required to determine the maximum estimated MAS data, using both the IAA and WAA methods of calculation for the same hand locations as during the MAS collection, and 3) the comparisons between measured MAS and the maximum estimated MAS as calculated using the IAA and WAA methods The collected JAS data will be used to complete the two different calculations that have been highlighted in the figure, as indicated by the orange arrows. The empirically collected MAS data was compared to the MAS estimations of the IAA & WAA methods, as indicated by the red arrows. The blue arrows indicate that the MAS estimations of the IAA and WAA methods of calculation were compared to the measured MAS data. The purple box contains the comparison that was made in this study.

1.5 – Hypothesis

It was hypothesized that, even when using a participant specific JAS database, 3DSSPP outputs (using the IAA method) would be statistically different, and would not correlate well with the collected participant specific MAS data. This hypothesis was stated, even though my analysis provided a “best case scenario” comparison for the 3DSSPP model to predict actual measured force production. In terms of the comparison between the WAA predictions, and the collected MAS data, I hypothesized that the WAA would have reduced error between the estimated value and the collected MAS data, when compared to the IAA predictions. However, I hypothesized that the WAA predictions would still be significantly different than the empirical MAS values. If the initial hypothesis, regarding the IAA, was shown to be true, it would indicate that the method of strength prediction used by 3DSSPP contains some errors that need to be addressed. If the two hypotheses associated with the WAA were shown to be true, then it would indicate that the WAA could be a potential replacement for the IAA within 3DSSPP

Chapter 2 – Literature Review

2.1 – 3DSSPP

Currently, tools like 3DSSPP, greatly assist ergonomists in performing biomechanical analyses when assessing a task in a workplace. This software-based tool uses linked segment models that have been programmed to use the inputs of anthropometry and external forces (direction and magnitude) to calculate joint moments throughout the body. Next, using a series of strength equations that are specific to each joint axis, 3DSSPP estimates the percentage of the population that would be capable of performing a specific static task (based on posture and load demands). In turn, by using these population percent capabilities, this program attempts to establish task acceptability. The data sets, which 3DSSPP uses to perform its strength calculations, includes work completed over several studies by Clarke (1966), Schanne (1972), and Stobbe (1982), with a large majority of the data stemming from the study collected by Stobbe (1982).

The primary goal of Stobbe's (1982) thesis was to develop a series of standardized strength tests (eg. work place tasks involving pushes, pulls, and lifts in a standing or sitting posture) that are best suited for predicting 16 functional strengths (eg. elbow flexion & extension) about various joint axes. Stobbe (1982) determined that the prediction of these 16 functional group muscle strengths could be achieved using seven standardized strength tests, four of which pertained exclusively to the upper extremity. Using the inputs of the measured standardized strengths, Stobbe (1982) developed a series of regression equations that are capable of predicting the functional muscle group strengths. The standardized strengths that were included were chosen based on how commonly used they are in industrial settings. An attempt was made to try to include all of the functional muscle groups that were measured into the chosen standardized strength tests. Stobbe (1982) found the correlations to be statistically significant between the measured standardized strengths and the functional strengths (correlations ranging from 0.61 to 0.91 for the seven different tests).

Stobbe (1982) tested the functional strength of 67 participants (35 males & 32 females) that ranged from 19 to 57 years of age. These participants were obtained from two different populations that included the local university student population (10 males & 10 females) and the local industrial plant worker population (25 males & 22 females). The functional strengths were tested by Stobbe (1982) about a series of JAS. A total of

16 JAS were tested by Stobbe (1982) and, out of these, eight pertained specifically to the upper extremity (Figure 2.1). These JAS included lateral humeral rotation, medial humeral rotation, horizontal extension, horizontal flexion, adduction, abduction, elbow flexion, and elbow extension. By testing these JAS across a large breadth of participants, Stobbe (1982) was able to create a strength database for the whole body. Specifically, in regards to the upper extremity, these eight JAS are the basis of the strength axes about the shoulder and elbow within 3DSSPP. Using these data, the University of Michigan was essentially able to set a strength anchor point within 3DSSPP for each strength axis based on the population strength data collected by Stobbe (1982).

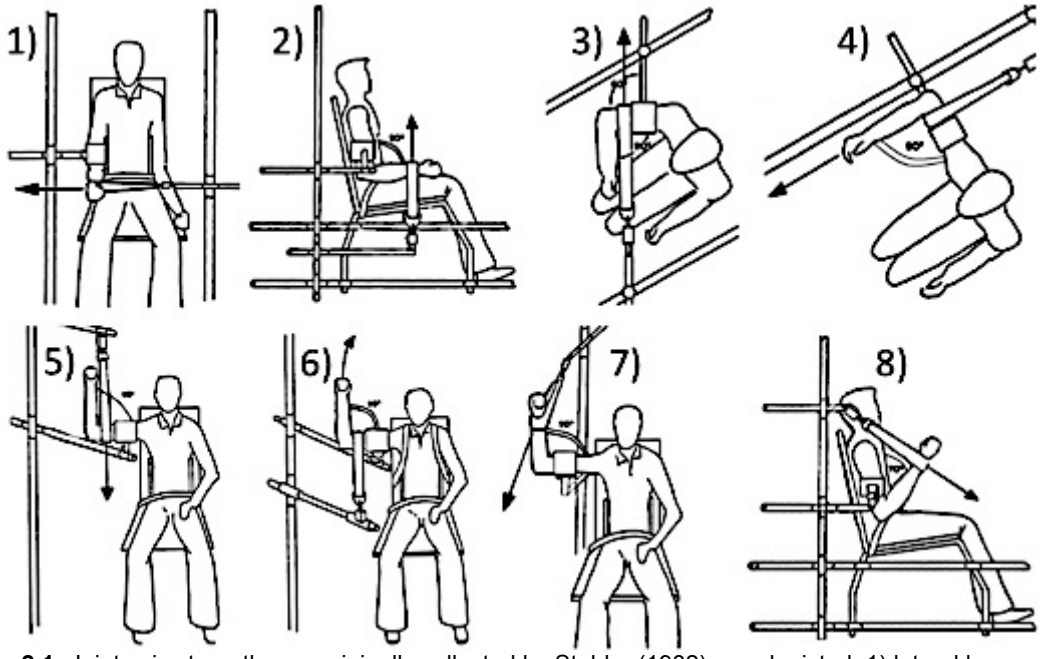

Figure 2.1: Joint axis strengths, as originally collected by Stobbe (1982), are depicted: 1) lateral humeral rotation, 2) elbow flexion, 3) horizontal extension, 4) horizontal flexion, 5) adduction, 6) abduction, 7) medial humeral rotation, and 8) elbow extension.

Specifically, with regards to the upper extremity, the strength anchor points from Stobbe (1982) were corrected using a series of regression equations developed by Schanne (1972), based on joint angle. The overall goal of Schanne (1972) was to develop a 3D isometric maximal voluntary hand force capability model for the arms and torso. Overall, there were three inputs into the model, which included: 1) participant anthropometrics (stature, weight, sex, body segments lengths, strength coefficients, and the ranges of motion of the various joint centers), 2) body configuration and direction of external force loading at the center of the grip of the hands, and 3) a gravitational constant. The resulting model outputs consisted of: 1) maximum hand force capability of the participant for a given body position & external force direction, 2) limiting muscle

group strength at the maximum hand force, and 3) the predicted & maximum voluntary strength at maximum hand force for each articulation. The developed 3D model represents a human in a seated posture as a system of linked segments.

Schanne (1972) had two different sets of data collections. The first collection, termed the “single subject phase”, was designed to collect data to build the 3D isometric model. The second collection, termed the “multi-subject phase”, was designed to collect data to test and validate the developed 3D isometric model. For the “single subject phase”, only one male participant was used to collect all of the data. A total of 20 different muscle group strengths were tested, eight of which pertained exclusively to the elbow and shoulder, including: 1) elbow flexion, 2) elbow extension, 3) shoulder horizontal rotation - forward, 4) shoulder horizontal rotation - backward, 5) shoulder vertical abduction, 6) shoulder vertical adduction, 7) humeral rotation - lateral, and 8) humeral rotation - medial. After the participant's body was positioned in a specific orientation for a particular muscle group, the participant performed maximum voluntary exertions for 5-seconds each trial. The central 3-seconds of the trial were used to determine the average force, as it was deemed that the initial and final 1-second portions of the trial were used for ramping up and down force levels. To finish the testing protocol for all 20 muscle groups, testing on this single participant lasted approximately 7-months. During this 7-month period, testing sessions occurred every other day. On each testing day, 2 separate testing sessions occurred, 90-minutes in the morning, and 90-minutes in the late afternoon, to minimize the effects of fatigue. A total of 35 different positions were tested per testing session, with a work-to-rest ratio of 1:24 given for rest (eg. after a 5-second exertion 120-seconds of rest was given). Additionally, after every 10 exertions the participant was given an extra 10-minute rest period prior to the next exertion. The work-to-rest ratio, in combination with the 10-minute rest, was deemed sufficient in terms of alleviating any fatigue. A total of 1,350 tests were conducted across all 20 muscle groups. All of the strength testing was completed while the participant was in a seated posture with either a cuff wrapped around the distal end of the humerus or distal end of the radius & ulna, or while grabbing a handle with their hand. Both the cuff and handle were attached to a specifically designed strain ring using a cable. The custom strain ring was designed by mounting a series of strain gauges within in a stainless steel ring. It was decided that the average of the participant's maximum force plateau would be used as the participant's maximum strength for each specific muscle group tested.

Prior to strength testing, Schanne (1972) determined how various muscle groups are affected by variations in joint angles at different joints (termed body angles). For example, changes to both the elbow and shoulder angles would contribute to elbow flexion strength, as the biceps brachii crosses both the elbow and shoulder joints. This information, for each of the 20 tested muscle groups, was important in regards to developing the predictive regression equations. For each muscle group, it was determined that several angles affected the strength [eg. 5 different angles that affect elbow strength: 1) forearm rotation, 2) elbow, 3) humeral rotation, 4) horizontal shoulder, & 5) vertical shoulder angle]. For each of these angles, the participant's range of motion was first determined. Next, the test position for each of these angles was determined (eg. degrees of elbow flexion/extension). These positions were defined as a series of angles within the joint's range of motion (eg. every 45°) (Figure 2.2)**.** Photographs were used to document the participants' whole body posture (upper and lower body) in terms of the various joint angles throughout the various exertions trials. In total, three different cameras, aligned perpendicular to each other, were used to take simultaneous photographs of the participant while they were completing a maximal voluntary isometric contraction for a given muscle group. The photographs were used to determine the 3D position of any point on the surface of the participant's body (e.g. the lateral epicondyle of the humerus), as long as the point could be seen on at least two out of the three photographs. Reflective markers were positioned over specific palpable anatomical landmarks to allow for the identification of specific joint center coordinates, and ultimately to determine the participant's body configuration for a given muscle group test. It was decided that the necessary joint centers, required for determining both body configuration and torque computations for the upper body, included: 1) hand center of grip, 2) wrist, 3) elbow, 4) shoulder, 5) L5 vertebral process (L5), and 6) T7 vertebral process (T7). The overall goal of this "single subject phase" was to produce a set of regression equations that could predict individual muscle group strengths as a function of joint angles. For each of the 20 muscle groups, three separate regression models were created (first, second, and third order polynomials). The selection of the best model to represent each muscle group was based on a series of five criteria: 1) residual mean square error equal to population variance, 2) correlation coefficient, 3) simplicity, 4) prior knowledge, and 5) prediction validity. The equations for each of the 8 muscle groups pertaining to the upper extremity are presented in Figure 2.3**.** Each stepwise regression equation contains a constant term, and several additional terms, which account for the

differences in various joint angles. The University of Michigan used these equations within 3DSSPP to allow the program to predict strength for each strength axes over a wide range of joint angles. As previously mentioned, the program uses the strengths from Stobbe (1982) as anchor points for each strength axis. Next, each of these regression equations developed by Schanne (1972) essentially forms a strength curve, as force production changes with a change in joint angle. Thus, by fitting the curves generated by these equations through the Stobbe (1982) strength anchor points, 3DSSPP predicts strength in a variety of arm postures and load exertion directions for the population. In turn, this allows 3DSSPP to output percent capabilities for a specific task based on the population strengths corrected for joint angle.

Table 3.4

Elbow Strength Test Position Data*

Angle	Positions Assumed
Forearm Rotation	0°
Elbow	40,60,90,120,150,180
Humeral Rotation	-30,0,45,90
Horizontal Shoulder	-90,-45,0,45,90,135
Vertical Shoulder	0,20,45,90,135

Total number of different test positions = 8?

*Unless otherwise stated all other angles are equal to zero except for trunk forward flexion-extension angle which is 90°. This holds true for all strength test positions in this chapter.

Figure 2.2: This table, as presented in Schanne (1972), outlines the five different angles that were determined to affect elbow strength, as seen in the left hand column. In the right hand column, the angular positions for each of the five angles at which elbow strength would be tested are provided. A table similar to this is provided for each of the different muscle groups tested.

(1) Elbow Flexion

$T_E = 336.294 + 2.088\alpha_E - 0.015\alpha_E^2 - 3.364\alpha_{VS} + 0.019\alpha_{VS}^2$

$r = 0.603 \quad r^2 = 0.363 \quad n = 75$

(2) Elbow Extension

$T_E = 264.153 - 0.575\alpha_E - 0.425\alpha_{VS}$

$r = 0.649 \quad r^2 = 0.421 \quad n = 70$

(3) Horizontal Shoulder Rotation - Backward

$T_S = 235.872 + 0.320\alpha_{HS} - 0.661\alpha_{VS}$

$r = 0.461 \quad r^2 = 0.213 \quad n = 79$

(4) Horizontal Shoulder Rotation - Forward*

$T_S = 226.272 + 0.161\alpha_E + 0.132\alpha_{HS} - 0.553\alpha_{VS}$

$r = 0.494 \quad r^2 = 0.244 \quad n = 63$

(5) Vertical Shoulder Abduction

$T_S = 227.338 + 0.525\alpha_E - 0.372\alpha_{HR} - 0.296\alpha_{VS}$

$r = 0.660 \quad r^2 = 0.435 \quad n = 82$

(6) Vertical Shoulder Adduction*

$T_S = 149.392 - 0.161\alpha_{HS} + 0.0086\alpha_{HS}^2 - 0.099\alpha_{VS}$

$r = 0.539 \quad r^2 = 0.291 \quad n = 69$

(7) Lateral Humeral Rotation

$T_{UA} = 92.731 + 0.477\alpha_{HR} + 0.553\alpha_{HS}$

$r = 0.790 \quad r^2 = 0.620 \quad n = 36$

(8) Medial Humeral Rotation

$T_{UA} = 155.373 + 0.422\alpha_{HR} - 0.003\alpha_{HR}^2 + 1.271\alpha_{HS} - 0.0099\alpha_{HS}^2$

$r = 0.750 \quad r^2 = 0.570 \quad n = 41$

Figure 2.3: The eight different regression equations from Schanne (1972) to represent strength in the 8 different axes modeled for the upper extremity. For each equation, the correlation coefficient (r), the coefficient of determination (r^2), and the sample size (n) on which the hand force prediction model is based, are provided. The variables within each equation are defined as follows: α_E = elbow angle (always greater than 0), α_{VS} = vertical shoulder angle (always positive), α_{HR} = humeral rotation angle (medial >0, lateral <0), and α_{HS} = horizontal shoulder angle (always positive). The α^2_{HR} α^2_{HS} terms are the same as the previously defined terms, however, they have been squared prior to entering them into the model.

2.2 – Potential Issues with 3DSSPP

Chaffin & Erig (1991) examined the sensitivity of 3DSSPP to errors in postural input and anthropometric data. In the study, these researchers initially completed an empirical validation of the predictions by 3DSSPP. To do this they used a static strength database collected by Warwick et al. (1980). This strength database consisted of 29 males who performed four different exertions (lift up, press down, push forward, and pull backward) and a variety of postures. Forces were measured using a force cell with an attached handle. The force cell was positioned at two different heights: knee height (60 cm from floor) and shoulder height (142 cm from floor). To determine the postures of the participants during strength trials, three orthogonal photographs were taken. In total, 56

different tasks were performed (14 postures X 4 exertions/posture) by each participant. The mean stature and weight of the 29 male participants was entered into the 3DSSPP model to create the models anthropometric database. These researchers proposed that if the model was unbiased then, for any given task, it would predict joint muscle strength requirements that only 50% of the participant population could perform. This study developed a regression line that fit the mean hand force data from the 56 different tasks such that the data had an expected percent capable value of 53.7% with a standard deviation of 5.9% (Figure 2.4). This prediction is 3.7% greater than the expected 50%, however, it was statistically determined, through a student t test, that this 3.7% difference was not significant. However, the researchers decided that, for some specific reason, the model tends to over predict strength by 3.7%.

Overall, the study found that, for the given set of exertions that were used to validate the model, the elbow and shoulder strengths appeared to be the most frequent limiting joints. After completing the model validation, and discovering this evidence about the limiting joint, it became apparent to the researchers that the model was very sensitive to model input values. As such, a subsequent sensitivity analysis was performed in which Chaffin & Erig (1991) systematically manipulated the input values for stature, body weight, and joint angles, to determine the effect on the percent capable predictions by the model. Of specific relevance to the present study, was the sensitivity analysis conducted for the postural angle inputs. To test the effect that changing the joint angle had on the percent capabilities, Chaffin & Erig (1991) initially identified the joint that was determined to be the most limiting in terms of percent capabilities for a specific task simulation. Next, using the model, the joint was rotated every 10° through a range of motion that was +/-30° of the static angle at the joint in question that was recorded in the photographs for each specific task simulation. Depending on which joint was being tested, joint angles were manipulated in the vertical, horizontal, or frontal planes. After completing these sensitivity simulations for all 56 tasks, the study found that the press-down task were the most sensitive to changes in the postural input angles. It was shown that changes of +/-10° in the limiting joint resulted in approximately a +/-30% variation in joint percent capabilities (Figure 2.5). The lifting and pulling tasks were shown to be the next most sensitive as a +/-10° change in the joint input angle resulting in approximately a +/-12% variation in percent capability outputs (Figure 2.5). Finally, the pushing tasks were shown to be the least sensitive, as a +/-10° angle change only caused a small change in the percent capabilities (Figure 2.5). Chaffin & Erig (1991) also found that the

standard deviations changed throughout the sensitivity analysis. For all tasks combined, the standard deviation in percent capable was 5.9% (Figure 2.4). However, when looking at the sensitivity analysis for each task individually, as the limiting joint angle was manipulated there was a large increase in the standard deviations of the percent capabilities (Figure 2.6). The sensitivity analysis indicated that it is very important to measure joint input angles correctly prior to running an analysis using 3DSSPP, as errors as little as 10° can have a large effect on the range strength calculations and subsequent percent capabilities.

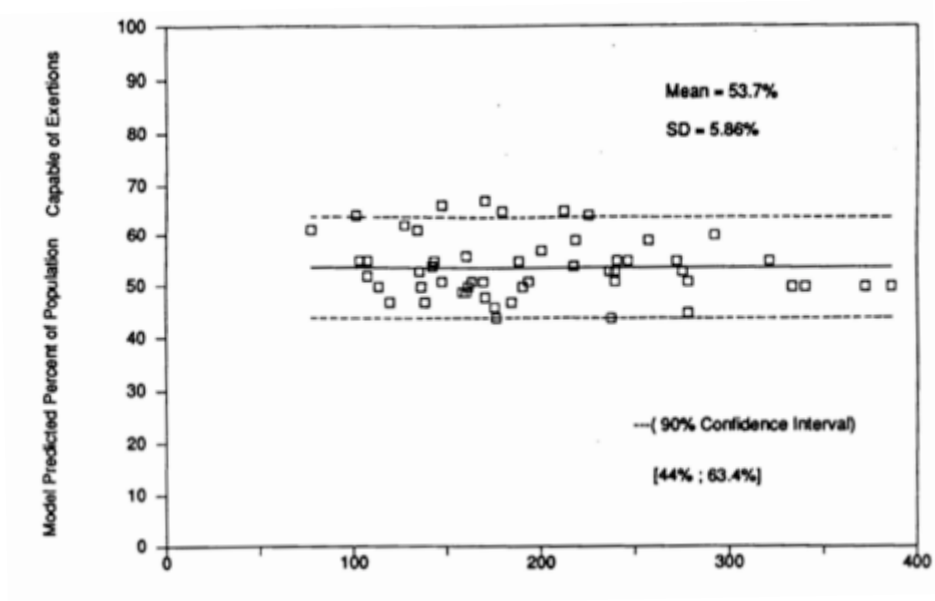

Figure 2.4: This graph from Chaffin & Erig (1991) shows the comparison between the models predicted percent capable values (on the Y axis) and the mean hand forces (N) (on the X axis) that were recorded in the study completed by Warwick et al. (1980). The solid black line on the graph indicates the regression line that was developed to fit the data, and fits through the mean of the data at 53.7%, with a standard deviation of 5.86%. The dashed lines indicate the 90% confidence interval. Each square represents a task that was simulated using 3DSSPP (n = 56).

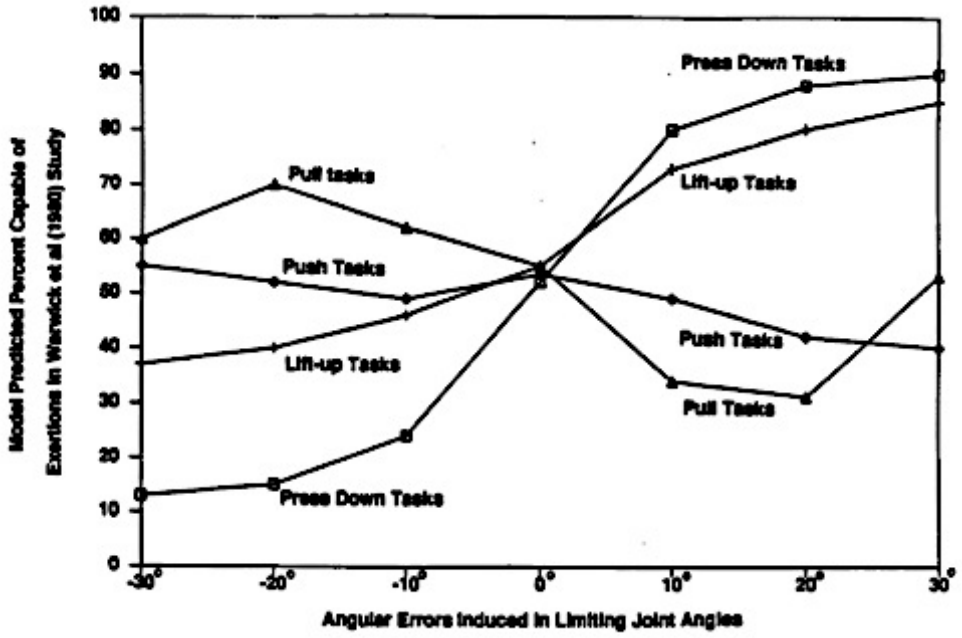

Figure 2.5: This graph from Chaffin & Erig (1991) depicts the results from the sensitivity analysis that was conducted. It depicts the effect that errors in the angular inputs (X-axis) of the limiting joint had on the models predicted percent capabilities (Y-axis). Each black line on the graph indicates the average results for the 4 different types of exertions that were measured (pull, push, lift-up, press down). This graph shows that press down tasks were the most influenced by errors in input angles, as a change of +/-10° resulted in about a +/-30% variation in predicted percent capabilities. The lift-up and pull tasks both were shown to be equally sensitive to angular input errors, as a +/-10° resulted in about a +/-12% variation in predicted percent capabilities. The push tasks were shown to be the least sensitive to input angle errors, as it resulted in only a small variation in the predicted percent capabilities.

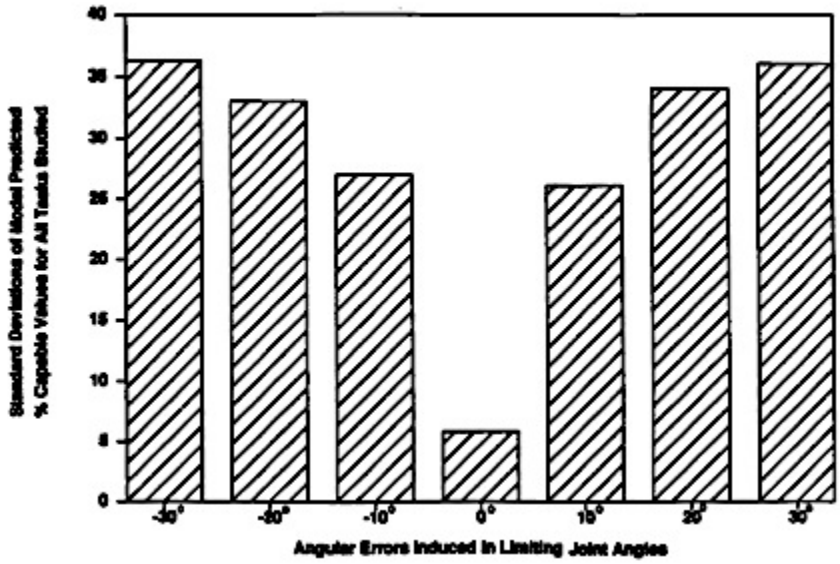

Figure 2.6: This graph, as presented in Chaffin & Erig (1991), indicates the change in the standard deviation (Y-axis) of the models predicted percent capabilities as a result of input errors (X-axis) of the joint angles of the limiting joints. The graph indicates that with a 0° error, the standard deviation is only 5.9% (as in Figure 2.4), however, with only a 10° error, the standard deviation jumps to over 25%, and 30° errors resulting in over a 35% standard deviation. This indicates that even a small error in joint angle can have a large effect on the variability of the predicted percent capabilities from the model.

2.2.1 – Addressing the 3DSSPP Problem

The inherent issues of 3DSSPP have been outlined over the course of the introduction and through the study conducted by Chaffin & Erig (1991). La Delfa (2011) tested some of the inherent issues in 3DSSPP where he measured MAS in the 1-Dimensional (1D, e.g. push), 2-Dimensional (2D, e.g. push & up), and 3-Dimensional (3D, e.g. push & up & lateral) exertion directions and to evaluate the importance of knowing the exact arm posture and specific joint locations in 3D space when estimating maximal MAS. A secondary purpose of his study was to analyze the relationship between 3DSSPP arm strength outputs and the empirical strength data measured in the lab. La Delfa (2011) recruited 17 healthy university aged female participants. A custom adjustable laboratory apparatus, complete with a vertically oriented padded handle attached to a tri-axial load cell, was used to measure force exertions. The adjustable apparatus allowed La Delfa (2011) to position the load cell in a variety of specific hand locations based on the participant's anthropometrics. Participants were positioned in front of the apparatus (see Figure 2.7). A telescoping post extended from the apparatus to the participant's sternum to ensure a constant participant right shoulder location relative to the apparatus. The various hand locations tested were defined by the horizontal angle of the arm relative to the sagittal plane (0°, 45°, & 90°), and their vertical height of the hand relative to the body (umbilicus, shoulder, & overhead). A total of eight different hand locations were tested, and these included umbilicus height at 0°, 45°, & 90°, shoulder height at 0°, 45°, & 90°, and overhead height at 0° & 45°. All eight hand locations were set specifically such that the hand was at 80% of their total reach distance from the shoulder.

At each hand location, participants were tested in 26 different exertion directions that included combinations of 1D (n = 6), 2D (n = 12), and 3D exertions (n = 8). In total, each participant was required to complete 208 exertions (26 exertion directions X 8 hand locations), over four different 1-hour testing sessions. Participants were given at least one minute of rest between exertions, as well as three days of rest in between each testing session, to account for any fatigue effects. Participants were fitted with a series of reflective markers to allow for the collection of postural kinematic data during exertion trials. The end goal of this study was to create a regression equation (termed M_{NP}) that could predict MAS based on the horizontal (H), vertical (V), & lateral (L) position of the hand relative to the contact point within the glenohumeral joint, the unit vectors in each of the three axes (up/down, push/pull, medial/later), and the resultant shoulder 3D moment arms. This regression equation did not have the postural inputs from the

kinematic data that were collected; hence the "NP" in the term M_{NP} stands for "no posture". An additional equation (termed M_{ALL}) was made with the added postural variables including the moment arm of the resultant force about the elbow, elbow flexion angle, horizontal shoulder angle, and vertical shoulder angle. This equation was termed M_{ALL}, as it included "ALL" of the inputs from the M_{NP} equation, plus the input of the postural data. These two separate equations were created to determine if the added postural variables increased the M_{ALL} equation's predictive strength compared to M_{NP}. M_{ALL}, explained 75.4% of the variance, with a root mean square error (RMSE) of 9.1 N (Figure 2.8). M_{NP} explained only slightly less variance (67.3%) with an RMSE of 10.5 N (Figure 2.9).

The secondary purpose of La Delfa (2011) was to conduct an analysis of the relationship between 3DSSPP arm strength outputs and empirical strength data measured in the lab. La Delfa (2011) compared the 1D exertions from a total of 44 different hand locations (8 of which came from his own thesis) to the corresponding 3DSSPP outputs. The other 36 hand locations came from a series of three other data collections that used similar methodologies (Potvin et al. 2010). The mean MASs collected from 88 different participants [71 from the studies compiled in Potvin et. al., (2010), & 17 from La Delfa (2011)] were compared with the 3DSSPP outputs using a comparable 50-percent capable female manikin of matching anthropometrics. For each of the 44 hand locations, all six 1D exertion directions (up, down, medial, lateral, push anterior, pull posterior) were simulated using 3DSSPP. A function within 3DSSPP has the ability to predict the posture the manikin will assume, based on the location of the hand. The hand location inputs for this posture prediction function are based on the H, V, and L location of the hand. Prior to activating this function, the manikins were positioned in the neutral stand posture and the posture-locking feature was applied to lock all body segments in place, except the right arm. Once the posture was predicted, a biomechanical analysis could be performed on the manikin. For each of the tested hand locations, the maximum acceptable force in each of the six 1D exertion directions was determined for a 50^{th} percentile female. Using the hand load (force) tool, the load in the appropriate direction was increased iteratively by 0.5 N until one of the moments exceeded the predicted strengths about the three shoulder, three wrist/forearm or one elbow axes. The highest force that was obtained for that hand location and force direction, acceptable to 50% of the female population, was taken as the maximum force for that hand location and exertion direction. La Delfa (2011) made a total of 264

comparisons, (44 hand locations X 6 exertion directions) (Figure 2.10). Overall, this comparison resulted in a very poor explained variance (r^2 = 0.093) between the manual strength data and the outputs from 3DSSPP, with an accompanied very high RMSE of 39 N (~4 kg).

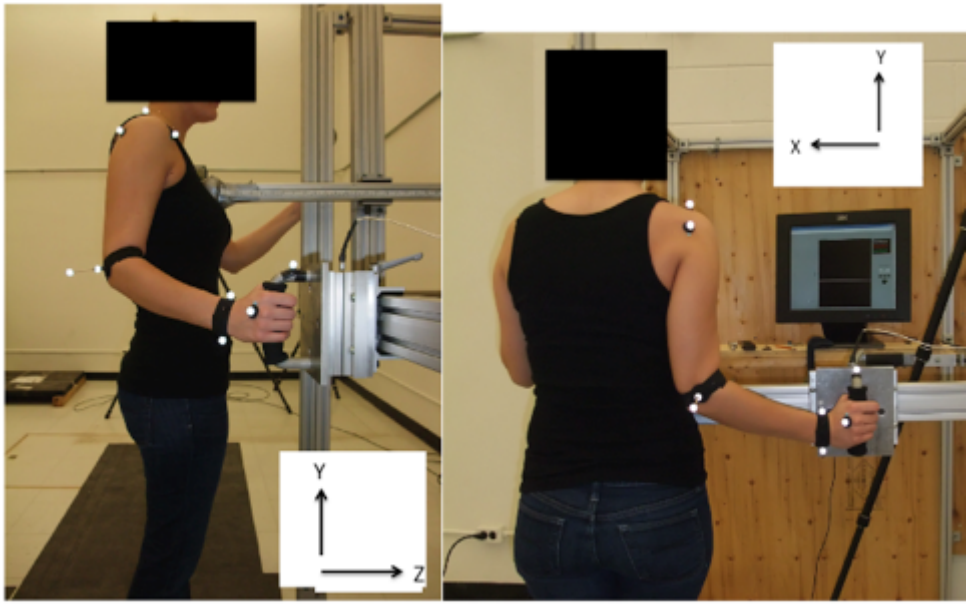

Figure 2.7: La Delfa's (2011) custom laboratory apparatus is shown with a participant positioned in front, while grasping the vertically oriented handle that is attached to the load cell. Reflective markers were positioned on the participant's hand, wrist, elbow, and shoulder to collect kinematic data. A telescoping post, extending from inside the apparatus, was positioned on the participant's xiphoid process to control the participant's trunk position.

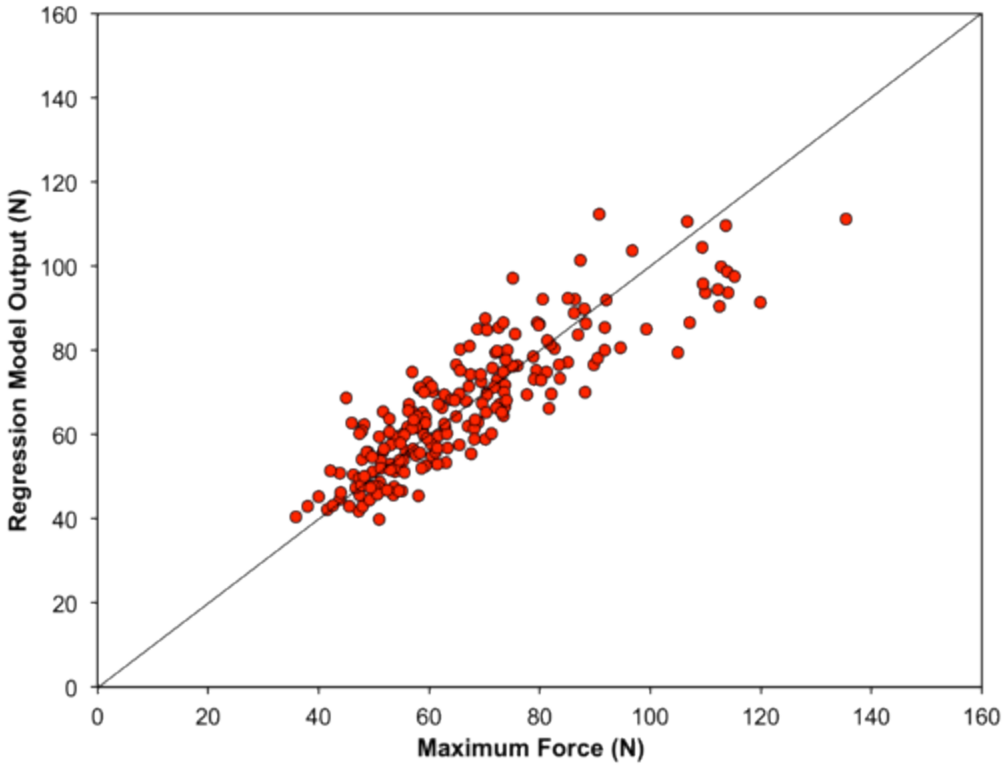

Figure 2.8: The results from the M_{ALL} regression equation created by La Delfa (2011) with a line of perfect prediction. The R-square was 0.754 with an RMSE of 9.1 N (n = 208, 8 positions x 26 exertion directions).

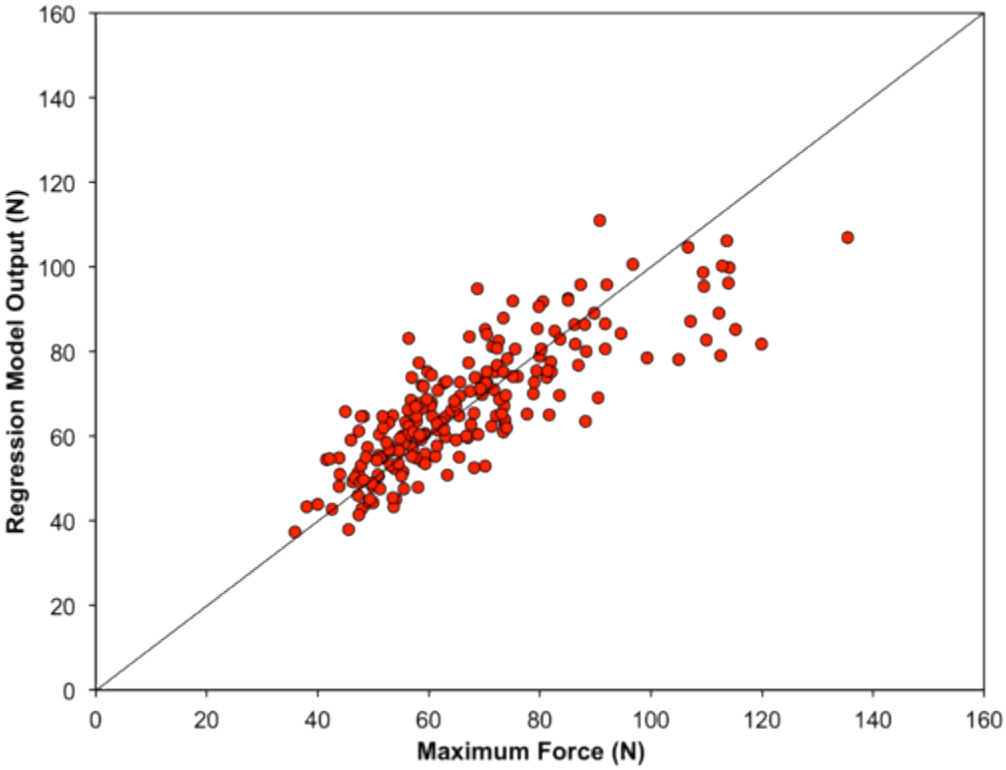

Figure 2.9: The results from the M_{NP} regression equation created by La Delfa (2011) with a line of perfect prediction. The R-square was 0.673 with an RMSE of 10.5 N (n = 208, 8 positions x 26 exertion directions).

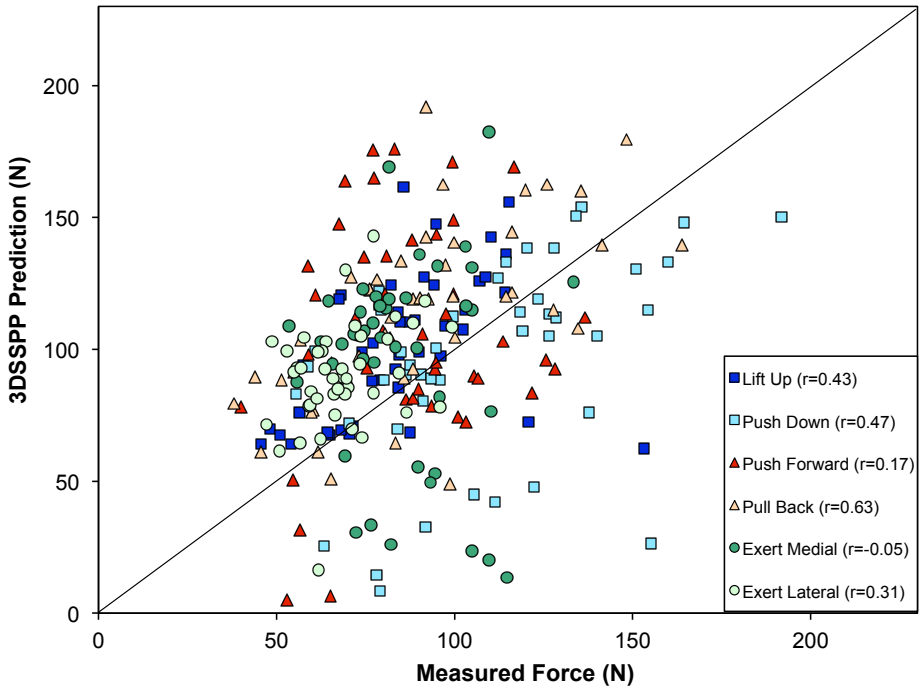

Figure 2.10: A scatter plot showing the comparison (r^2 = 0.093 & RMSE = 39 N) between measured manual arm strength data (X-axis) with the predicted strength outputs from 3DSSPP (Y-axis) for 44 different hand locations (8 from La Delfa (2011) and 36 from three other data collections) and 6 different exertion directions (n = 264) (La Delfa, 2011).

2.3 – The Weighted Average Approach

2.3.1 – Rationale for this Approach

The IAA, which is currently used in several ergonomics tools, works under the assumption that strengths act independently of each other about each of the three orthopedic axes about the shoulder. It is then assumed that the resultant of these strengths can be taken to predict the tri-axial strength of the shoulder. However, the physiological validity of this approach is questionable, considering the vast complexity of the shoulder.

One particular reason for this is how the direction of each muscle's moment arm changes depending on the exertion direction and lines of action are rarely aligned with the orthopaedic axis. Holzbaur et al. (2005) desribed the musculoskeletal model of the entire upper extremity, currently available in OpenSim (simtk.org). Of particular interest to the present study, were defining the moment arm of the shoulder muscles based on experimental data collected from several other studies. Three different figures were created that represent the moment arms for the rotator cuff muscles (Figure 2.11), the

deltoids (Figure 2.12), and the other shoulder muscles (Figure 2.13). For Figure 2.11, the shoulder rotation and abduction moment arms for the muscles were calculated while the shoulder was in 60° of abduction and 0° of axial rotation. While for Figures 2.12 and 2.13, the shoulder was in a neutral posture when the shoulder flexion and abduction moment arms were calculated. These three different figures show how the moment arms, and muscles involved, vary depending on the type of exertion that is required. If the independent axis approach is anatomically feasible, then all the markers would be along the lines defining zero for either the horizontal and vertical axes. However, this is not the case one or more muscles do not simply act independently about a single axe to generate moments. Instead, it is a combination of muscles that work about multiple axes to complete a required exertion while maintaining the joint stability necessary. As such, I believe that the WAA makes more physiological sense, as it allows the various muscle strengths to work together to complete a task, opposed to working independently.

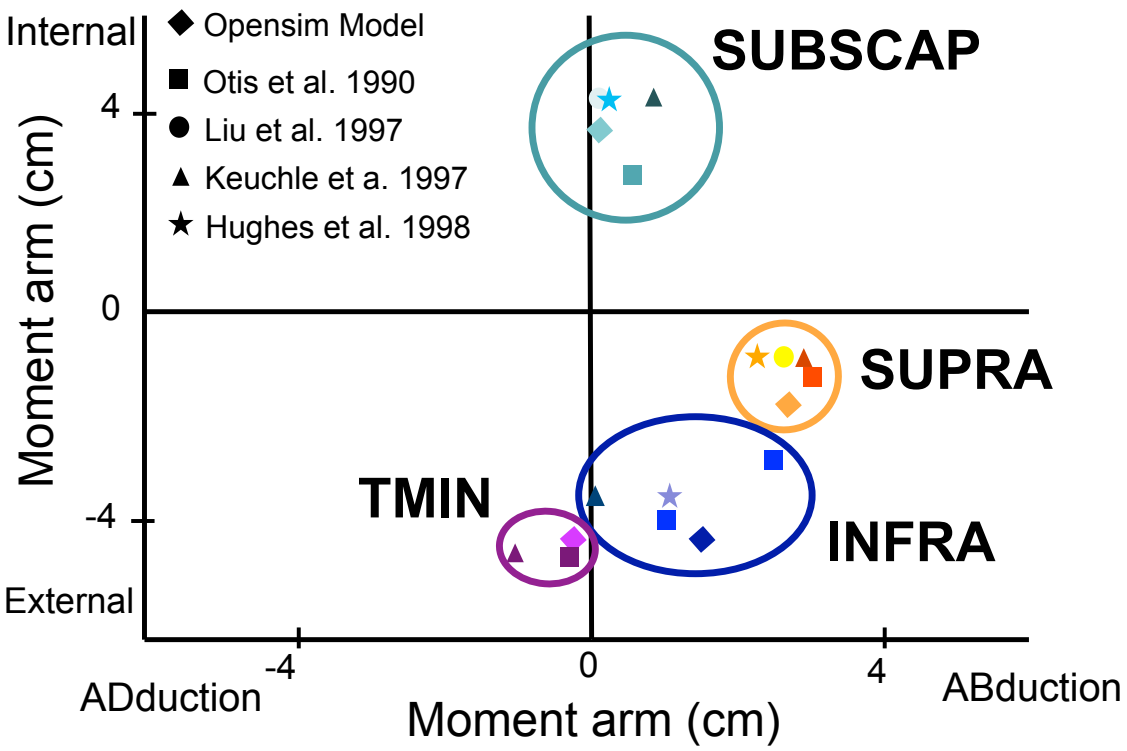

Figure 2.11: Moment arm lengths for the rotator cuff muscles, including subscapularis (SUBSCAP), supraspinatus (SUPRA), infraspinatus (INFRA), and teres minor (TMIN). The X-axis and Y-axis represent the moment arm lengths for adduction/abduction and internal/external rotation exertions, respectively. The diamond markers for each muscle represent the OpenSim model estimation, while different markers, as defined by the legend, represent experimental data from several studies. Model estimations were made while the arm was in 60° of abduction and 0° of axial rotation. This figure was originally presented by Holzbaur et al. (2005), and has been adapted by Hodder & Potvin (2014), as presented here.

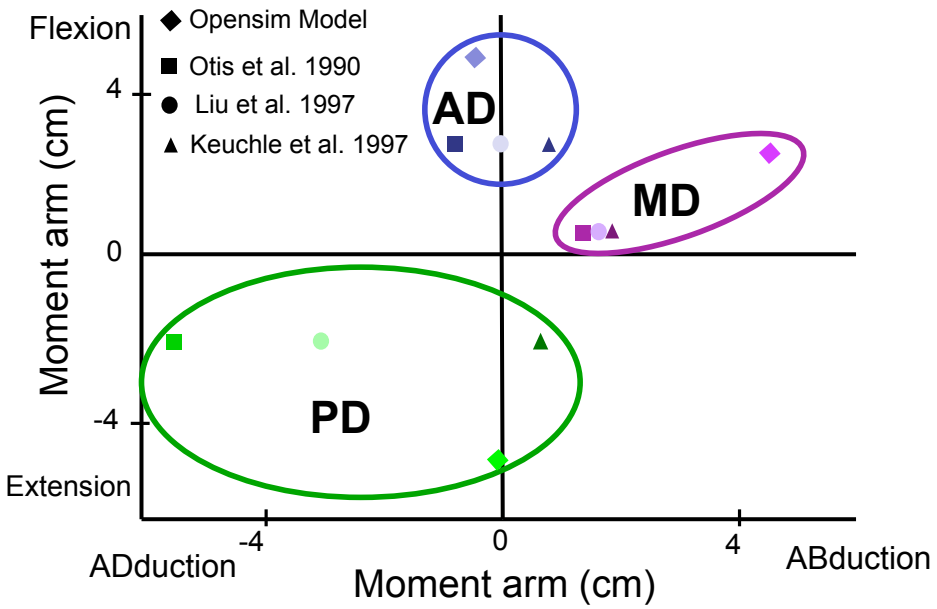

Figure 2.12: Moment arm lengths for the deltoid compartment muscles, including anterior deltoid (AD), middle deltoid (MD), and posterior deltoid (PD). The X-axis and Y-axis represent the moment arm lengths for adduction/abduction and flexion/extension exertions, respectively. The diamond markers for each muscle represent the OpenSim model estimation, while different markers, as defined by the legend, represent experimental data from several studies. Model estimations were made while the arm was in neutral arm posture. This figure was originally presented by Holzbaur et al. (2005), and has been adapted by Hodder & Potvin (2014), as presented here.

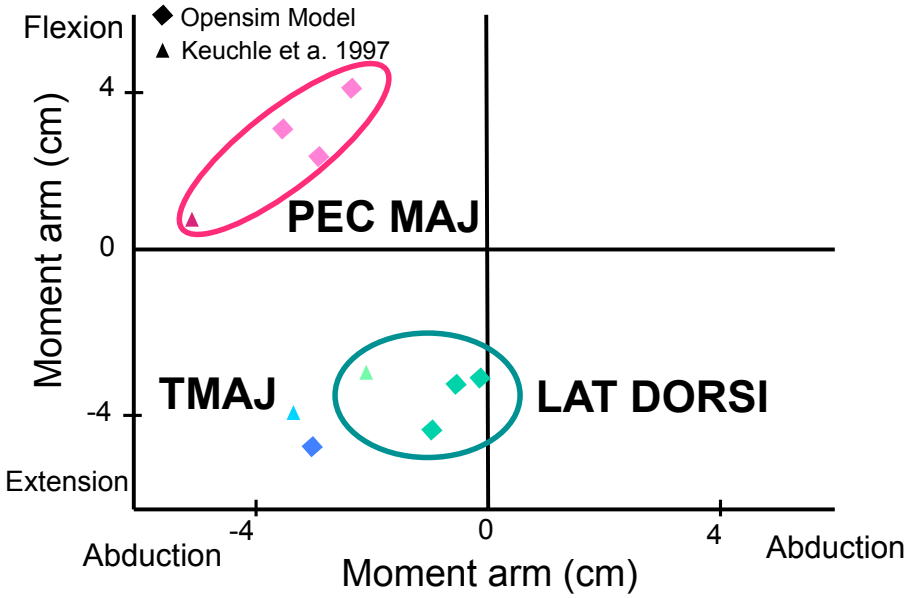

Figure 2.13: Moment arm lengths for the other shoulder muscles, including pectoralis major (PEC MAJ), latissimus dorsi (LAT DORSI) and teres major (TMAJ). The X-axis and Y-axis represent the moment arm lengths for adduction/abduction and flexion/extension exertions, respectively. The diamond markers for each muscle represent the OpenSim model estimation, while different markers, as defined by the legend, represent experimental data from several studies. Model estimations were made while the arm was in neutral arm posture. This figure was originally presented by Holzbaur et al. (2005), and has been adapted by Hodder & Potvin (2014), as presented here.

2.3.2 – Evaluating the Potential of the Weight Average Approach

As discussed, the WAA has a potential physiological basis of support, as evidence provided by Holzbaur et al. (2005) fits this WAA theory. Hodder & Potvin (2014) applied this to a study completed by Makhsous et al. (1999) who developed a series of strength profiles about the scapular plane of the shoulder. Both experimental strength profiles (as determined from data collected in the study) and theoretical strength profiles (as determined using a previously developed shoulder model) were created in the study. Specifically in regard to testing the WAA, the experimental data from this study was important. The study used seven male right hand dominant participants that varied in age from 23-59 years and two different arm postures (titled case A & case B) (Figure 2.14) were tested on all of the participants using a specially designed ring shaped force transducer to collect strengths. Strength was measured at the distal end of the humerus after the participant had been positioned in the correct posture. Specifically, participants were required to perform maximal exertions on the device in the humerus-perpendicular plane (Figure 2.14). To do this, the participant's arm was placed inside the circular strain ring and then positioned in the appropriate posture. Throughout testing, the participant was restrained such that only the arm could be used to complete the maximal isometric exertions. Both a training period and a warm up session occurred prior any strength testing occurring. For each arm posture, testing was divided into eight different parts. For each part, eight different maximal exertions were performed, all in different directions in the scapular plane. Following each exertion, participants were given a 2-minute rest period between consecutive exertions, and after the eight maximal exertions, participants were given an additional 10-minute rest period. The eight different parts of testing for each arm posture lasted approximately 3-hours, and a total of 64 measurements were recorded for each arm posture such that the whole range of the humerus-perpendicular plane was covered. After data collection, two circular strength profiles were created, one for each arm posture, for each participant (Figure 2.15). To generate each strength profile, the forces in each direction were presented as the force relative to the maximal force produced by participant throughout the testing period. The profiles from all seven participants were summated onto one graph for each arm posture (Figure 2.16). Since exertions were completed in every direction, the strength profile developed for each participant depicts how that participant's strength changes as they complete maximal exertions in each direction of the humerus-perpendicular plane.

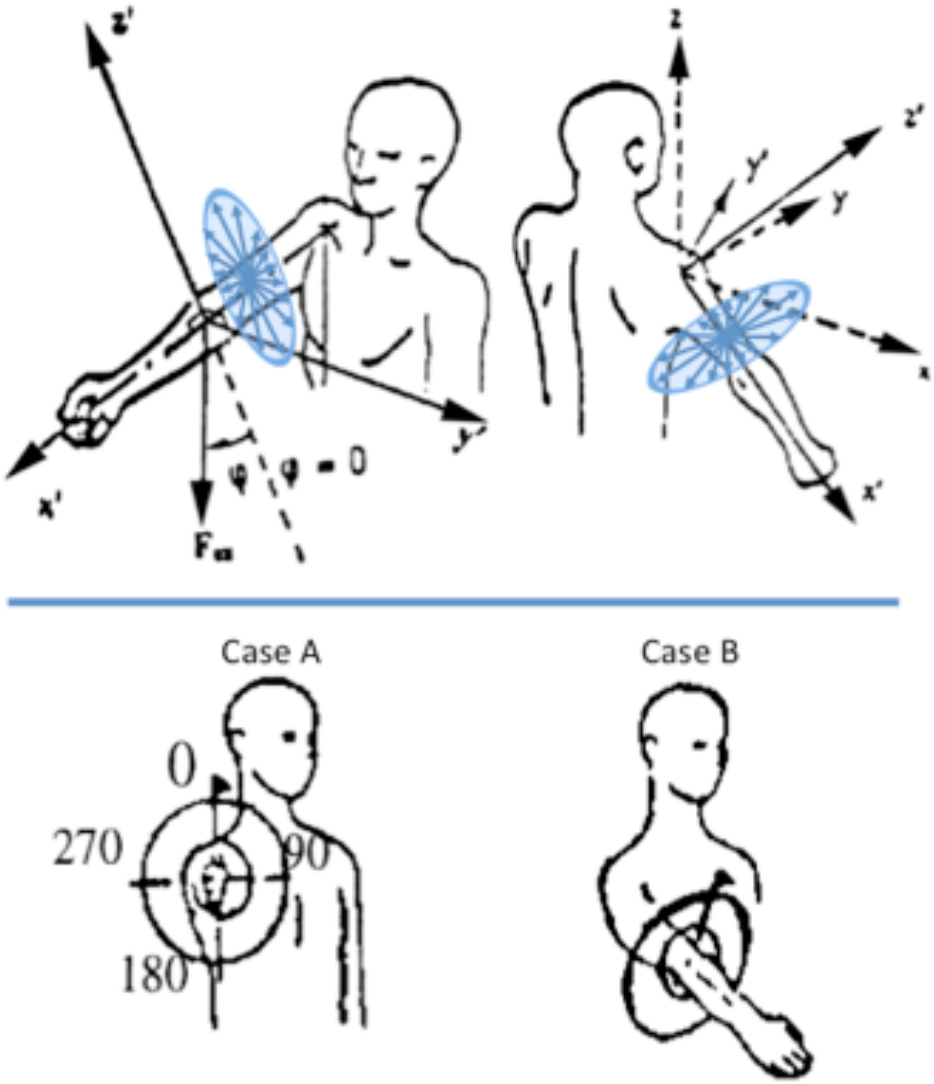

Figure 2.14: The two diagrams at the bottom of the figure represent the two different arm postures that were tested by Makhsous et al. (1999). The two different arm postures were defined as follows: Case A: the arm was in a 45° abducted position away from the centerline of the shoulder. Case B: the arm was in 45° abduction and 45° of humeral flexion in the frontal plane from a neutral, 0° of flexion, position. The two diagrams at the top of the figure show the humerus-perpendicular plane in which participants completed maximal exertions as measured at the distal end of the humerus. The blue circle at the distal end of the humerus represents the plane, while the arrows originating from the center of the circle points outwards indicate that the participants were required to complete maximal isometric exertions in all directions in this plane to create the strength profile. This humerus-perpendicular plane can also be seen in the bottom diagrams labeled case A and B. It should be noted that the top diagrams do not correspond directly with the bottom diagram in terms of the two different arm postures, as illustrated by the blue dividing line.

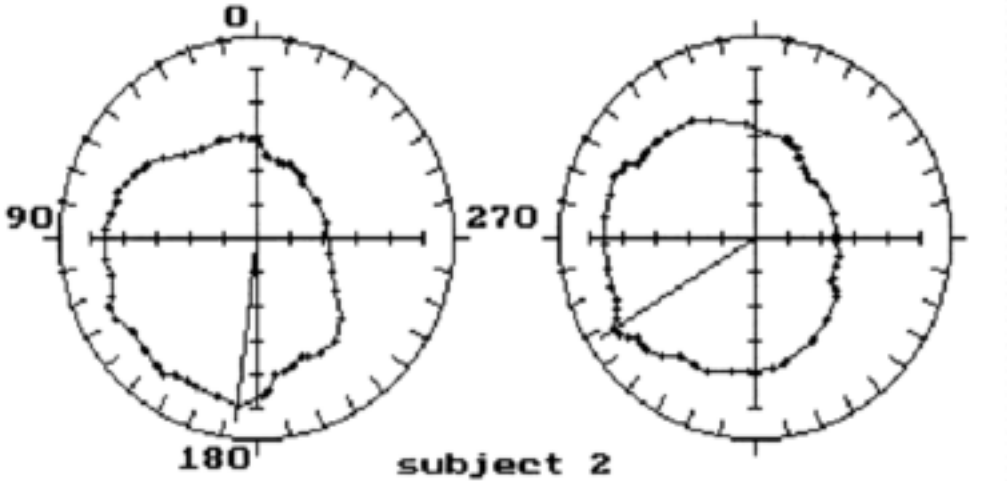

Figure 2.15: An example of an experimental strength profile for one participant in Makhsous et al. (1999). Each graph corresponds with the strength profile for two different arm positions, termed case A (on the left) and case B (on the right). The numbers on the graph correspond with the angle of the exertion within the humerus-perpendicular plane; 0° represents a pure up exertion, 90° a pure medial exertion, 180° a pure down exertion, and 270° a pure lateral exertion. Data points from 64 different exertions are plotted, and then joined together to form the circular strength profile. The interior line, extending from the origin to a point on the graph, represents the maximum relative strength for that participant and arm posture. Each tick on the axes represents 20% of the maximal force that was produced specifically by that participant.

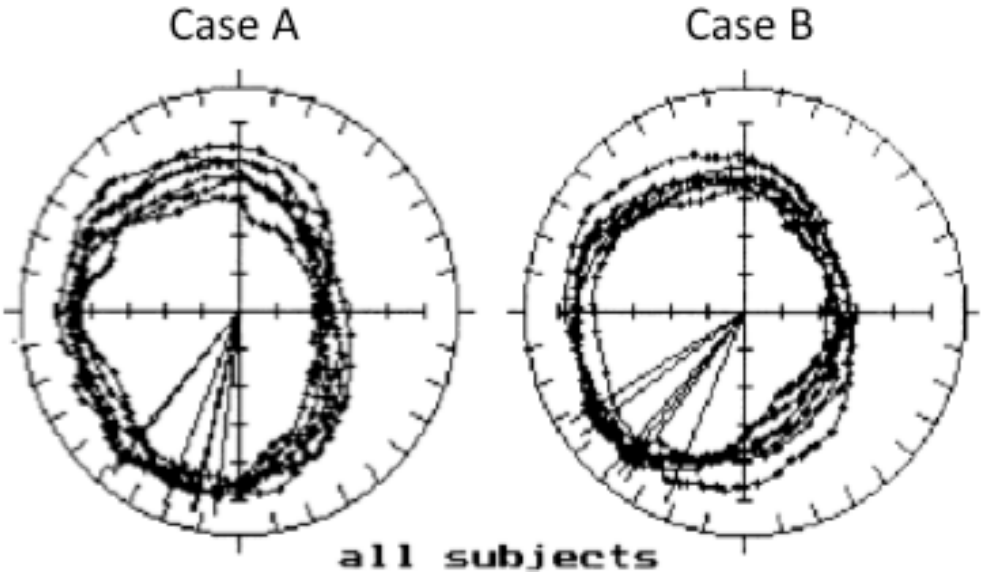

Figure 2.16: The combined strength profiles for all 7 participants for case A and case B as presented by Makhsous et al. (1999). See Figure 1.5 for the description of the exertion directions. Each unit on the axes represents 20% of the maximal force that was produced specifically by each participant. The peak force exertions for each participant are once again show by the interior lines within each strength profile.

Hodder & Potvin (2014) applied the WAA to the data collected by Makhsous et al. (1999) to determine if this WAA method actually applied to physiological data to predict shoulder strength, compared to the IAA used by 3DSSPP and Jack (Figures 2.17). To do this, arbitrary force values were onto each axis in 100 newton (N) increments, starting

from 0. Next, he estimated the approximate average peak force value from the Makhsous et al. (1999) curves for the up, down, medial, & lateral directions based on the strength profiles of the seven participants. For example, for case B (Figure 2.17), the average peak force in the up, down, medial and lateral exertions were estimated to be approximately 360 N, 360 N, 460 N, and 260 N, respecitively. It should be noted, that the example for the case A arm posture, was already presented in Figure 1.4. Using the WAA, the maximum shoulder forces were estimated at each angle and then superimposed onto the strength profiles developed by Makhsous et al. (1999). This WAA appears to be valid as it follows the Makhsous et al. (1999) curves very closely for both of the shoulder postures they tested (Figures 2.17).

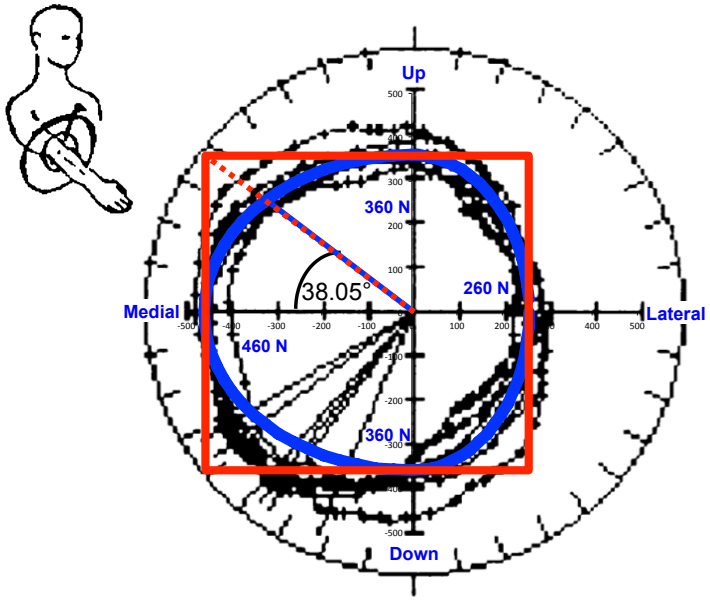

$\theta = \text{Tan}^{-1}(360/460)$
$= 38.05°$

IAA:
$= (360^2 + 460^2)^{½}$
$= 584.12$ Nm

WAA:
$= (460\cos 38.05)^2+(360\sin 38.05)^2)^{½}$
$= 424.79$ Nm

% Difference:
$=(584.12/424.79)*100$
$= 138\%$

When the IAA is used (as in 3DSSPP) the predicted force is 138% of the force that is predicted using the WAA.

Figure 2.17: The independent axis approach (IAA) and weighted average approach (WAA) have been applied to the experimental shoulder strength profile, as created by Makhsous et al. (1999), for the case B arm posture by Hodder & Potvin (2014). Next, they determined the curve that the WAA would predict for the strength profile using the average peak forces of 360 N, 360 N, 460 N, & 260 N, for the up, down, medial, and lateral exertion directions, respectively. The calculations for the IAA and WAA have been applied using the same convention as completed in Figure 1.3. The strength profiles of Makhsous et al. (1999) follows fairly well with the WAA curve that was overlayed. In this example, the assumed task is a maximal exertion in a combination of the up and medial directions. The blue oval represents the strength curve estimated with the WAA, and the red rectangle represents what the stregth according to the IAA. The red dashed line, extending from the origin to the corner of the IAA rectangle, shows what the IAA would calculate the strength to be for this example, while the solid blue line represents what the WAA would calculate the strength to be. In this example, the IAA results in a predicted strength that is approximately 38% greater than the WAA, at 38.05° from the horizontal.

In addition to the evaluating the WAA using the data collected by Makhsous et al. (1999), Hodder & Potvin (2014) also conducted their own test of the WAA, using their own empirically measured data. The primary purpose of the study was to determine if the WAA produced more accurate shoulder strength predictions than the IAA, assuming the WAA is a more anatomically appropriate method of strength estimation. Hodder & Potvin (2014) tested 15 female participants while they performed maximal isometric shoulder strength exertions with their right arm fixed in a rigid brace, just proximal to the elbow. The brace was attached to a tri-axial load cell that could be moved superior/inferior and anterior/posterior to accommodate the varying participant anthropometrics. While in the brace, the participant's arm was positioned such that it was in 90° of abduction with the elbow flexed to 90°, such that the forearm was in a vertical position (Figure 2.18). Participants were required to preform two exertions in each of the following directions while their arm was in this specific posture: 1) horizontal flexion (cross-flexion), 2) horizontal extension (cross-extension), 3) abduction, 4) adduction, and 5) at a 45° angle between each of the directions (n=8). They then had participants perform maximum isometric exertions where they were instructed to trace a square that would represent their strength predicted with the IAA. Four repetitions were performed, randomly starting in one of the orthopaedic axis directions. The IAA and WAA were then used to predict the moments that were measured using the load cell. Hodder & Potvin (2014) found that the moments (Nm) measured during the second set of exertions lined very well with the strengths predicted by the WAA (Figure 2.19). This result was similar findings when the WAA and IAA were applied to the data of Makhsous (1999). When examining strengths in the most extreme cases (at 45° between each of the axes), the study found that the IAA over predicted strength by 21-22% and 3-4% for exertions from adduction and abduction, respectively. On the other hand, the WAA either predicted strengths that were no different than the measured strengths (from adduction), or under predicted strength by 8-9% when completing abduction exertions (Table 2.1). The results from both Hodder & Potvin (2014) and Makhsous (1999) indicate that the WAA is a more physiologically viable method of strength prediction, compared to the IAA, and is something that should be investigated further with the hope of eventually integrating it into current ergonomics tools.

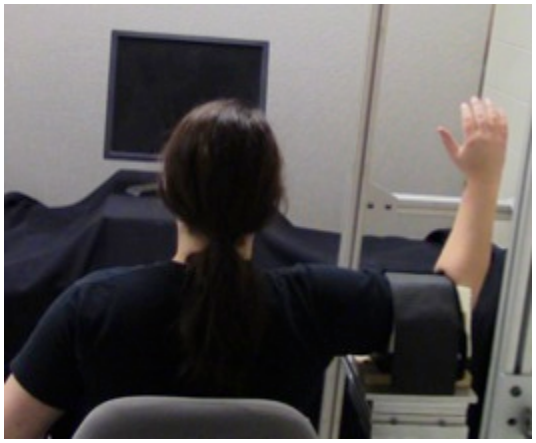

Figure 2.18: The arm posture used by Hodder & Potvin (2014) to test the WAA and IAA. Participants were seated in a chair with their arm in 90° of abduction with the elbow flexed to 90° such that the forearm was in a vertical position. All of the required exertions were completed while in this same posture. The arm brace that was used was full padded and its position could be adjusted to accommodate a wide range of participant anthropometrics.

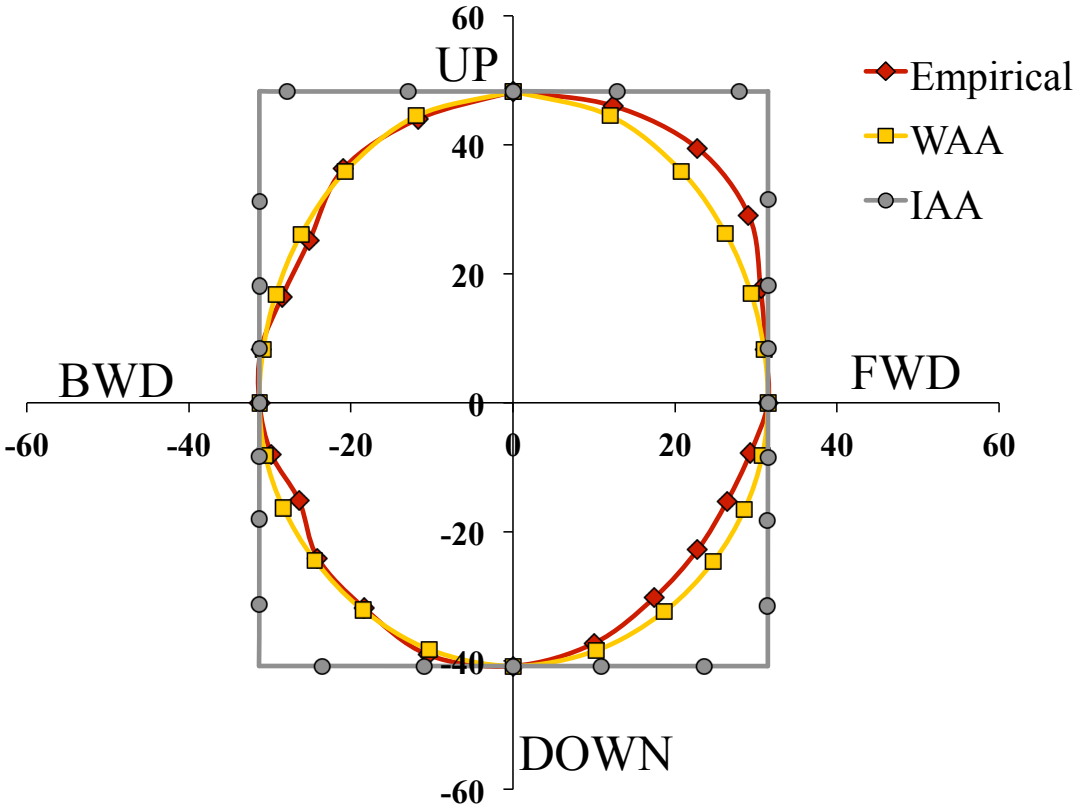

Figure 2.19: This figure depicts how both the WAA and IAA predicted moments (Nm) in the study completed by Hodder & Potvin (2014) (n=15). Along the X and Y-axes are the strengths (Nm) for forward/backward and abduction (up)/adduction (down). The red line represents the actual measured strength, and the yellow and grey lines represent the predicted strengths by the WAA and IAA, respectively. Each point on the lines represents where a measurement was taken.

Table 2.1: Summary of the measured and predicted strengths (Nm), by the IAA (resultant method) and WAA methods at the extreme 45° exertion directions (Hodder & Potvin, 2014). The mean and standard deviation for the measured strength is provided (n=15), while only the mean predicted strengths are provided for the IAA and WAA.

	Maximum Strength (Nm)		
45° Angle Between:	Measured	Resultant Method	WA Method
Flexion & Abduction	32.4 ± 11.7	33.5	29.3
Extension & Abduction	30.9 ± 8.2	32.1	28.4
Extension & Adduction	26.5 ± 7.4	32.1	26.6
Flexion & Adduction	27.4 ± 8.4	33.5	27.4

2.4 – Shoulder Strength Prediction

Ergonomists rely heavily on current software packages, such as 3DSSPP and Jack, to predict joint moments and compare them to strength literature to determine task acceptability. However, due to the previously outlined potential sources of error within these programs, whether or not the moment predictions are trustworthy should be called into question. To this point, there have been many studies since Stobbe (1982) that have attempted to develop different methodologies to predict shoulder strength based on inputs such as; posture, exertion direction, gender, and age (Chow & Dickerson, 2009; Das & Wang, 2004; Garg et al. 2005; Haslegrave et al. 1997; Hughes et al. 1999; MacKinnon 1998; Makhsous et al. 1999; Peebles & Norris, 2003; Roman-Liu & Tokarski, 2005).

One such study, by La Delfa et al. (2014), developed a series of regression equations that predicted MAS for a wide variety of hand locations and force directions. The study included a total of 71 right-hand dominant female participants. The equations that were developed predicted MAS based on: 1) the location of the hand, relative to the shoulder joint, and 2) the direction cosines of the exertion force vector. Participants were required to produce isometric maximal exertions in six primary 1D exertion directions: 1) push up, 2) push down, 3) push anterior, 4) pull posterior, 5) push medial, and 6) push lateral. Participants completed exertions while grasping a vertically orientated handle attached to a tri-axial load cell. In total, three separate data collections, using the same methodologies, were conducted to obtain the data in the study. Overall, 28 different hand locations were examined, as 20, 4, & 4 hand locations, were tested in the first, second, and third data collections, respectively. In total, 29, 30, & 12 participants, respectively, completed each of these studies. All of the exertions were completed while

participants were in a standing posture. All of the tested hand locations were based on the H, V, & L locations of the hand relative to the center of the glenohumeral joint. The hand locations were tested in various combinations of: A) hand height (overhead, stature, eye, shoulder, and waist height, B) the degree of rotation away from the sagittal plane: (20°, 0°, 45° and 90°), C) the percentage reach distance based on the maximum reach distance as measured from the center of the glenohumeral joint to the first knuckle of the third finger. Participants were required to perform ramped maximal exertions for a period of 5-seconds, in which they ramped up the force to maximum for 1-second, held the contraction for 3-seconds, and then ramped down the contraction for 1-second. Throughout the exertion, participants received visual feedback of their force application. If the resultant force was not at least 90% in the intended direction, then the trial was re-collected. The force that was measured during each trial defined each participant's MAS for that hand location and exertion direction. After data collection, La Delfa et al. (2014) developed regression equations to estimate MAS for each of the six 1D exertion directions for each hand location. These equations used only the inputs of hand location in terms of the anterior H, V, and L position of the hand relative to the acromion of the shoulder. These inputs were also squared (H^2, V^2, L^2), cubed (H^3, V^3, L^3), and multiplied by each other (H*V, H*L, V*L) in order to maximize the explained variance by including non-linear variables into the equations. These equations performed very well as they resulted in an overall r^2 of 92.5% with an RMSE of only 6.4 N (Figure 2.20). The high explained variance and the low RMSE, indicated that this method of arm strength prediction could potentially be a valid alterative to improve strength predictions. As mentioned, currently in 3DSSPP, the database that is present contains strengths that were measured about each axis for each joint (eg. three at the shoulder). Then, using those strengths in each axis as anchor points, strength equations were applied to predict how strength changed with a change in joint angle. This population strength database was then fed into the linked-segment model within 3DSSPP to calculate moments about the various joints when different forces and exertion direction were applied at the hand. The method developed by La Delfa et al. (2014) essentially treats the entire arm as a piston, and only measures force produced at the hand. Then, using a set of input variables based on the location of the hand and the developed MAS database, the regression equations to predict strength could be developed. These equations could now be used to predict MASs at the hand using only the inputs of hand location.

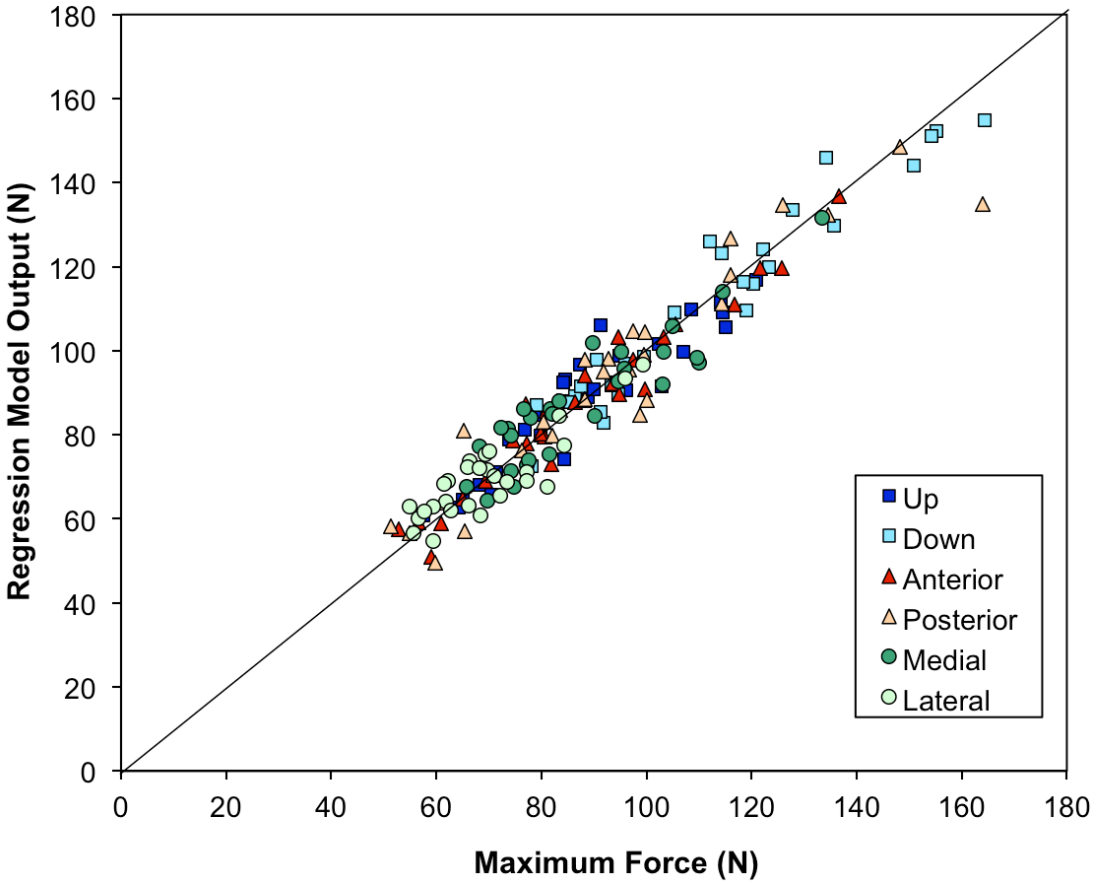

Figure 2.20: A scatter plot depicting the overall results for the regression equations that were developed (r^2 = 92.5% & RMSE = 6.4 N) (n = 28 for each exertion direction). The diagonal line represents a perfect prediction by the model and collected manual arm strength data (La Delfa et al. 2014).

Chapter 3 – Methods

3.1 – Participants

A total of 15 right-hand dominant, healthy females, from the McMaster University student population, were recruited for this study. These participants were free of any upper body acute injuries and/or chronic disorders for a period of one year prior to the onset of data collection. Prior to the commencement of the study, participants were required to read and sign a written consent form (Appendix A). During this process, participants were informed of the purpose of the study, the methods of data collection that were used, and any potential risks that were associated with the protocol. Any questions participants had concerning their involvement were answered.

Prior to data collection, anthropometric measurements, pertaining to each individual participant, were recorded and entered into an electronic spreadsheet. Descriptive data on the average participant anthropometrics can be found in Table 3.1. These measurements included height (cm), weight (kg), age (years), maximum arm reach (cm) (as measured from the center of the glenohumeral joint to the midpoint between the base of the third metacarpal and the line connecting the radial and ulnar styloid processes), shoulder breadth (cm), shoulder height while sitting (cm) (measured from the floor to the center of the glenohumeral joint), sternum height while sitting (cm) (measured from the floor to the xiphoid process), umbilicus height while sitting (cm) (measured from the floor to the umbilicus), eye height while sitting (cm) (measured from the floor to eye level) humeral length (cm) (as measured from the center of the glenohumeral joint to the olecranon process), forearm length (cm) (as measured from the olecranon process to the radial styloid process), wrist to knuckle length (as measured from the centre point between the radial & ulnar styloid processes to the base of the third metacarpal), and the wrist width (cm) (as measured from the dorsal to palmer surfaces at the wrist joint centre). Once these values were entered into the spreadsheet, they were used to help determine the specific tested hand locations for each participant.

Table 3.1: Descriptive data for the average participant anthropometrics (n = 15).

	Height (cm)	Weight (kg)	Age (years)
Average	169.2	64.1	24.5
St. Dev.	8.3	12.5	2.7
Min	158.0	48.3	20.0
Max	185	93.8	32

3.2 – Instrumentation and Data Acquisition

For this study, a custom laboratory apparatus was constructed (Figure 3.1). This setup consists primarily of a metal cube constructed of slotted rail (80/20 Inc., Columbia City, IN). A tri-axial load cell (500 lbs. XYZ Sensor, Sensor Development Inc., Lake Orion, MI) was fixed on a horizontally mounted piece of 80/20 slotted rail positioned between the two anterior vertical rails. The tri-axial load cell, and the horizontal piece of slotted rail, were able to translate medial/lateral and superiorly/inferiorly using sliding brakes affixed underneath the load cell and at either end of the horizontal rail. This allowed for the load cell to be easily positioned to accommodate an acceptable range of hand locations and arm postures. A linear force transducer (100 lbs., Omegadyne Inc., Laval, QC, Canada) was also be used to measure force in this study (Figure 3.2). This transducer was mounted to both vertical rails, the horizontal rail, and a rail fixed to the baseboard of the chair that the participants sat in. These multiple mounting positions (Figure 3.2) allowed for the desired force to be measured accurately as the transducer had the ability to slide along the lengths of each of the slotted rails. Attached to the transducer was a non-stretch climbing rope that was attached to a padded wrist cuff (Figure 3.2).

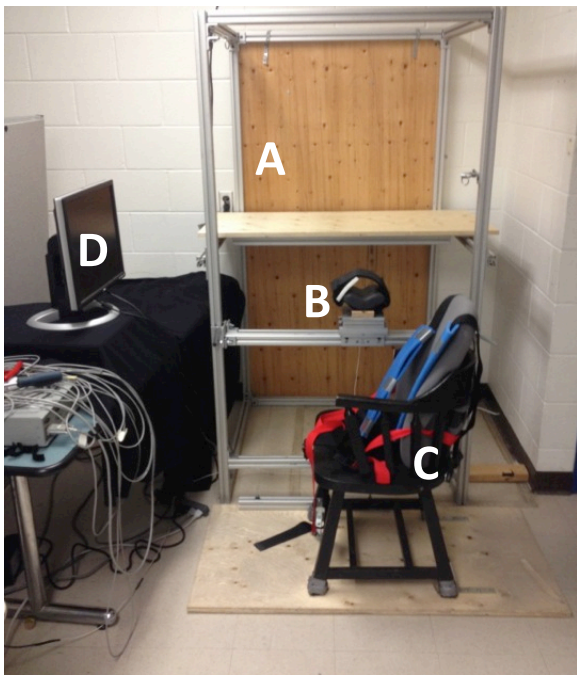

Figure 3.1: Overview of the custom apparatus. A) the 80/20 slotted rail structure. B) the tri-axial load cell mounted to the horizontal 80/20 slotted rail. C) the chair participants were seated in during data collection. This chair was moved around to accommodate the various anthropometrics of the participants, the red waist belt, and blue shoulder straps helped to keep participants in a seated and secured posture. D) the screen on which participants received feedback on the direction of their exertion.

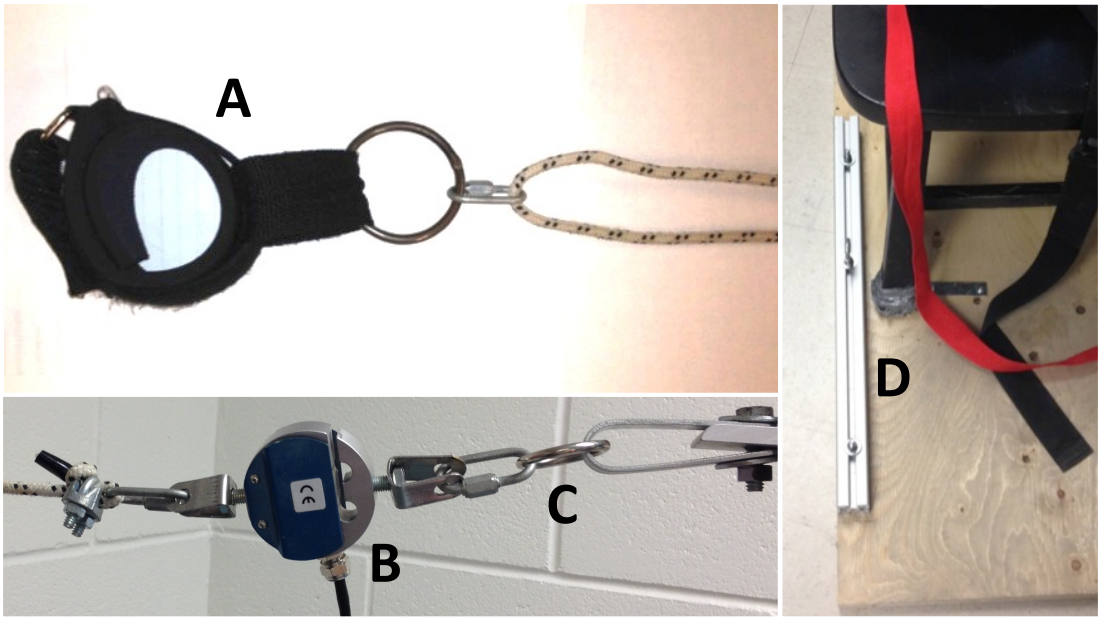

Figure 3.2: This diagram presents the linear force transducer and the various attachment points. A) the padded wrist cuff that participants used to perform the required exertions. B) the linear force transducer attached to a steel screw ring. C) the attachment point for the linear force transducer on the vertically oriented 80/20 slotted rails. D) the slotted rail attached to the baseboard of the chair. A screw ring can slide along the rail to adjust the position for which the linear force transducer can be attached.

This study consisted of collections for: 1) joint axis strengths (JAS), and 2) manual arm strengths (MAS). The instrumentation shown in Figure 3.1 & 3.2 pertains to the JAS collection, however, the same tri-axial load cell (Figure 3.1) was also used during the MAS collection. Additionally, during the MAS collection, kinematic data was also collected using the 6-degree-of-freedom Fastrak electromagnetic system (Polhemus, Colchester, VT.), with a sample rate of 30 Hz. This system used four separate sensors, fixed to the dorsal surface of the hand (over the midpoint between the base of the third metacarpal and the line connecting the radial and ulnar styloid processes), on the forearm (on the dorsal surface, in the centre of the forearm, just proximal to the padded wrist cuff), elbow (over the lateral epicondyle), and shoulder (over the acromion process). This allowed for the determination of the joint locations and joint angles throughout the MAS collection.

For both for the JAS and MAS data collections, custom LabVIEW software (National Instruments, Austin TX) was used to collect the data with a PC computer. All of the force data was sampled at 100 Hz using this software, and converted by a 12-bit A/D card (National Instruments, Austin TX). Participants received visual feedback on the direction and magnitude of the resultant force exertion throughout each JAS and MAS trial on a screen placed in front of them.

3.2.1 – Joint Axis Strength Setup

As mentioned, this study was divided into two separate data collections; 1) JAS, and 2) MAS. To complete the former, the apparatus was configured such that the same postures used by Stobbe (1982) could be tested (see Figure 2.1). Specifically, using the slotted rail setup, eight different strengths in four separate axes (three about the shoulder, & one about the elbow) were tested for each participant. These strengths included the individual's horizontal shoulder flexion (forward), horizontal shoulder extension (backward), abduction, adduction, medial humeral rotation, lateral humeral rotation, elbow flexion, and elbow extension.

Each of the JAS magnitudes (Figure 2.1) were tested in same arm postures as originally tested by Stobbe (1982). Throughout all of the JAS testing, participant's were seated and firmly strapped into the seat using a waist strap and a strap that came over the left shoulder & crisscrossed the chest. Each participant's level of comfort was checked after the strapping was secured. For the horizontal flexion and extension strengths, the padded wrist with the non-stretch climbing rope (Figure 3.2) was mounted to the tri-axial load cell using a screw. To test these JAS, the participant was seated in the chair, positioned either parallel (horizontal extension) or perpendicular (horizontal flexion) to the slotted rail apparatus (Figure 3.4). For horizontal flexion, their arm was strapped in using the padded wrist cuff while in 90° of abduction, 90° of elbow flexion, 0° of horizontal flexion, and 0° of humeral rotation posture. For horizontal extension, their arm was also strapped in using the padded wrist cuff while in the same posture, except their arm was in 60° of horizontal forward flexion (Figure 3.4). To test abduction and adduction, a custom arm strap apparatus (Figure 3.3) was mounted to the tri-axial load cell. The participant remained in almost the same posture as for testing horizontal flexion, however, the humerus was rotated 90° laterally (Figure 3.5). Finally, to test lateral humeral rotation, and elbow flexion and extension, again the padded wrist strap attached to the linear force transducer was used, and the participant was seated in the chair with 0° of abduction/adduction, 90° of elbow flexion, 0° of horizontal flexion, and 0° of humeral rotation (Figure 3.6).

Figure 3.3: The custom padded arm strap apparatus is seen here. The participant rested their humerus inside the cuff, and then the padded arm strap was secured on the humerus just proximal to the elbow.

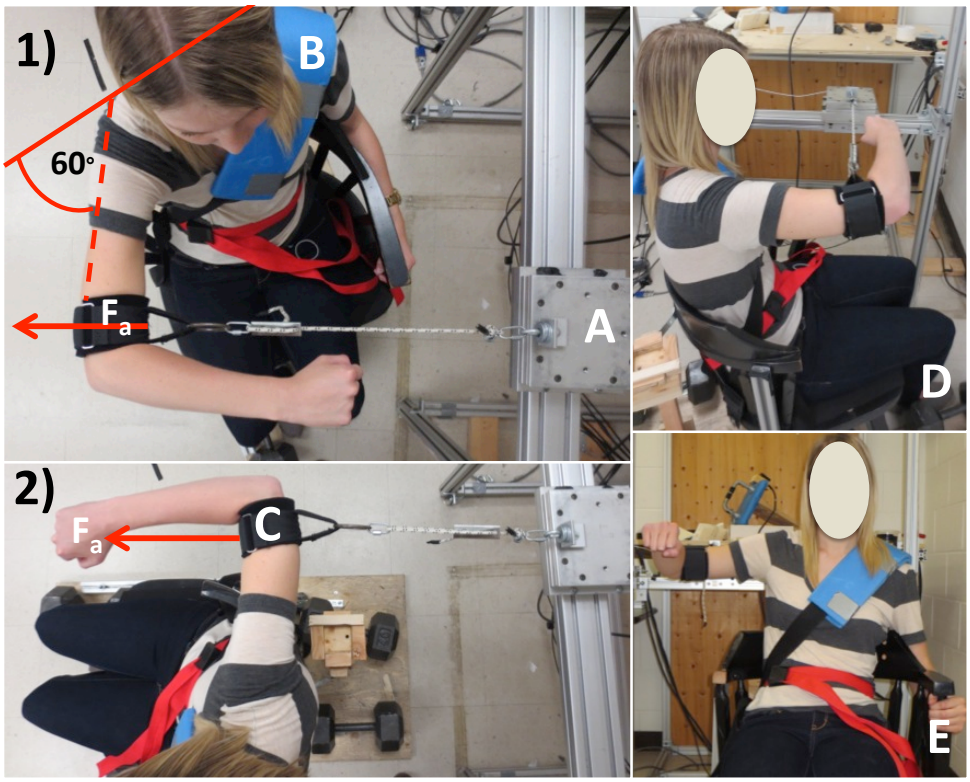

Figure 3.4: This diagram shows the two arm postures that were used to test the horizontal extension (backward) (1) and horizontal flexion (forward) (2) strengths, as seen in Figure 2.1, pictures 3 & 4, respectively. For both postures, the humerus is placed into 90° of abduction, with the elbow bent to 90° of flexion. For the horizontal backward trial, the participant was positioned such that the humerus was in a 60° forward flexed position. The red arrows indicate the direction of the applied force (F_a). A) the tri-axial load cell that measured force production. B) the left shoulder strap that helped to secure the participant into the chair. C) the padded cuff that was secured to the humerus.. D) a sagittal view of the horizontal backward strength trial. E) a frontal view of the horizontal forward strength trial.

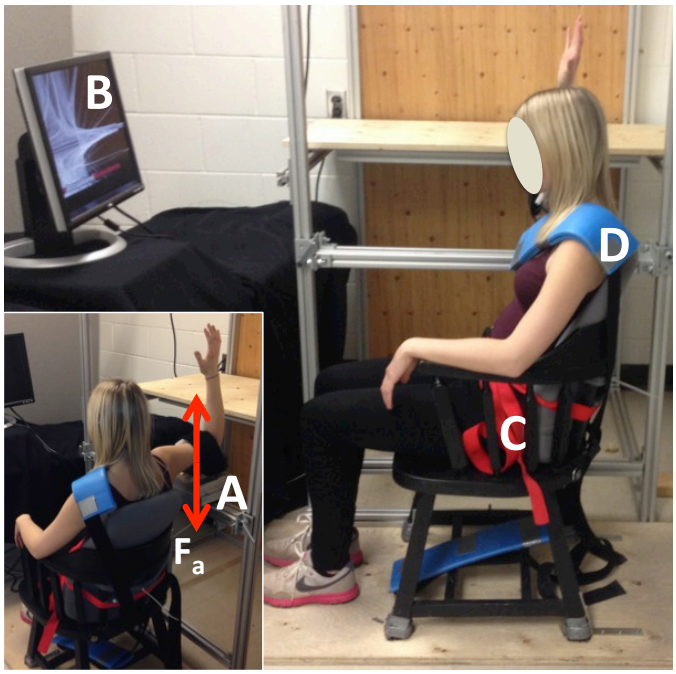

Figure 3.5: This diagram shows a sagittal view of the adduction and abduction JAS tests, as seen in Figure 2.1, pictures 5 & 6, respectively. Both of these strengths used this same posture as the humerus is placed into 90° of abduction, with the humerus rotated 90° laterally, and the elbow bent to 90° of flexion. The red arrows indicate the direction of the applied forces (F_a). A) the tri-axial load cell to measure force production, B) the monitor which participants received feedback on the direction of their exertion, C) the waist strap used to help secure the participant into the chair, D) the left shoulder strap used to help secure the participant into the chair.

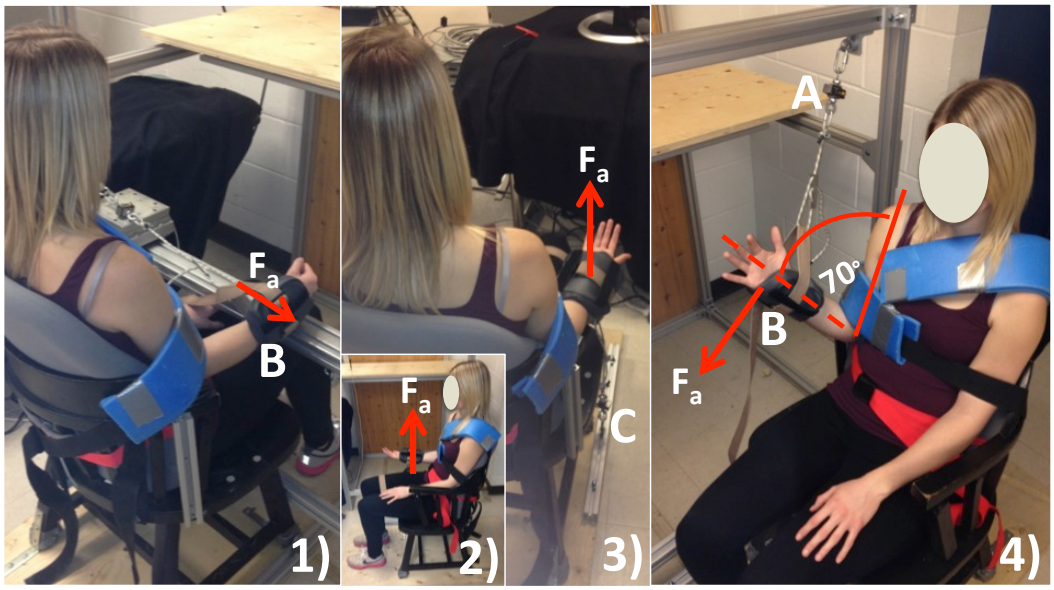

Figure 3.6: This diagram shows several views of the lateral humeral rotation (1), elbow flexion (2 & 3), and elbow extension (4) JAS tests, as seen in Figure 2.1, pictures 1, 2 & 8, respectively. All of these strengths were tested while the humerus was in a neutral position with the elbow in 90° of flexion, except for elbow extension, which starts with the elbow in 70° of flexion. The red arrows indicate the direction of the applied force (F_a). A) the linear force transducer mounted to the inferior surface of the horizontal 80/20 rail, B) the padded wrist cuff, C) the linear force transducer attached directly below the wrist to the piece of slotted rail that is fixed to the baseboard of the chair.

For the medial humeral rotation strength, the participant was seated in the chair with their arm fixed into the arm strap apparatus; the same as the adduction and abduction JAS. During this strength test, the arm strap apparatus served as a stabilization device, as no measurements were collected using the tri-axial load cell (Figure 3.7). Instead, the padded wrist cuff was attached to the linear force transducer via the non-stretch climbing rope, and was secured to the palmar surface of the wrist just proximal to the styloid processes of the radius and ulna. The linear force transducer was positioned such that it was perpendicular with the length of the radius with the elbow flexed 90°. This ensured that the rope, leading from the wrist cuff to the linear force transducer, was parallel with the horizontally mounted piece of slotted rail (Figure 3.7).

For the lateral humeral rotation, and the elbow flexion/extension trials (Figure 3.6), participants were seated perpendicular to the apparatus. Their humerus was stabilized using an additional strap that ran across the participants chest and around the right arm just proximal to the 90° bent elbow (Figure 3.8). Originally, Stobbe (1982) used a telescoping post with a pad that was strapped to the arm, however, since the only purpose of this was to secure the humerus so only the elbow could flex, the strap was sufficient for this purpose. For lateral humeral rotation measurements, the linear force transducer and padded wrist cuff were moved within the apparatus on the vertical side support bars, such that the cable was parallel with the floor, at the correct distance such that the arm was in a static posture (with 0° of arm flexion and 90° of elbow flexion) when completing an exertion. For the lateral humeral rotation test, the padded wrist cuff was attached to the dorsal surface of the wrist, just proximal to the styloid processes of the radius and ulna. For the elbow flexion and extension efforts, participants were in the same humeral restraint setup as for lateral humeral rotation, however, the position of the force transducer was changed. For flexion, it was mounted directly below the participants wrist along the rail that was secured to the base board of the chair and, for extension, it was mounted to the inferior surface of the horizontal rail that supports the tri-axial load cell (Figure 3.6). The padded wrist cuff, for the elbow flexion & extension tests, was positioned on the radial & ulnar surfaces of the wrist, respectively, just proximal to the respective styloid process.

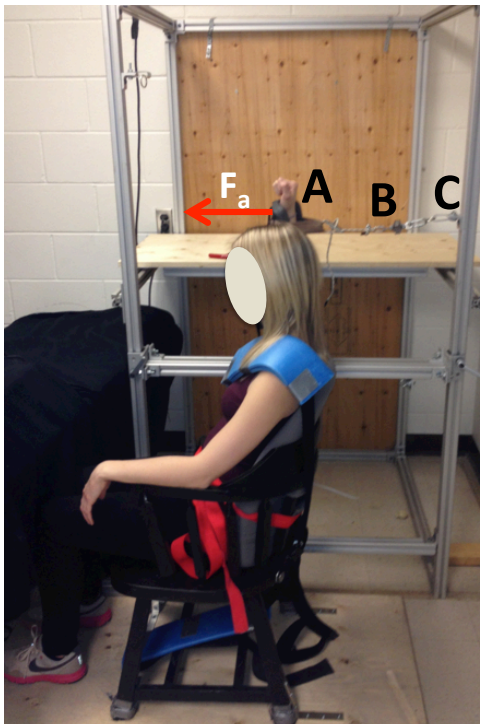

Figure 3.7: A sagittal view of the medial humeral rotation JAS is shown. In this test the tri-axial load cell, with the attached padded arm cuff, was used as a mechanism to support the humerus, as the linear force transducer was used to measure the force that was generated by the participant. The red arrow indicates the direction of the applied force (F_a). A) the padded wrist cuff. B) the linear force transducer. C) the attachment of the linear force transducer to the vertical 80/20 slotted rail.

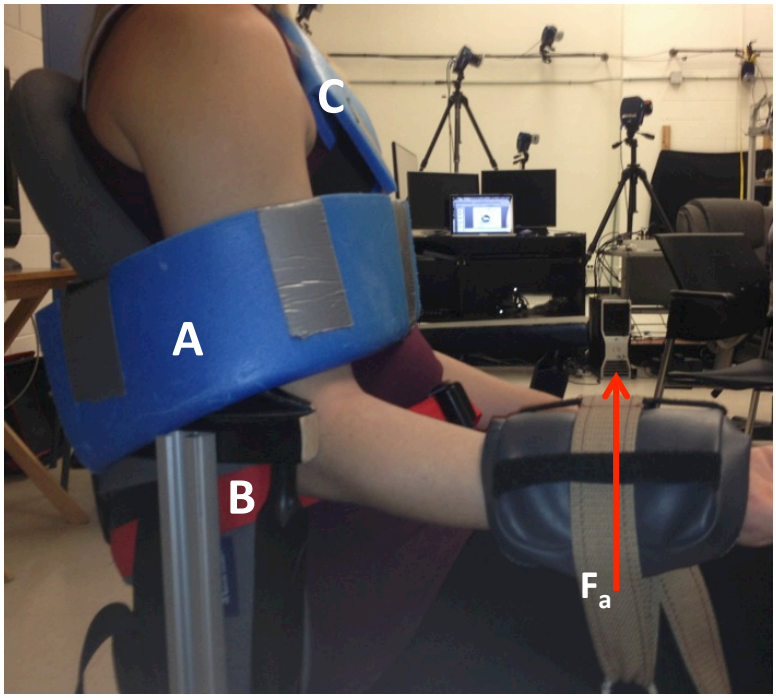

Figure 3.8: The arm strap support is shown for testing the lateral humeral rotation, and the elbow flexion & extension strengths. In this diagram specifically, the elbow flexion strength test is shown. A) the shoulder strap that holds the humerus in place just proximal to the elbow joint, B) the waist strap used to secure the participant into the chair, C) the left shoulder strap that was used to secure the participant into the chair.

3.2.2 – Manual Arm Strength Setup

The second half of this study required the collection of MASs for each participant. This was completed using the same setup that was described for the JAS collection. The only structural variation to the setup was that a different attachment replaced the horizontal arm strap apparatus. This attachment consisted of a vertically oriented handle that was secured to the tri-axial load cell (Figure 3.9). Each participant's MAS was tested while their wrist was positioned within the handle, or coupled to the handle using a padded wrist strap (Figure 3.10a). This was done to eliminate the wrist as the limiting joint while performing maximum exertions. During the MAS trials, participants' wrists were positioned relative to the handle such that the participant was able to perform the appropriate exertion (Figure 3.10a & Figure 3.10b). Prior to MAS testing, participants were first fitted with the four Fastrak sensors that were used to record the three-dimensional (3D) position of the arm. The participant was then seated in the chair positioned perpendicularly to the apparatus, with their waist and torso secured using the waist strap and shoulder strap over the left shoulder (Figure 3.11). While positioned parallel to the apparatus, participants were able to reach the handle within their reach envelope. This setup allowed participants to be in a comfortable wrist/arm posture for the various hand locations and exertion directions that were tested.

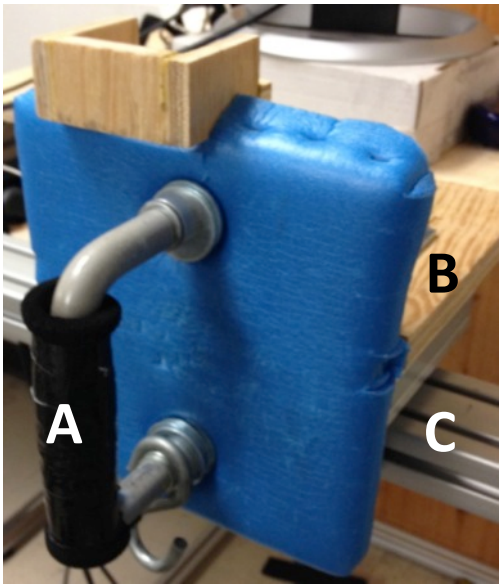

Figure 3.9: The vertical handle attachment for collecting manual arm strength (MAS) is shown. A) the vertical handle which participants were coupled to using the padded wrist strap (Figure 3.10a). B) the tri-axial load cell. C) the horizontal slotted rail that allowed the tri-axial load cell to translate medial and lateral along the rail.

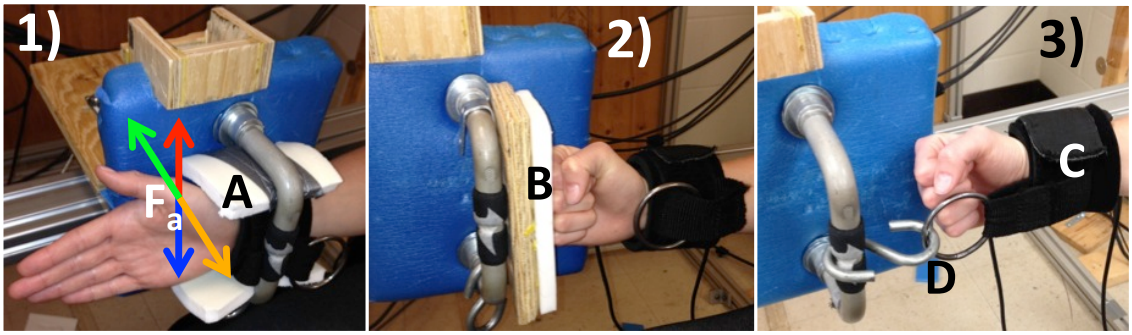

Figure 3.10a: The six different exertion directions that were tested for the manual arm strength (MAS) collection when the participant was in the umbilicus 0°, 60°, and eye 45° hand locations (Figure 3.12) are shown. See Figure 3.10b for how these exertions were tested for the eye 0° hand location. 1) up, down, medial, lateral, 2) push; for the push exertion, the participant simply pushed into the padded plate while making a fist, 3) pull; the participant wore a padded wrist strap that has a metal hook that can be hooked onto the handle to complete the pull exertion. During the up, down, medial, and lateral exertions, participants slid their hand and wrist inside the handle (as shown), while wearing the padded wrist cuff. Foam padding was then positioned superior and inferior to the wrist to ensure it was positioned both snugly and comfortably. It should be noted that the tri-axial load cell was able to be moved medial/lateral on the horizontal bar such that the hand was in the same location for each of the wrist-controlled postures.

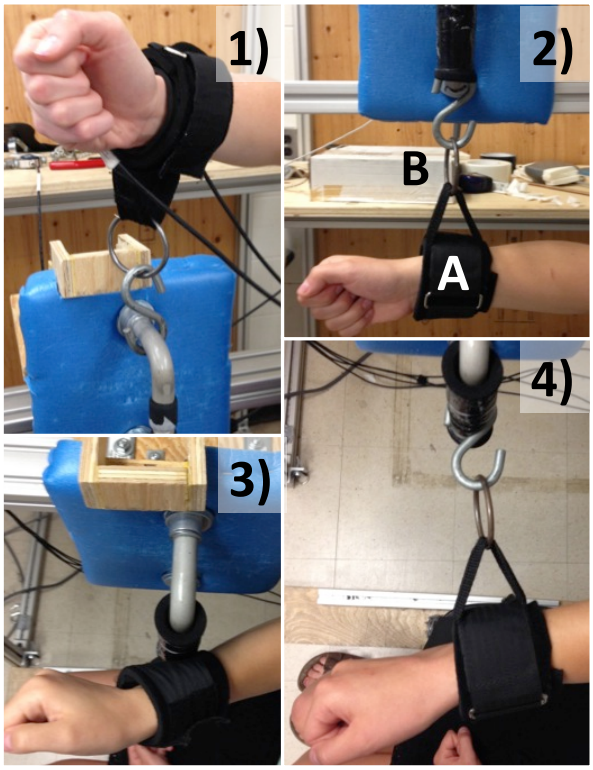

Figure 3.10b: How the six different exertion directions were tested for the manual arm strength (MAS) collection when the participant was in the eye 0° hand location (Figure 3.12) is shown. A separate set of coupling strategies had to be applied due to the awkwardness of this hand location for most participants. 1) up, 2) down, 3) lateral, and 4) medial. Please note that pictures 1 and 2 are sagittal views, while picutres 3 and 4 are superior views. The padded wrist strap was either used to hook the participant's wrist on the handle (up, down, medial) or to press on the handle (lateral).

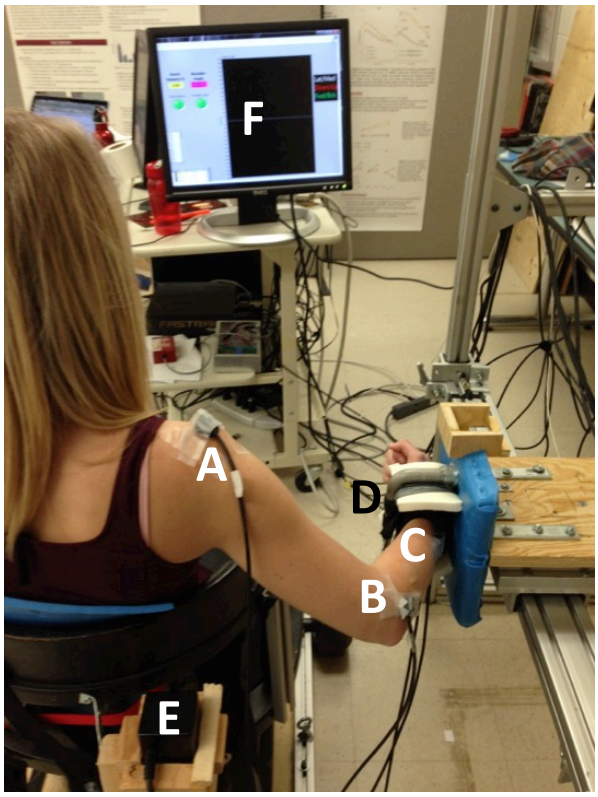

Figure 3.11: A participant strapped into the chair for a manual arm strength (MAS) exertion trial in the umbilicus 60° hand location. A) the acromion Fastrak marker. B) the lateral epicondyle elbow Fastrak marker. C) the forearm Fastrak marker positioned on the dorsal surface, in the centre of the forearm, just proximal to the padded wrist cuff. D) the hand positioned inside the handle. What cannot be seen is the hand Fastrak marker, which was positioned over the midpoint between the base of the third metacarpal and the line connecting the radial and ulnar styloid processes. E) the Fastrak source mounted to a post on the chair, such that it is always positioned posterior to the right shoulder in a constant location.

Similarly to the JAS measurements, the horizontal 80/20 slotted rail, which the tri-axial load cell and vertical handle attachment were fixed on, was able to slide freely superior and inferior on the anterior vertical side rails. Additionally, the tri-axial load cell was also able to slide medial/lateral on the rail, which allowed for specific hand locations to be set for each participant. Similar to the JAS testing, participants received feedback on a screen of the resultant direction of their force exertion.

3.3 – Experimental Protocol and Procedures

3.3.1 – Study Overview

Data collection for this study was completed over the course of two 1-hour sessions for each participant. During the first session, anthropometric measurements were taken, the participant was familiarized with the protocol they were about to complete (JAS or MAS), and they completed that day's protocol (whether they completed the JAS or MAS

protocol first was randomized). During the second session, the participant was familiarized with the protocol they were about to complete (JAS or MAS), and they completed that day's protocol. Participants were provided with a minimum of two days of rest in between the two testing sessions, to account for any fatigue effects.

3.3.2 – Joint Axis Strength Testing Protocol

During the strength trials, participants completed approximately 3-5 second strength exertion trials, as they were required to ramp up exertions over a period of approximately 1-2 seconds until they reached their maximal peak exertion, held the peak exertion for approximately 1-second, and then ramped down their exertion strength over a period of 1-2 seconds. During the exertions that were measured using the tri-axial load cell (horizontal flexion & extension, abduction, & adduction), participants were provided with visual feedback as to the direction and magnitude of the force applied. They were required to apply the force in the intended direction that was at least 90% of the resultant in order for the collection trial to be deemed valid. If this criterion was not met, then the trial was recollected. For the exertions (medial & lateral humeral rotation, and elbow flexion & extension) that were completed using the linear force transducer, participants were provided with visual feedback in terms of only the magnitude of force application, as the linear force transducer did not permit directional feedback to be displayed. They were given a minimum of 90-seconds of rest between exertions, in order to abate any fatigue effects. Participants completed three trials for each of the eight JASs that were tested (n = 24).

3.3.3 – Manual Arm Strength Testing Protocol

Each participant's MAS was tested in six different exertion directions, and at four different hand locations (n = 24) (Table 3.2). All of the exertions were completed using their right hand and all participants will be right hand dominant. The exertions that were tested were the primary 1-dimensional (1D) exertion directions. These included up, down, push (anterior), pull (posterior), medial, and lateral. Participant's wrists were either positioned within the handle, or coupled to the handle using a padded wrist strap (Figure 3.10a & 3.10b). These two wrist-controlled coupling methods were implemented such that MAS data could be collected while the participant's wrist strength was not a limiting factor.

The hand locations were defined by the location of the hand relative to the center of the glenohumeral joint of the shoulder. The range of hand locations were based on the angle that the arm made with the sagittal plane intersecting the shoulder, and this was termed “sagittal shoulder angle”. The angle estimates were completed by the custom Lab View software. The three different sagittal shoulder angles, that were used to define the hand locations in this study, were 0°, 45°, and 60°. The percentage of maximal reach distance was also used to define the hand locations, and this was set at 80% of maximal reach distance for each of the four hand locations. Finally, the height of the hand, relative to the body, was also used to define the hand locations. The two different heights were umbilicus and eye height while sitting. The four different hand locations, based on these definitions, that were tested include; 1) umbilicus height at 0°, 2) umbilicus height at 60°, 3) eye height at 0°, and 4) eye height at 45° (Figure 3.12).

After the hand location was determined and set, based on the participant’s anthropometry, the their right wrist was then coupled to the handle using one of the two previously mentioned coupling strategies (based on the exertion to be performed), while their arm/hand was in a semi-prone forearm posture. Next, participants were asked to perform exertion trials as they were presented in a random order, which had been blocked on hand location. Each exertion was collected for a period of 5-seconds, and participants were requested to perform the same type of ramped exertions performed in the JAS data collection. They were provided with visual feedback on the direction and magnitude of the current force application, similar to the feedback system used during the JAS tests. Again, to deem a trial valid, 90% of the result direction had to be in the intended direction. Participants were provided with a minimum of 90-seconds of rest in between each trial to abate any fatigue effects.

Table 3.2: Summary of the manual arm strength conditions that were tested. The second column outlines the four different hand locations that were tested. The top row outlines the six different exertion directions that were tested at each hand location, as indicated by the check marks.

		Exertion Direction					
		Up	Down	Push	Pull	Medial	Lateral
Hand Location	Eye 0°	✔	✔	✔	✔	✔	✔
	Eye 45°	✔	✔	✔	✔	✔	✔
	Umbilicus 0°	✔	✔	✔	✔	✔	✔
	Umbilicus 60°	✔	✔	✔	✔	✔	✔

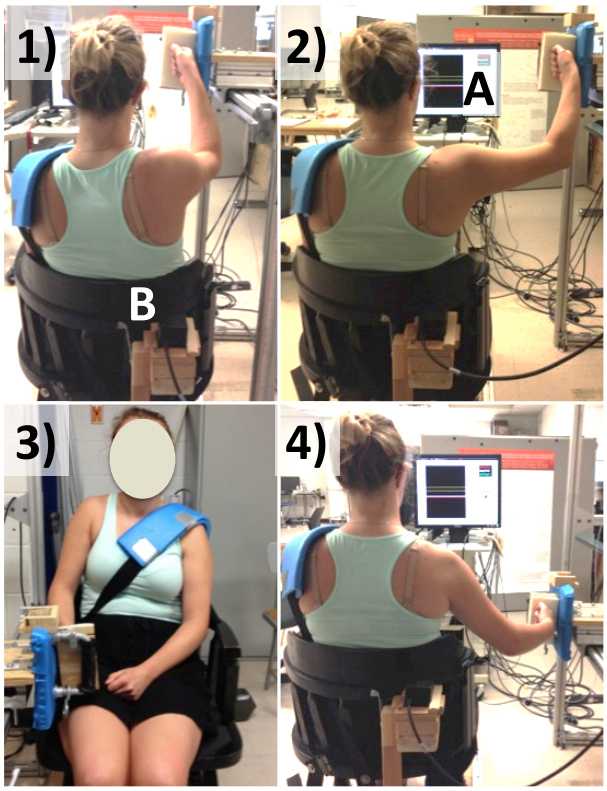

Figure 3.12: The four hand locations that were tested during the manual arm strength (MAS) collection are shown. 1) eye height with 0° of sagittal shoulder flexion, 2) eye height with 45° of sagittal shoulder flexion, 3) umbilicus height with 0° of sagittal shoulder flexion, 4) umbilicus height with 60° of sagittal shoulder flexion. A) the screen on which participants received feedback about the direction of their exertion.

3.4 – Data Analysis

The analysis of the data was completed in three stages.

1. I used the participant's specific anthropometric length measures, their mass, and the same assumptions used in 3DSSPP (e.g. the percentage of body mass present in the upper arm) to calculate the joint moments for each participant.
2. Two sets of input data were entered into a specifically developed linked segment biomechanical model, which include:
    a. the strength data collected from the JAS testing, and
    b. the kinematic data that are collected from the MAS testing.
3. Both of these data fed into this biomechanical model that:
    a. calculated the joint angle for each of the four axes (vertical shoulder angle, horizontal shoulder angle, humeral rotation angle, and elbow included angle),
    b. calculated the moment strengths at the elbow (flexion/extension) and the three 3DSSPP-specific strengths at the shoulder (forward/backward, abduction/adduction, humeral rotation), based on:

i. the equations used by 3DSSPP
ii. the specific joint postures
iii. the subject-specific strengths in the Stobbe postures

c. iterated through forces at the hand (in increments of 0.1 N), in the intended direction, until one of the joints reaches it's maximum

For each participant, these analyses were conducted for each hand location/exertion direction combination (n = 24), as the force and kinematic postural data were different for each trial. To complete the first half of the data analysis, a total of 360 (24/participant X 15 participants) of these analyses had to be conducted. The second stage of the data analysis consisted of conducting a similar analysis, however, using the WAA to estimate each individual's MAS. The same joint moment calculations were conducted, using the same assumptions in 3DSSPP as applied during the IAA analyses. Again a specially designed biomechanical model used the inputs of the: 1) JAS data, and 2) the kinematic data from the MAS collection, to estimate each individual's MAS, however using the WAA, opposed to the IAA.

This second stage of the data analysis required another 360 of these analyses to be completed. It is important to note that the participants' peak strengths, for both the JAS and MAS collections, were determined using a 1-second moving average over the span of each 5-second exertion collection period. For the JAS trials specifically, the peak force, that was determined for each of eight strengths, was taken as the highest recorded 1-second moving average from the three separate trials collected.

3.4.1 – Estimating the Joint Centres

Since my kinematic data were based on markers that were positioned superficially on the skin, an estimation of the joint centres had to be completed prior to entering the data into the linked segment model. For the shoulder and elbow, the joint centres were estimated using the procedure outlined by Nussbaum & Zhang (2000). For the wrist and knuckle, however, a different method of estimation had to be used. This was because the padded wrist strap interfered with the positioning of the marker over the wrist joint centre, and the hand marker could not be placed on the knuckle due to how the forward exertion had to be performed (by making a fist and pressing against a padded plate). For the wrist, the marker was placed on the dorsal surface of the arm, in the middle of the forearm, just proximal to the padded wrist cuff. For the hand, the marker was placed over the midpoint between the base of the third metacarpal and the line connecting the radial

and ulnar styloid processes. This point was a measured distance from the wrist joint centre. To determine the wrist joint centre location, the forearm marker was translated the length of the forearm (a known length) along a vector that ran from the elbow marker through the forearm marker, to form a surface marker for the wrist. This position was then translated into the wrist a distance that was half of the wrist width (half of the dorsal to palmar surface distance at the wrist). This was done by first taking the unit vector of the cross product between the elbow-forearm vector and a purely vertical vector. Next, this unit vector was multiplied by half the width of the wrist and adding it to the virtual surface wrist marker. The location of the knuckle was estimated by first multiplying the elbow-to-wrist distance (based on the markers) by the sum of the hand length and forearm length (both know lengths, measured on the participant). Next, this product was divided by the measured forearm length and then added to the elbow joint centre location. The locations of these two virtual markers, for the wrist and hand joint centres, and the locations of the two virtual markers for the shoulder and elbow, were the inputs for the kinematic data within the linked segment model.

3.5 – Statistical Analysis

The statistics for this study were fairly simple, as the primary comparison to be made in this study was between the 1) 3DSSPP (IAA) manual arm strength estimations, 2) the WAA manual arm strength estimations, and 3) the collected MAS values (Figure 3.13).

To compare these three methods, a 4 x 6 x 3 repeated measures analysis of variance (ANOVA) was completed with the independent variables of: 1) hand location (n = 4), 2) exertion direction (n = 6), and 3) method of MAS measurement/prediction (n = 3). The purpose of the ANOVA was to indicate the differences in MAS estimation between the IAA, WAA and MAS methods. Since the MAS method was the “gold standard”, this comparison teased out which method (IAA or WAA) was closer to the actual measured MAS at each hand location and exertion direction.

The correlation between the two strength prediction methods (IAA & WAA) and the measured MAS was also completed and presented in a series of plots, similar to Figure 2.10. It is important to note that these correlations were conducted on an individual basis for each participant. Additionally, the absolute and relative RMSEs between each of the prediction methods, and the MAS, were presented for the four hand locations and separately for the six exertion directions. La Delfa (2011) conducted a similar statistical analysis, however, that study used the mean MAS data collected and

the population strength database present in 3DSSPP to complete the analysis. Additionally, he only examined the IAA method of MAS estimation, inherent in 3DSSPP. My study used each participant's MAS compared to the current 3DSSPP (IAA) estimation, and the hypothesized WAA method of estimation, using their own strength database, such that each comparison was specific to each participant.

The predicted limiting strengths for the IAA predictions were also evaluated for all 360 exertions. This allowed for insight into which joint strengths (forward, backward, adduction, abduction, medial humeral rotation, lateral humeral rotation, elbow flexion, and elbow extension) were most often the limiting for: 1) all efforts, 2) pooled within the four hand locations and 3) pooled within the six exertion directions.

Finally, the ratios of the IAA-to-MAS and WAA-to-MAS were also examined. This allowed for a determination of whether the IAA and WAA were under- or over-predicting the MAS. Average ratios less than 1.00 would indicate an tendency to under-predict the measured MAS.

This study allowed for the most direct comparison between IAA & WAA methods of strength estimation, and the empirically collected MAS data, and ultimately gave 3DSSPP (via the IAA) the best chance to make accurate predictions.

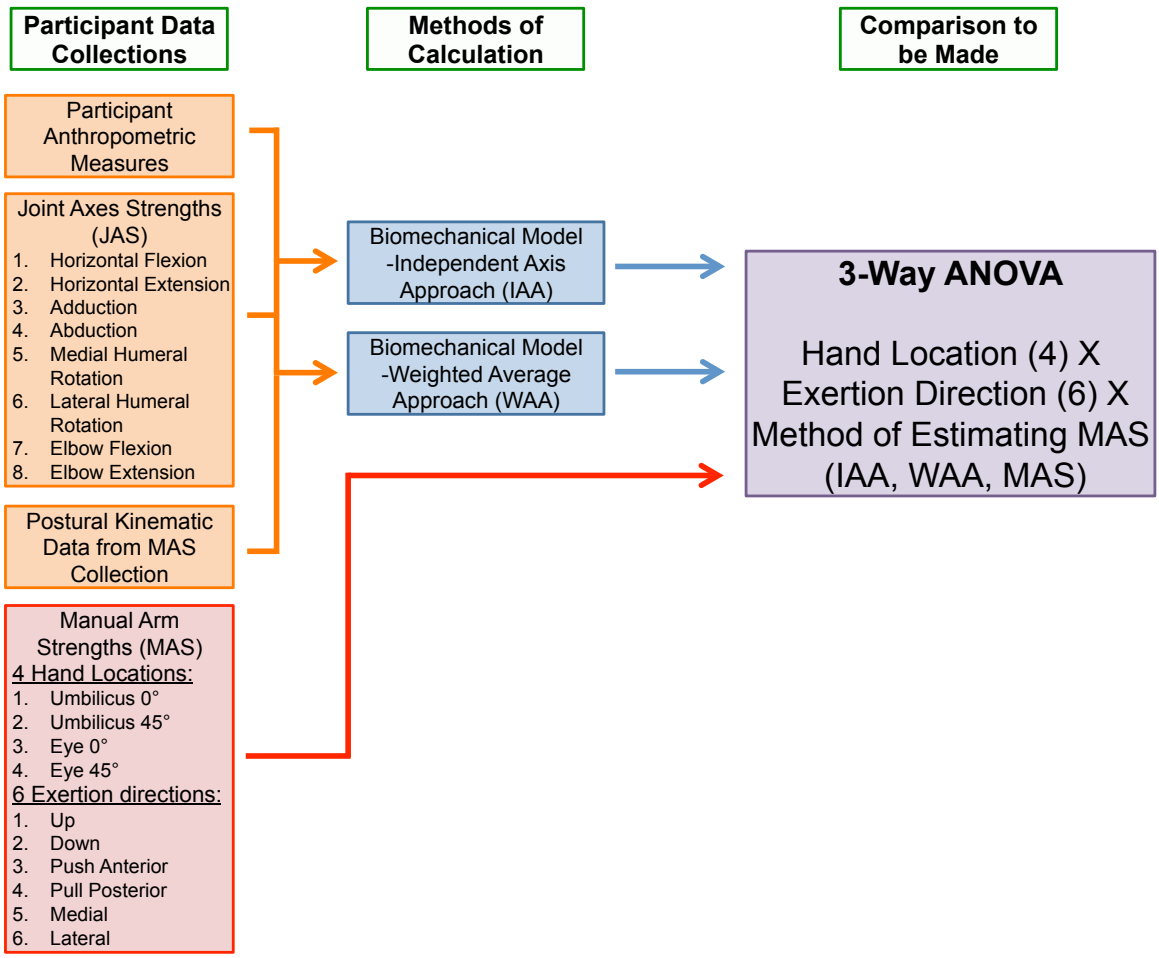

Figure 3.13: The outline of the study is presented. The orange boxes and arrows indicate inputs for the two developed biomechanical models (blue boxes) that calculated the predicted manual arm strengths (MAS) using the independent axis approach (IAA) and weighted average approach (WAA). These inputs included: 1) participant specific anthropometric measures, 2) the eight different joint axis strengths (JAS) that are collected, and 3) the postural kinematic data from the MAS collection. The predicted outputs from the two biomechanical models (as indicated by the blue arrow) were compared to each participant's MAS (as indicated by the red box and arrow) at every hand location (n = 4) and exertion direction (n = 6) through a 3-way ANOVA, as indicated by the purple box.

Chapter 4 – Results

4.1 – IAA Model Validation

My replication of the 3DSSPP software (IAA model) was tested using data from the "average" participant in terms of body weight, height, and JAS strength. This model performed very well, and was able to replicate the same calculations capable by 3DSSPP, with a very high level of accuracy. In terms of the peak hand load prediction for the average participant, the model explained 100% of the variance between values predicted by the model and 3DSSPP, with a RMSE of only 0.89 N (Figure 4.1). Further information in regards to the validation of the IAA model can be found in Appendix B.

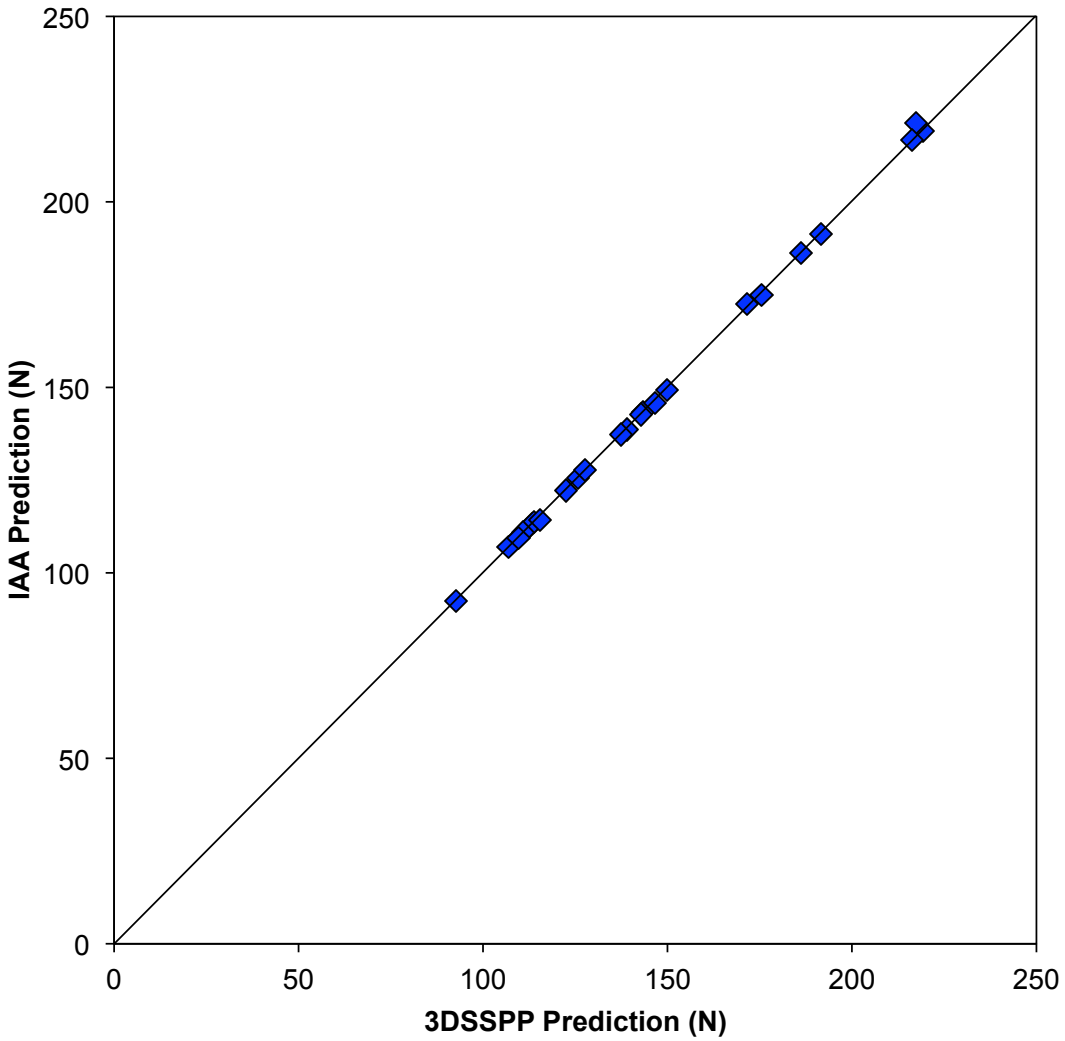

Figure 4.1: IAA model validation for maximum hand load, comparing the predicted peak hand loads from the IAA model and 3DSSPP for the average participant (n = 24 comparisons: 4 hand locations x 6 directions). The diagonal line represents a perfect prediction. The r^2 was 1.000 and the RMSE was 0.89 N.

4.2 – Mean Strength Data

4.2.1 – Manual Arm Strength

All of the individual resultant forces (N) for the MAS collection were averaged within each of the four hand locations and six exertion directions, and are presented in Table 4.1. Of the four different hand locations tested, on average, umbilicus 0° was the strongest location (146.72 ± 49.74 N), while eye 0° was the weakest location (116.98 ± 52.94 N). When looking at the six different exertion directions, on average the forward (push) direction was the strongest (180.61 + 48.89 N), while lateral humeral rotation was the weakest (91.55 ± 21.62 N).

Table 4.1: Mean MAS resultant forces (N) averaged within the four hand locations and the six exertion directions (n = 15). The associated standard deviation for each hand location and exertion direction combination is also presented. The overall means and standard deviations for hand locations and exertion directions are presented in the bottom row and the two most right columns, respectively.

	Eye - 0 deg		Eye - 45 deg		Umbil - 0 deg		Umbil - 60 deg		Overall	
Direction	Mean	SD	Mean	SD	Mean	SD	Mean	SD	Average	SD
Forward	189.70	50.14	169.63	42.59	213.20	43.30	149.92	26.37	180.61	46.89
Backward	127.19	41.66	133.02	41.20	155.94	45.48	120.09	40.84	134.06	43.42
Up	76.14	15.08	88.84	15.87	157.01	28.30	155.47	29.82	119.37	43.80
Down	141.25	42.70	145.39	31.19	154.59	17.46	156.96	23.19	149.55	30.10
Lateral	74.35	17.10	113.17	20.56	82.55	10.08	96.11	15.06	91.55	21.62
Medial	93.27	21.91	150.62	33.17	117.05	14.56	184.09	35.68	136.26	43.88
Overall	116.98	52.94	133.45	41.03	146.72	49.74	143.77	40.52	135.23	47.63

4.2.2 – Joint axis Strength

The individual peak moments (Nm) for the JAS collection have been averaged within each of the eight test postures and are presented in Table 4.2. The strongest posture was shoulder forward (63.04 ± 16.12 Nm), and the weakest test posture was lateral humeral rotation (17.52 ± 3.04 Nm). When comparing the collected JAS moments to those collected by Stobbe (1982), on average the moments from the current study were 124.9% of those from Stobbe (1982), and ranged between 88.0-161.2% of the Stobbe (1982) values.

Table 4.2: Mean JAS values averaged within the eight different test postures, and their associated standard deviations (n = 15). The Stobbe (1982) value (n = 32) for each posture is also presented, and a comparison to the mean value for each posture is made.

JAS	Mean	SD	Stobbe	Mean % of Stobbe
Elbow Extension	34.43	5.48	25.50	135.0%
Elbow Flexion	43.13	7.96	29.52	146.1%
Medial Rotation	24.95	6.31	21.44	116.4%
Lateral Rotation	17.52	3.04	19.90	88.0%
Shoulder Backward	39.88	7.60	34.02	117.2%
Shoulder Forward	63.04	16.12	39.09	161.2%
Shoulder Adduction	42.10	12.59	34.90	120.6%
Shoulder Abduction	42.48	11.52	36.95	115.0%
			Mean	124.9%

4.3 – Method Comparison (IAA & WAA vs. MAS)

4.3.1 – Primary Comparison

The primary purpose of my thesis was to allow for the most direct evaluation of the strength prediction method used by 3DSSPP (IAA), in terms of predicting the empirically collected MAS. The secondary purpose of this study was to also test if the WAA method would be a viable replacement for the IAA. As such a three-way repeated measures ANOVA was conducted, and revealed a significant three-way interaction between the method of force estimation, hand location, and direction of force application, $F(30, 420) = 11.41$, $p<0.0001$. For the purpose of this study, the primary concern is looking for any significant differences between the; 1) IAA and 2) WAA , and the empirically measured MAS. Post hoc testing using Tukey's honest significant difference (HSD) test revealed that, when comparing the IAA to the MAS, 15 out of the 24 means (4 hand locations x 6 exertion directions) where significantly different ($p<0.05$, max difference = 266.1 N) (Figure 4.2). When comparing the WAA to the MAS, 17 out of the 24 means were significantly different ($p<0.05$, max difference = 260.0 N) (Figure 4.2).

When looking at the six exertion directions at each of the four hand locations, across all 15 participants (n = 360 comparisons), the correlation between the IAA estimation and the empirically measured MAS was fairly low ($r = 0.42$). The IAA only explained 17.9% of the variance, with a large RMSE of 74.5 ± 68.2 N (Figure 4.3). Next,

examining the comparison between the WAA and the MAS data across all hand locations, exertion directions, and participants (n = 360 comparisons), the WAA did not fair that much better than the IAA. The correlation between the WAA and MAS was again low (r = 0.44), as the WAA only explained 19.1% of the variance, with a similarly large RMSE of 73.4 ± 60.6 N (Figure 4.4).

The absolute and relative RMSEs between the average predicted values by the IAA and WAA, and the empirically measured MAS values were also examined for the four hand locations and the six exertion directions. In terms of the four hand locations, the absolute RMSE ranged between 64.2-85.1 N and 61.2-87.9 N for the IAA vs. MAS and WAA vs. MAS, respectively (Figure 4.5). For the six exertion directions the absolute RMSEs for the six exertion directions, the values ranged between 36.5-92.4 N and 39.1-87.1 N for the IAA vs. MAS and WAA vs. MAS, respectively (Figure 4.6). The relative RMSEs for the four hand locations ranged between 45-60% and 41-57% for the IAA vs. MAS and WAA vs. MAS comparisons, respectively (Figure 4.7). Finally, the relative RMSEs for the six exertion directions ranged between 36-71% and 39-63%, for the IAA vs. MAS and WAA vs. MAS, respectively (Figure 4.8).

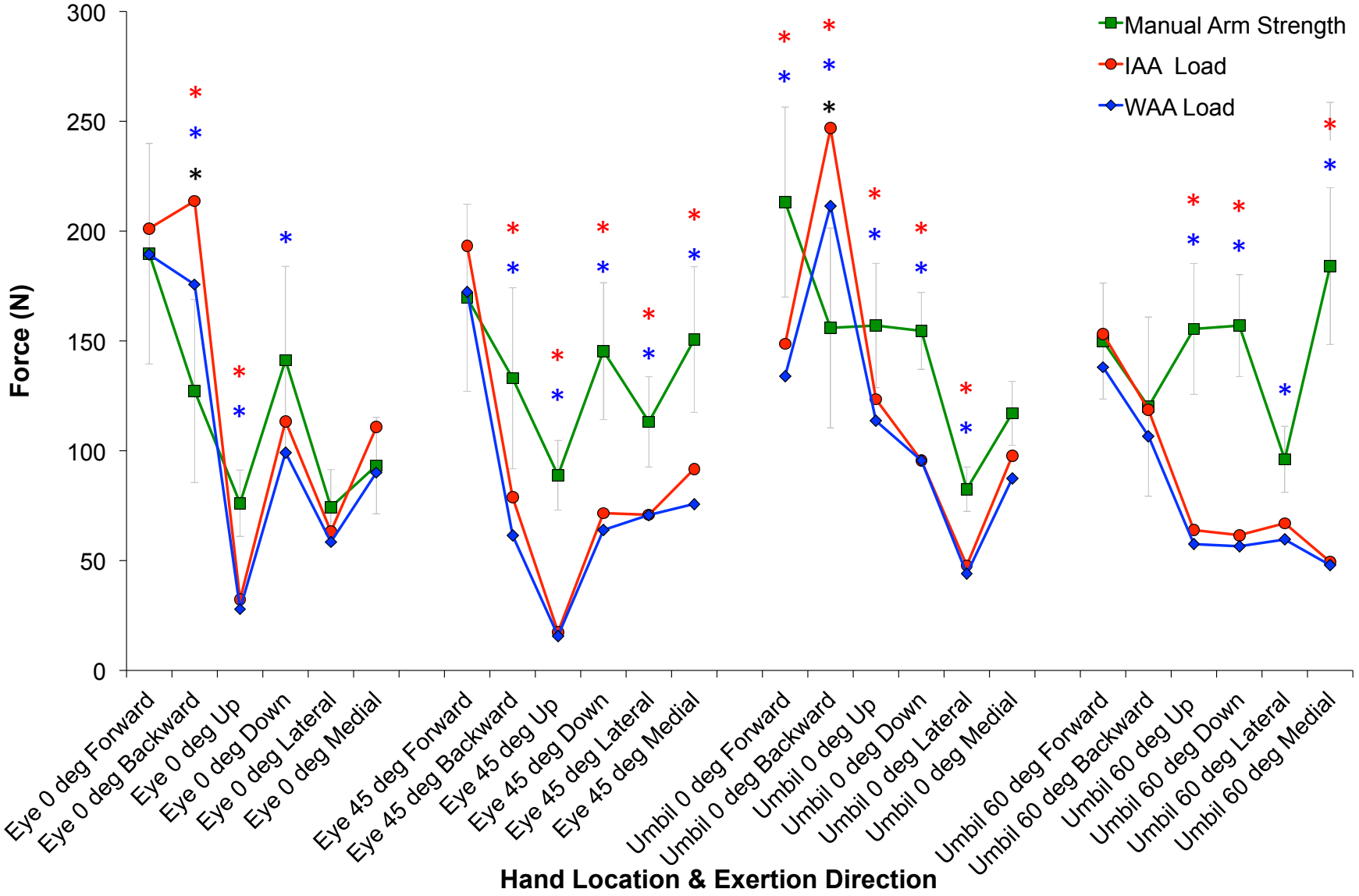

Figure 4.2: The significant three-way interaction between method of force estimation, hand location, and direction of force application, $F(30, 420) = 11.41$, $p<0.0001$. The X-axis shows the four different hand locations, and the six different exertion directions performed at each hand location. The Y-axis represents the force level (N) predicted (IAA or WAA) or measured (MAS). The red, blue, and black asterisks indicate post hoc significant differences between the IAA & MAS, WAA & MAS, and IAA & WAA means, respectively.

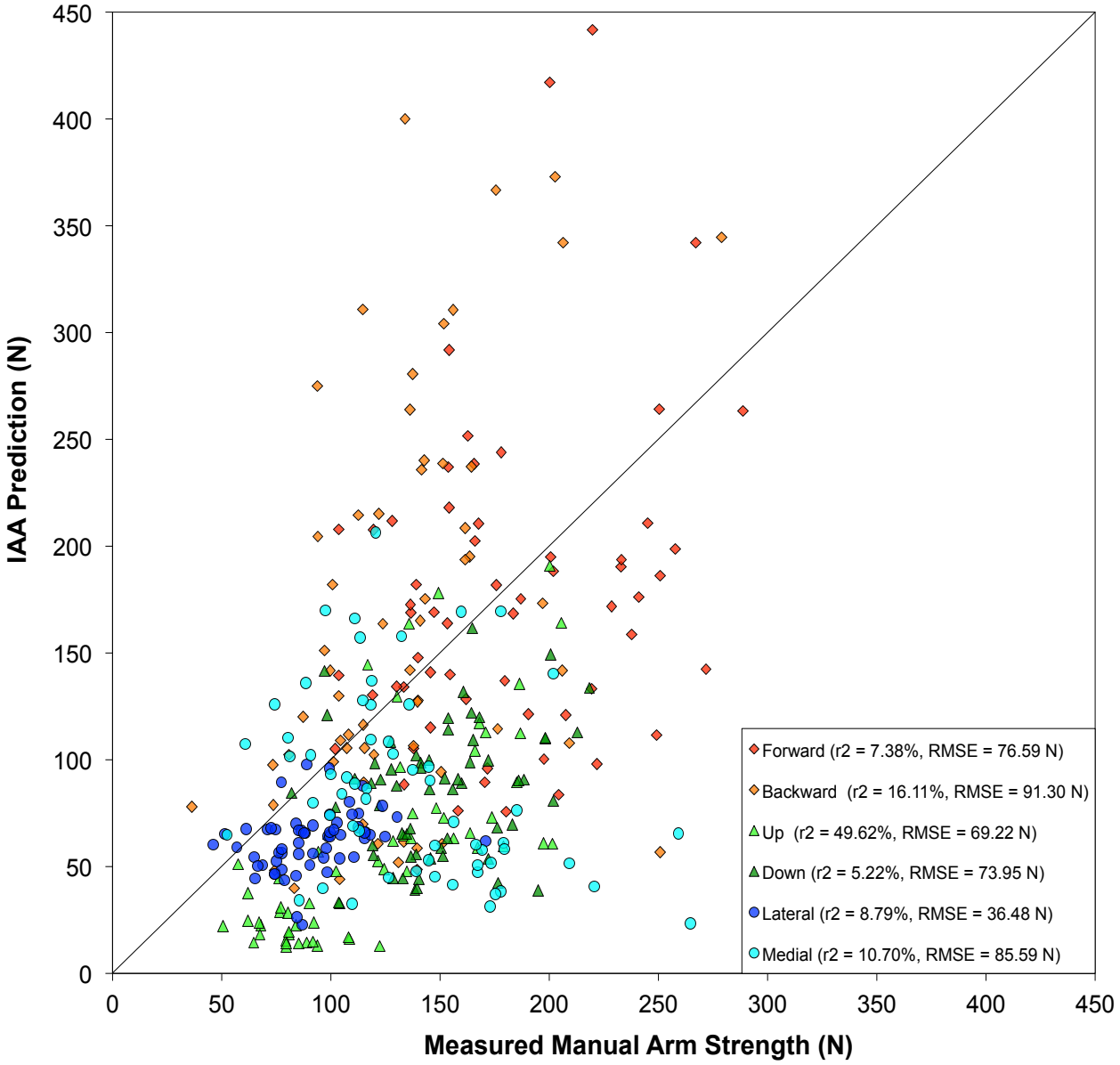

Figure 4.3: Correlation (r = 0.42) of the strength prediction by the IAA with the associated empirically measured MAS (n = 360 comparisons). The six different coloured markers represent the six different exertion directions. The X-axis and Y-axis represent the measured MAS (N) and predicted strength by the IAA (N), respectively. A line of perfect prediction runs diagonally across the graph. Any points falling on this line indicate that the IAA model has accurately predicted the MAS for that participant. Any values above the line indicate an over prediction by the IAA model, while values below this line indicate an under prediction of the MAS by the IAA. The RMSE for this correlation is 74.5 ± 68.2 N.

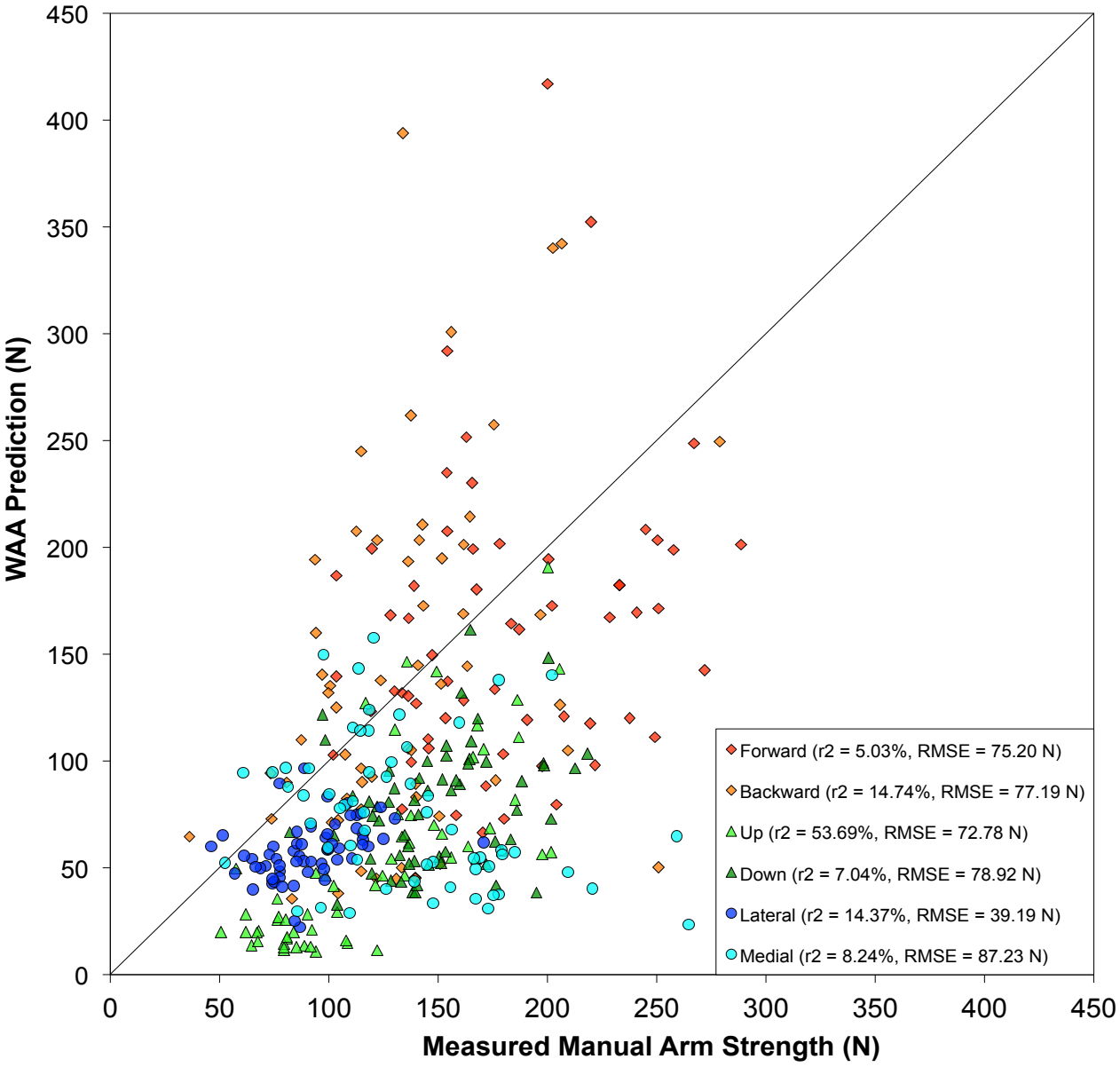

Figure 4.4: Correlation (r = 0.44) of the strength prediction by the WAA with the associated empirically measured MAS (n = 360 comparisons). The six different coloured markers represent the six different exertion directions. The X-axis and Y-axis represent the measured MAS (N) and predicted strength by the WAA (N), respectively. A line of perfect prediction runs diagonally across the graph. Any points falling on this line indicate that the WAA model has accurately predicted the MAS for that participant. Any values above the line indicate an over prediction by the WAA model, while values below this line indicate an under prediction of the MAS by the WAA . The RMSE for this correlation is 73.4 ± 60.6 N.

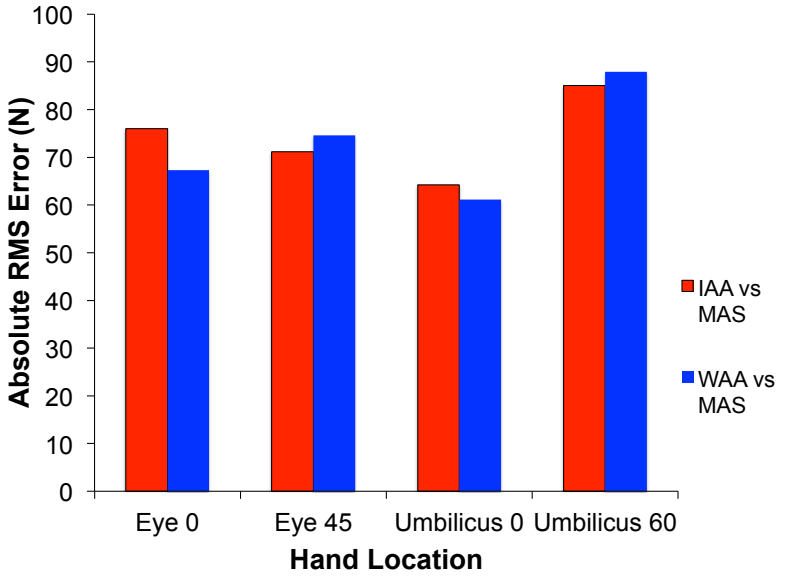

Figure 4.5: The absolute RMSE (N) (Y-axis) for the four different hand locations (X-axis) (n = 90 for each hand location). The different colour bars represent the IAA vs. MAS (red) and WAA vs. MAS (blue) comparisons.

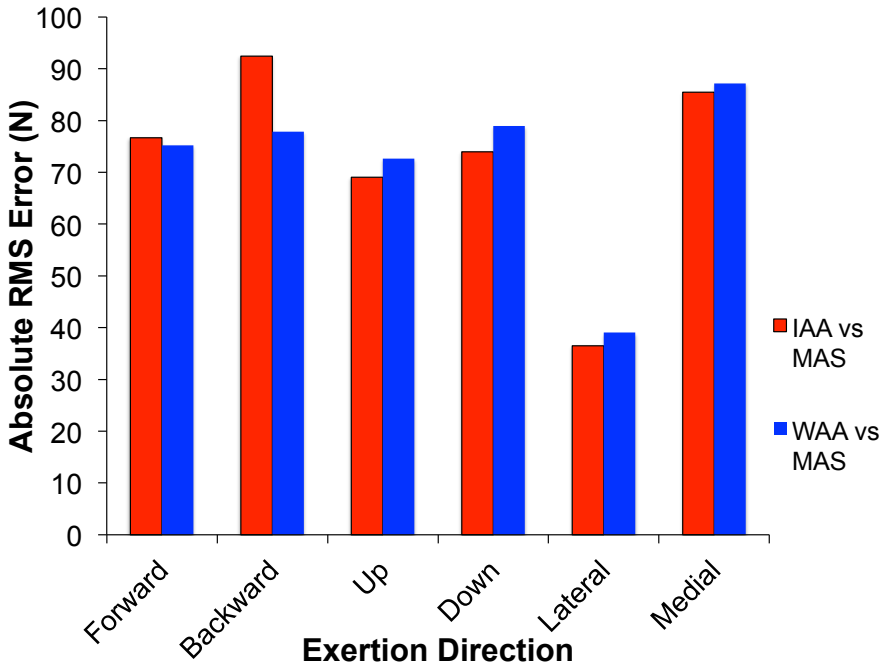

Figure 4.6: The absolute RMSE (N) (Y-axis) for the six different exertion directions (X-axis) (n = 60 for each direction). The different colour bars represent the IAA vs. MAS (red) and WAA vs. MAS (blue) comparisons.

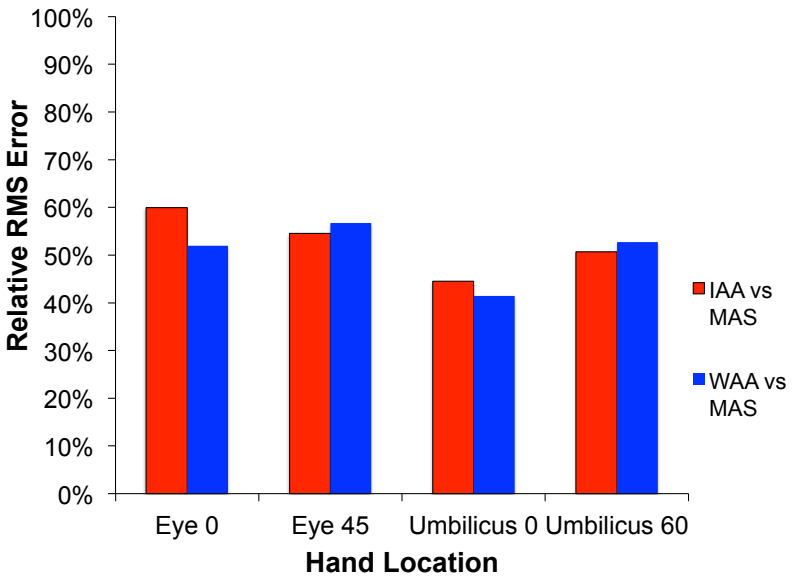

Figure 4.7: The relative RMSE (Y-axis) for the four different hand locations (X-axis) (n = 90 for each hand location). The different colour bars represent the IAA vs. MAS (red) and WAA vs. MAS (blue) comparisons.

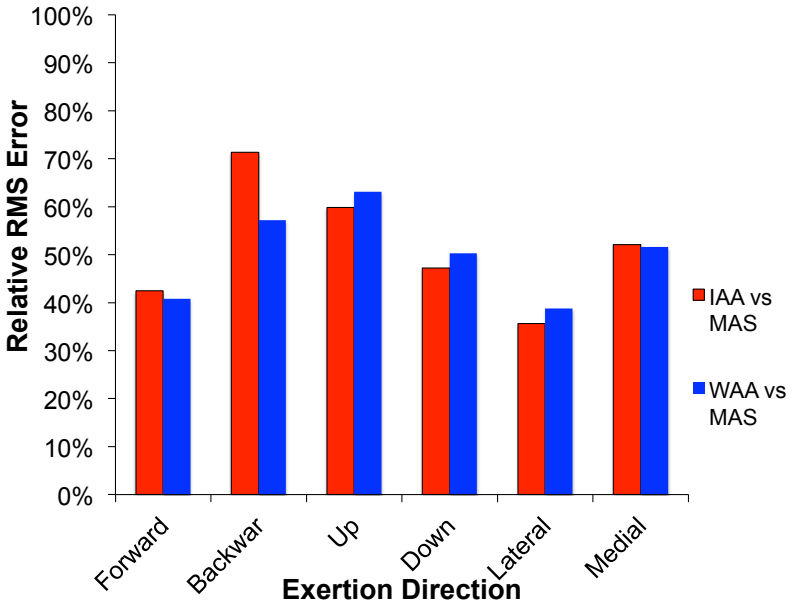

Figure 4.8: The relative RMSE (Y-axis) for the six different exertion directions (X-axis) (n = 60 for each direction). The different colour bars represent the IAA vs. MAS (red) and WAA vs. MAS (blue) comparisons.

4.3.2 – Limiting Strengths

The 3DSSPP (IAA) model, as it is currently designed, is able to predict which joint axis/direction limits the completion of a specific task given the posture of the arm (joint locations), and direction of force exertion. In this study, the limiting strengths were assessed to determine, on average, which strengths were limiting which tasks. Overall, lateral humeral rotation was the most limiting, as it was the limiting strength for 31.7% of the 360 trials evaluated. On the other hand, elbow flexion was the limiting strength for only 2.8% of trials (Figure 4.9). When pooling within the four different hand locations, it is evident that medial and lateral humeral rotations are the primary limiting strengths, as they combined to limit strength no less than 40.0% of the time (Figure 4.10). Similarly, examining the limiting strengths across the six exertion directions reveals that, when the humeral rotation strengths are combined, they limit the intended exertion at least 25.0% of the time (for the forward exertions), and up to a maximum of 74.0% of the time for the medial exertions (Figure 4.11).

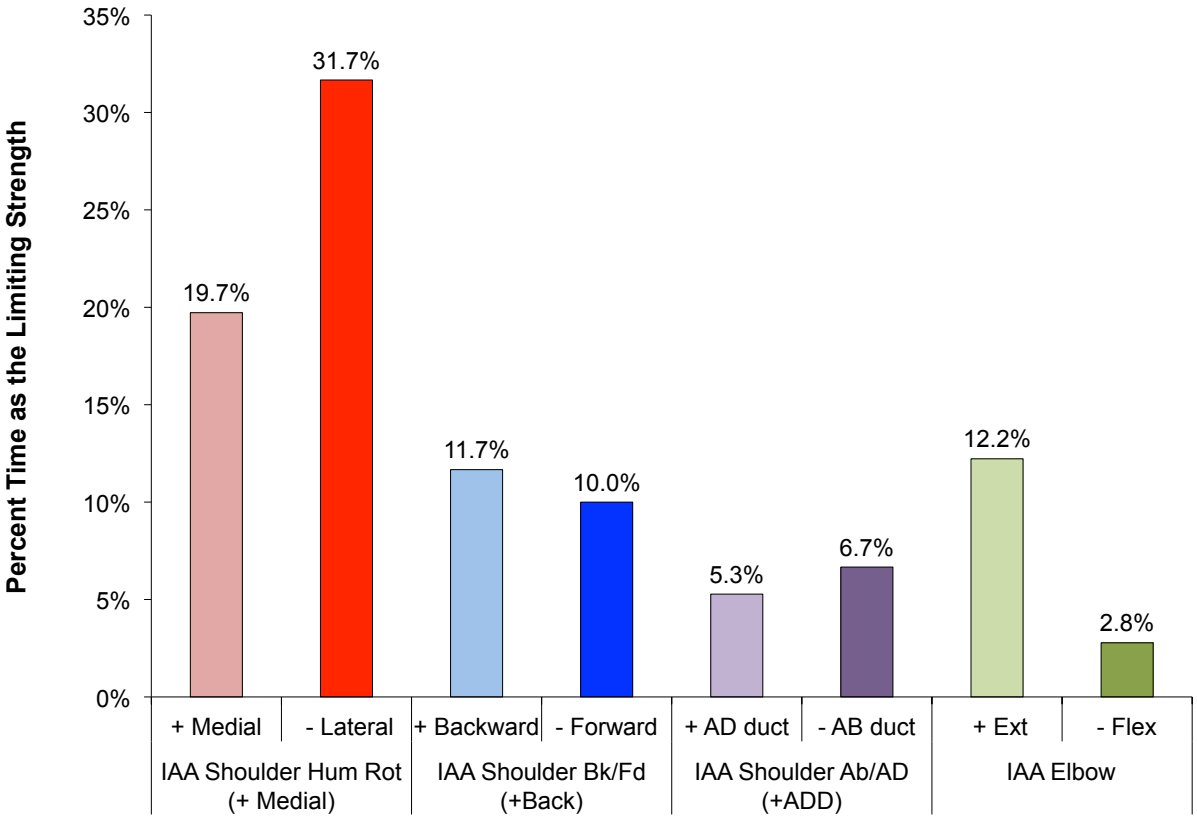

Figure 4.9: The percent of conditions that each joint axis limited strength (n = 360). The X-axis represents the eight different strengths present in 3DSSPP that pertain to the upper extremity, not including the wrist. The Y-axis represents the percentage of trials (n = 360) that each of the eight strengths were determined to be the limiting strength required to complete the exertion. The average percentage for each strength is provided above their respective bar.

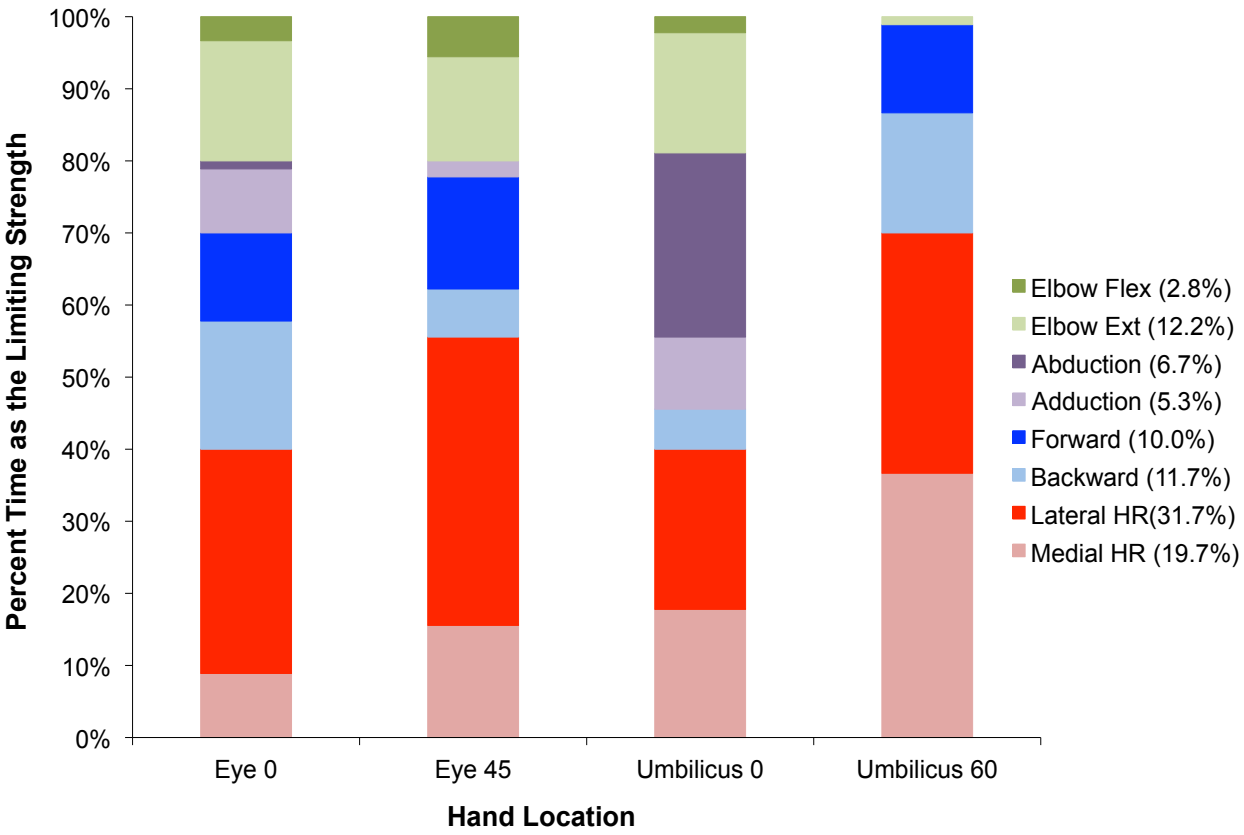

Figure 4.10: The percent of conditions that each joint axis limited strength for each of the four hand locations pooled across the six different exertion directions (n = 90 for each hand location) are presented. The four hand locations are listed along the X-axis, and listed along the Y-axis are the percentage of trials within each hand location (n = 90) that each of the eight strengths were determined to be the limiting strength required to complete the exertion. The eight different strengths are listed in the legend with their associated overall average limiting percentage (n = 360), as presented in Figure 4.9.

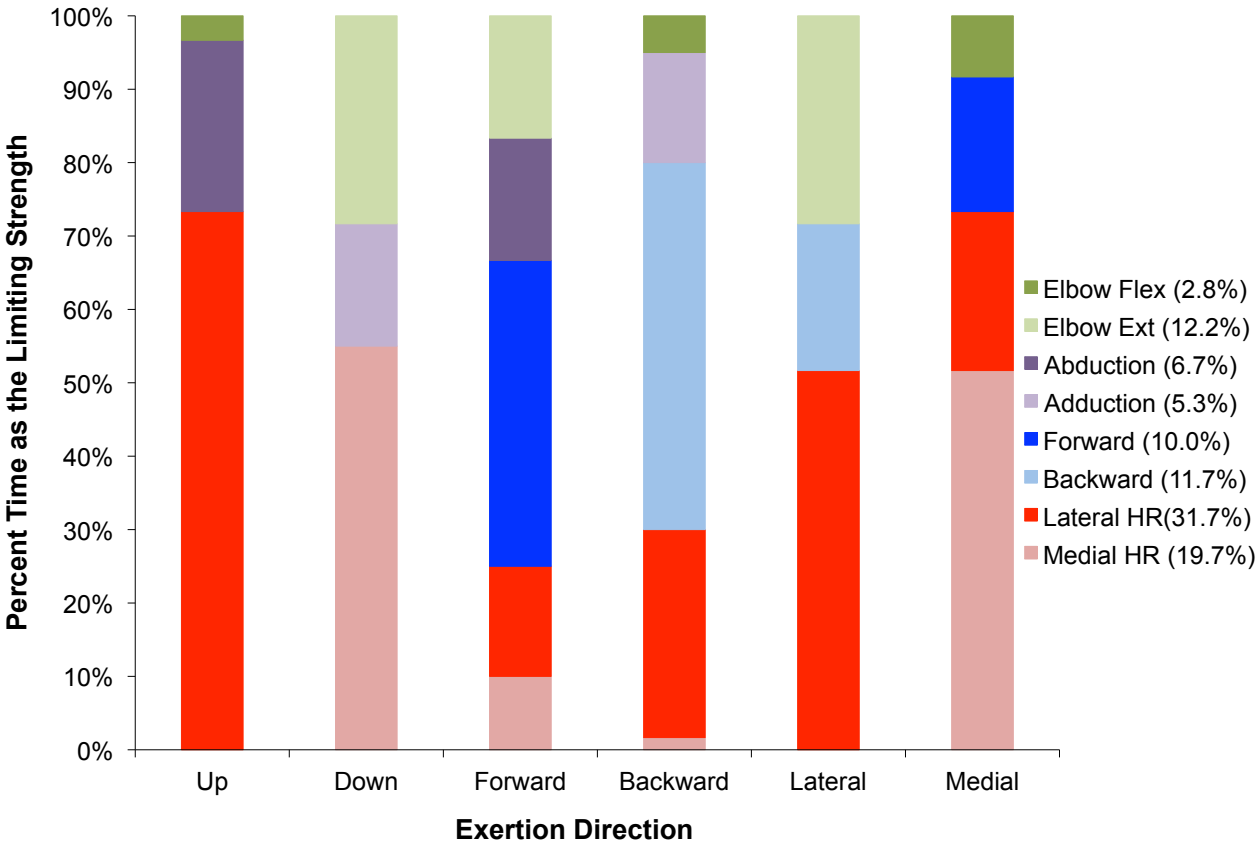

Figure 4.11: The percent of conditions that each joint axis limited strength for each of the six exertion directions pooled across the four different hand locations (n = 60 for each exertion direction) are presented. The six exertion directions are listed along the X-axis, and listed along the Y-axis are the percentage of trials within each exertion direction (n = 60) that each of the eight strengths were determined to be the limiting strength required to complete the exertion. The eight different strengths are listed in the legend with their associated overall average limiting percentage (n = 360), as presented in Figure 4.9.

4.3.3 – IAA/MAS & WAA/MAS Ratios

The resultant force levels that were predicted by the IAA and WAA methods were compared on a relative scale to the empirical MAS force levels by dividing the IAA or WAA predictions by the MAS value. This gave an indication as to whether the models were over or under predicting the correct MAS value. On average, the IAA predictions were 78.0% of the MAS values (e.g. IAA under predicted by 22.0%) (Figure 4.12). On average the WAA predictions were 69.4% of the MAS values (e.g. WAA under predicted by 30.6%) (Figure 4.12).

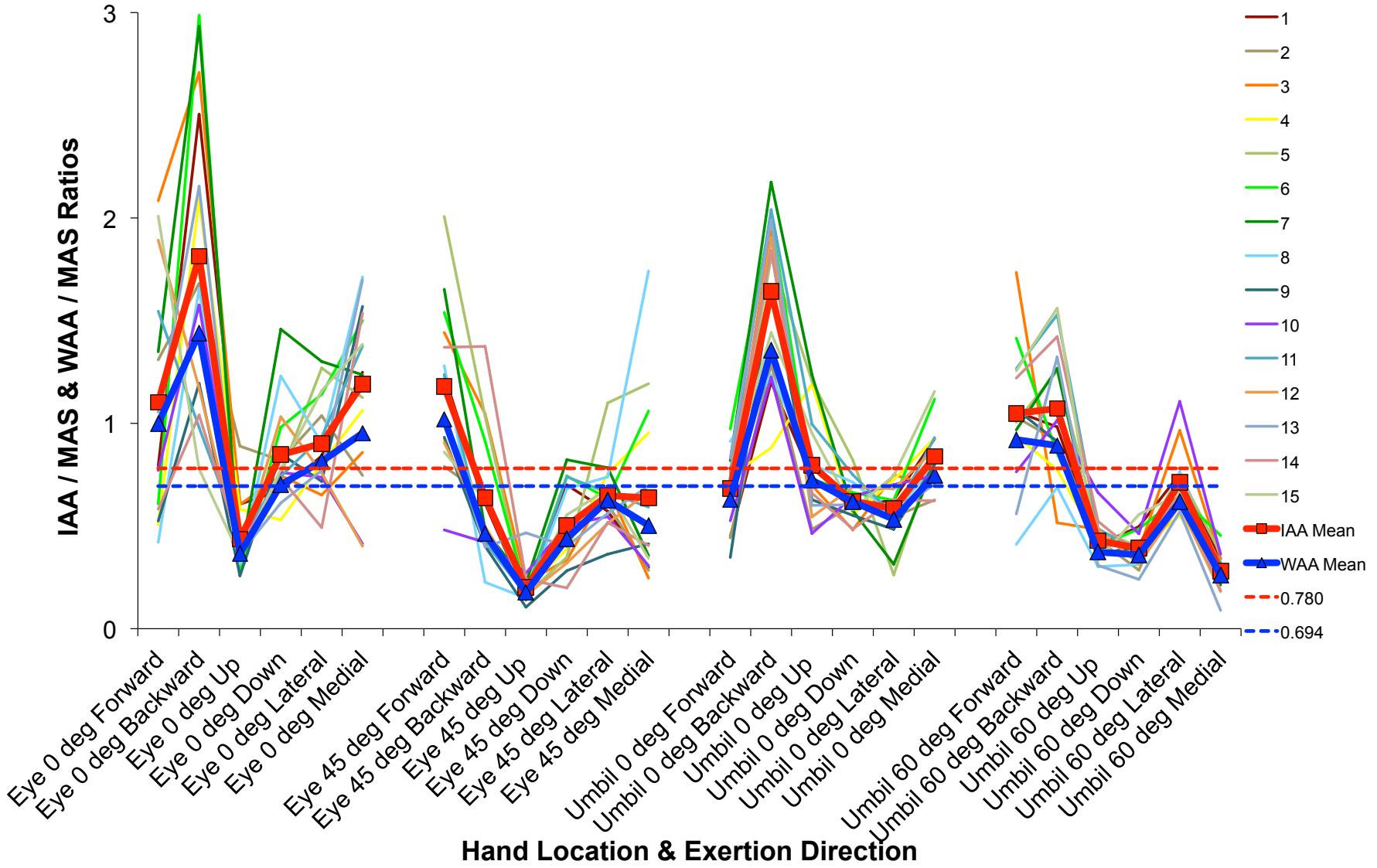

Figure 4.12: The ratio of the IAA prediction to measured MAS is presented for each participant at each hand location and exertion direction. In addition, the average ratio for the IAA and the WAA for each hand location and exertion direction (n = 15) are represented by the thick red line with the red squares (IAA) and the thick blue line with the blue triangles (WAA). The overall average ratio for the IAA:MAS and WAA:MAS were 0.780 and 0.694, respectively, and are represented by the dashed red and blue lines (n = 360).

4.4 – Strength Estimation Ignoring Humeral Rotation

As I determined that the humeral rotation strengths were the limiting factor for many of the tasks (51.4% of the time, when medial and lateral humeral rotation were combined), an additional comparison was run between the IAA and WAA models, and the empirically measured MAS, and it included only trials for which either medial or lateral humeral rotation were not the limiting strengths (n = 175 comparisons). Both the IAA and WAA methods saw a similar increase in their correlation with the MAS, by 5.1% and 6.5% increased correlation, respectively (Figure 4.13). Additionally, the unexplained variance decreased for both the IAA and WAA when the trials with the humeral rotation strengths were removed, by -2.4% and -3.3%, respectively. Both the IAA and WAA models, however, still had large unexplained variances overall of 79.5% and 77.6%, respectively (Figure 4.13). The biggest change with this comparison involved the change in the RMSE between the MAS and each model. The IAA saw only a 3.6% relative decrease in the RMSE, however, the WAA had a relative decrease of 13.3% in the RMSE, in comparison to the values for each when humeral rotation strengths were included. The absolute values, however, were still rather large with RMSEs of 71.6 N and 63.6 N for the IAA and WAA, respectively (Figure 4.13). All of these changes to the RMSEs, correlations, explained and unexplained variances due to the removal of the humeral rotation strengths for the IAA and WAA has been summarized in Table C1 in the Appendix.

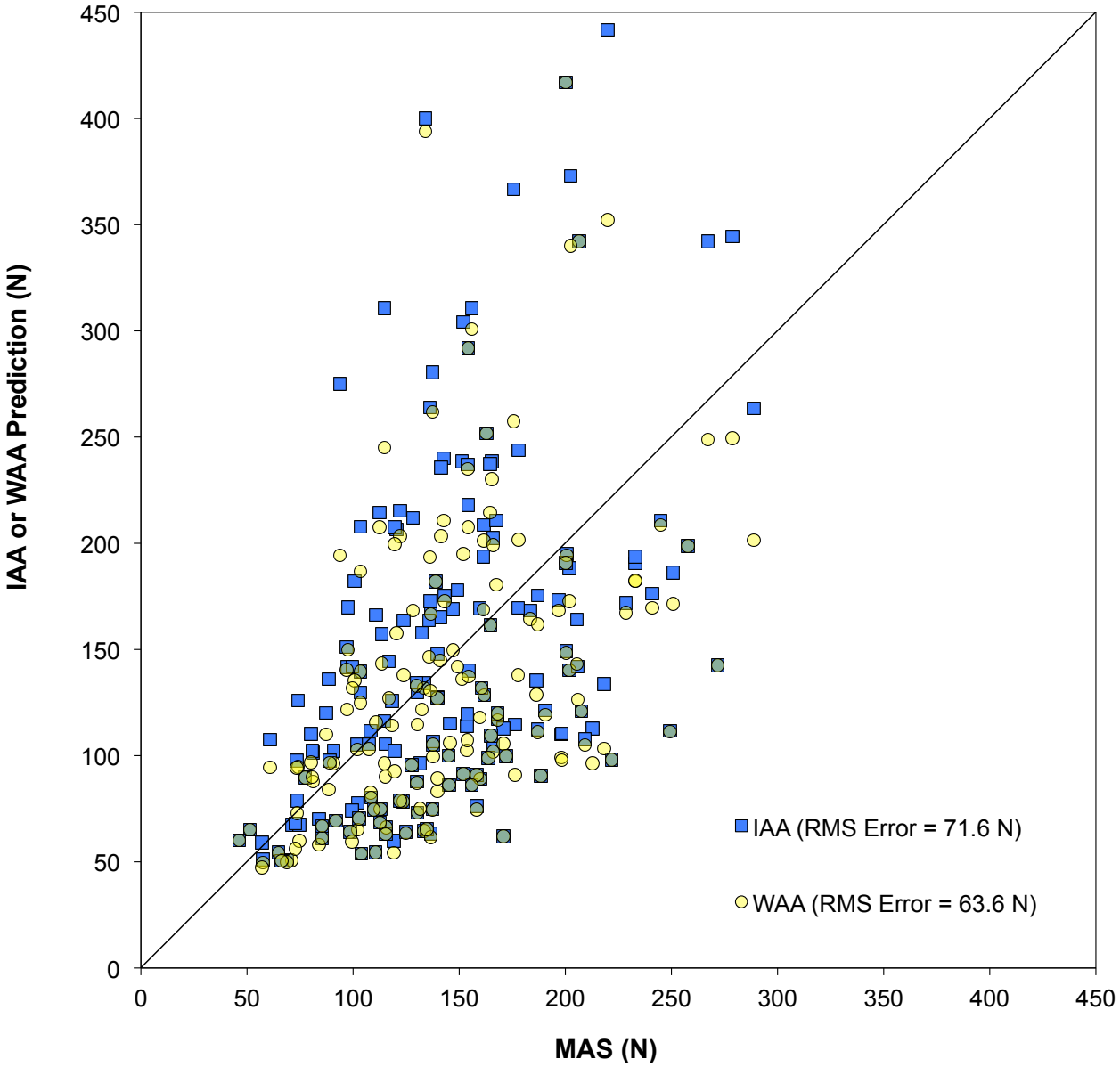

Figure 4.13: Correlation between the IAA & MAS (r = 0.45) and the WAA & MAS (r = 0.47) (n = 175 comparisons each) after removing trials for which humeral rotation was the limiting factor. The two different coloured markers represent the two different strength estimation models (IAA and WAA). The X-axis and Y-axis represent the measured MAS (N) and predicted strength by the IAA or WAA (N), respectively. A line of perfect prediction runs diagonally on the graph. Any points falling on this line indicate that the IAA or WAA model has accurately predicted the MAS for that participant. The RMSEs for the IAA and WAA correlations are 71.6 N and 63.6 N, respectively.

Chapter 5 – Discussion

The primary purpose of my thesis was to test the 3DSSPP model, and its use of the IAA, with participant specific joint locations and joint strengths. This afforded 3DSSPP the best chance to accurately predict each participant's manual arm strength. However, as hypothesized, the IAA performed very poorly when predicting the empirically measured MAS, as indicated by the significant three-way interaction. The post hoc tests showed that 15 out of the 24 means were significantly different between the IAA and MAS (Figure 4.2). The RMS error was 74.5 N and there was a maximum difference of 266.1 N (~59.7 lbs), which are ~100% and ~350% of Ford Motor Company's typical limit of 17 lbs (~75 N) for a one-armed effort. For ergonomists, who use 3DSSPP on a daily basis, these significant differences should be very alarming. Its important to remember that 3DSSPP is designed for populations, and makes strength predictions based on what the 50^{th} percentile female (for example) could do. My analysis, however, used the participant specific strengths, and made predictions based on what each individual could do. As such, these findings are more specific than what 3DSSPP would find but, even still, they indicate that the IAA was significantly different for approximately 60% of the trials.

The inaccuracy of 3DSSPP's prediction capability is very apparent when looking at the scatter plot for the IAA vs. MAS (Figure 4.3), which shows the large errors for a large proportion of the trials tested (n=360 comparisons). The IAA had an r^2 with the MAS of only 0.18, leaving 82.0% of the variance unexplained, with a large RMSE of 74.5 N (~16.7 lbs). La Delfa (2011) conducted a similar comparison (n = 264 comparisons), yielding a correlation of 0.305 and RMSE of 39 N (Figure 2.10) between the MAS and the 50% capable values produced by 3DSSPP. That comparison, however, used 3DSSPP with the pre-programed strength database. My study, used participant-specific strengths, which should have allowed 3DSSPP (IAA) to make more accurate predictions, however, the RMSE was almost double that found by La Delfa (2011). This truly shows how inaccurate the predictions by 3DSSPP (IAA) are.

The WAA was hypothesized as a possible replacement solution for the IAA, hence, the secondary purpose of my thesis was to also test the strength prediction accuracy of the WAA. However, the WAA was significantly different from the MAS for 17 out of the 24 conditions, which was actually two more than the IAA vs. MAS (Figure 4.2). Again there was a very large maximum difference (260.0 N). The correlation between

the WAA and MAS was 0.44 (Figure 4.4), leaving 80.9% of the variance unexplained with a large RMSE of 73.4 N (~16.5 lbs).

Overall, these results indicate that the independent axis approach is not accurate enough to be used as an effective proactive ergonomic tool. The premise of this approach is that it treats each axis (three at the shoulder and one at the elbow) as independent motors, even if some of the axes share various muscles. Particularly, the high degree of variability and large RMSE between the IAA and MAS, shown in both the present study and La Delfa (2011), are fairly definitive pieces of evidence that the IAA is not a suitable strength prediction tool for the upper extremity. In terms of the WAA, even though it is a more viable model from a physiological standpoint, it is not suitable to replace the IAA within 3DSSPP at this point in time, as it also performed very poorly in terms of predicting strength.

5.1 – Validation of Our 3DSSPP Replication Model

It is not possible to enter subject-strengths into 3DSSPP. Thus, we replicated the calculations of 3DSSPP related to joint angles, segment center of mass magnitude and location, joint strengths and joint moments. The validation process of the replicated calculations was fairy rigorous. Many different hand locations and joint angle postures were tested. Since the only inputs into the model could be: 1) the X, Y, Z joint centre locations, and 2) the eight JAS for each participant, validation of the model compared to 3DSSPP was essential. The outputs from the replicate model and 3DSSPP, for peak hand load (N), joint angles (degrees), and joint strengths (Nm), were compared for the 24 average conditions that I tested in my study (Figures 4.1, and Figures B.1 & B.2 in the Appendix). These 24 conditions, however, were not the only conditions tested to validate the IAA model. It was also tested in an additional 26 different conditions, all with unique hand location and exertion direction combinations. The results from that validation, were almost identical to those presented (Figure 4.1, and Figures B.1 & B.2 in the Appendix): the model accounted for 100% of the variance, with an RMSE of almost 0 N. The results from these 50 separate tests gave a high degree of confidence that our 3DSSPP replica was able to accurately predict the necessary outputs, just the same as 3DSSPP would predict them, with the added ability to enter specific strength values. Further information, in regards to the design of the replica model and its validation, can be found in the section B.1 of the appendix.

5.2 – Limiting Strengths

Beyond the main manual arm strength prediction, I was also interested in what the IAA predicted the limiting joint strengths to be. The JAS, that primarily limited tasks, were the lateral (31.7%) and medial (19.7%) humeral rotation strengths (total of 51.4% of the 360 trials) (Figure 4.9). This result, however, is not really that surprising. When examining the JAS strengths (table 4.2), the average humeral rotation strengths (lateral and medial) were only 56.5% and 57.7% of the forward/backward and abduction/adduction strengths, respectively. These values were determined by taking the average of the medial and lateral humeral rotations, and dividing it by the average of the forward/backward strengths and the abduction/adduction strengths. This is the reason why the forward (11.7%) and backward (10.0%) strengths only limited a combined total of 21.7% of the trials, and the adduction (5.3%) and abduction (6.7%) strengths combined to limit only 12.0% of the trials (n=360). When examining the elbow strengths, on average the humeral strengths were only 75.1% as strong as the elbow strengths. Similar to forward/backward and adduction/abduction, elbow flexion (2.8%) and elbow extension (12.2%) combined to limit only 15.0% of tasks, on average.

Of the six different exertion directions (Figure 4.11), the humeral rotation strengths often were the ones which most frequently limited a task (e.g. up and down). Often, when completing up and down exertions, participants would assume a posture similar to that shown in Figure 5.1. When performing an up exertion in this posture, for example, the individual must abduct the shoulder while laterally rotating the humerus. Since there is a large moment arm, as the point of force application at the hand is far from the shoulder and distal to the elbow, lateral humeral rotation strength becomes increasingly important to maintain the required arm posture to perform the exertion. While performing an up exertion, there is a tendency for the humerus to rotate medially, as a counter moment is created by the vertically oriented handle on the forearm in a direction opposite of the intended exertion. This is why lateral humeral rotation is important to maintain the required posture, as it must oppose this counter moment. Since lateral humeral rotation is only 54% of the abduction strength, eventually the exertion fails once the lateral humeral rotation strength reaches its maximum, while the abduction strength may only be ~50% of its peak strength. This is why the model determines lateral humeral rotation to be the limiting strength for this exertion.

This same kind of thought process can be applied to the down, lateral, and medial exertions (Figure 4.11). In terms of the forward and backward exertion directions,

these are primarily limited by the forward and backward shoulder JAS, respectively. A probable reason for this is that these exertion directions are more directly in line with the shoulder in comparison to the four other directions. As such, when completing the exertion at the hand, the forces translate directly through the shoulder such that the moments created at the hand on the arm require strength levels from the other six strengths that are less than the peak forward/backward strengths to maintain the desired arm posture.

The limiting strengths were also examined at each of the four hand locations (Figure 4.10). The combined limitation attributed to the humeral rotation strengths ranged from ~40% to ~70% of trials for each hand location (n=90). The most interesting finding was that for the eye 0° and umbilicus 0° hand locations, humeral rotation strengths combined to limit ~40% of the trials. When participants moved to the greater sagittal shoulder angle postures, eye 45° and umbilicus 60°, the humeral rotation strengths combined to limit ~55% and ~70% of trials, respectively. This is most likely due to the posture required by the arm to be in this hand location; somewhat similar to Figure 5.1. These hand locations generally required the arm to be in a more abducted position, with a bent elbow, and extended forearm, in comparison to the two 0° hand locations. As mentioned, when the arm applies a force at the hand on the handle, a counter moment on the forearm is created in opposition of the direction of force application. When the arm is in this abducted/extended posture (as described above), a large moment arm is created, hence, why the humeral rotation strengths play a key roll in maintaining the posture, as they must oppose the large counter moments.

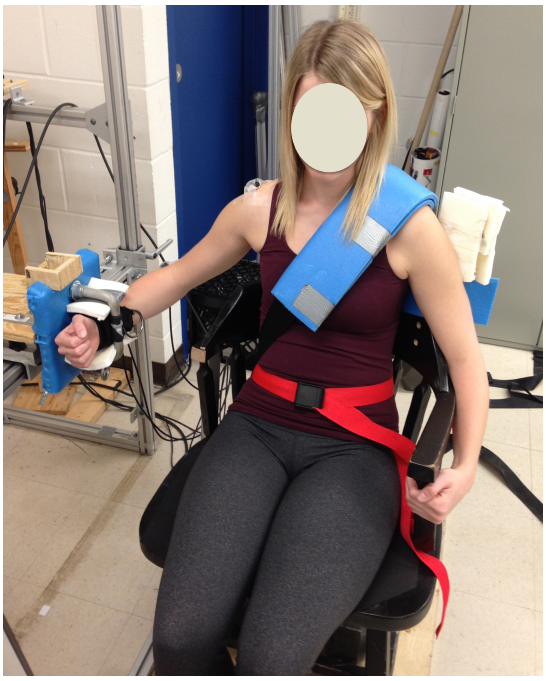

Figure 5.1: The umbilicus 60° hand location is shown. This and the eye 45° hand locations, both elicited this abducted and extended arm posture. This creates a large moment arm from the hand to the shoulder, which emphasizes the importance of the humeral rotation strengths to maintain the arm posture during certain exertions.

5.3 – Poor Performance of the Strength Prediction Models

The IAA and WAA performed poorly in terms of accurately predicting the empirical MAS. The significant differences shown in the post hoc tests, and the poor correlations accompanied by large RMSEs between each model and the empirical MAS values, are fairly definitive pieces of evidence in regards to the poor performance of both the IAA and WAA. This is the most important finding of this study, however, some insight can be provided regarding why 3DSSPP, with its IAA model, and the WAA were not accurate in terms of predicting strength.

5.3.1 – Poor Performance of the IAA

Prior to data analysis, it was expected that the IAA would perform poorly, based on past evidence by La Delfa (2011) and Chaffin & Erig (1991). After completing this study, there are several possible explanations of why the IAA is an inaccurate strength prediction tool. First, it became apparent that, when creating the IAA model, there was an inherent mistake in 3DSSPP in terms of the JAS input for lateral humeral rotation. All of the JAS within 3DSSPP come directly from Stobbe's (1982) thesis, and all but the lateral humeral rotation strength seems to have been entered correctly. According to Stobbe (1982), the

lateral humeral rotation strength should be 19.9 Nm (Table 4.2), however, this strength has been entered as 57.0 Nm (Figure 5.2) in 3DSSPP. These JAS strengths are specific to the posture in which Stobbe (1982) tested his participants. If the 57 Nm strength was, in fact correct, it would have been the strongest strength measured by Stobbe (1982), as it would be over 45% greater than the next strongest strength (Forward: 39.09 Nm – Table 4.2). The reality is, however, that lateral humeral rotation was the weakest strength measured by Stobbe (1982).

My thesis used the 3DSSPP algorithms (with the IAA) using a participant-specific JAS database, opposed to the population JAS database from Stobbe (1982). The average lateral humeral rotation JAS was 17.52 Nm (Table 4.2). This value is only 30.7% of the value entered into 3DSSPP (57 Nm), however, it is 88% of the correct Stobbe (1982) value (Table 4.2). Since 3DSSPP has never had a realistic value within the model, it is likely that the program's creators have never noticed this issue. If a more realistic value were present in the model, lateral humeral rotation would be a limiting strength much more frequently, as seen in my thesis, and most likely would have drawn some attention from the end users. The affects of this mistake are that 3DSSPP allows other strengths to continue to increase, even though lateral humeral rotation strength has probably passed its peak value. Eventually, this could potentially lead to an over prediction of the hand load in many cases, which was noted by both La Delfa (2011) and Chaffin & Erig (1991). In my thesis, however, I noticed the exact opposite, as the IAA tended to under predict strength on average by 22% (Figure 4.12). This result is most likely partly due to this correction in lateral humeral rotation.

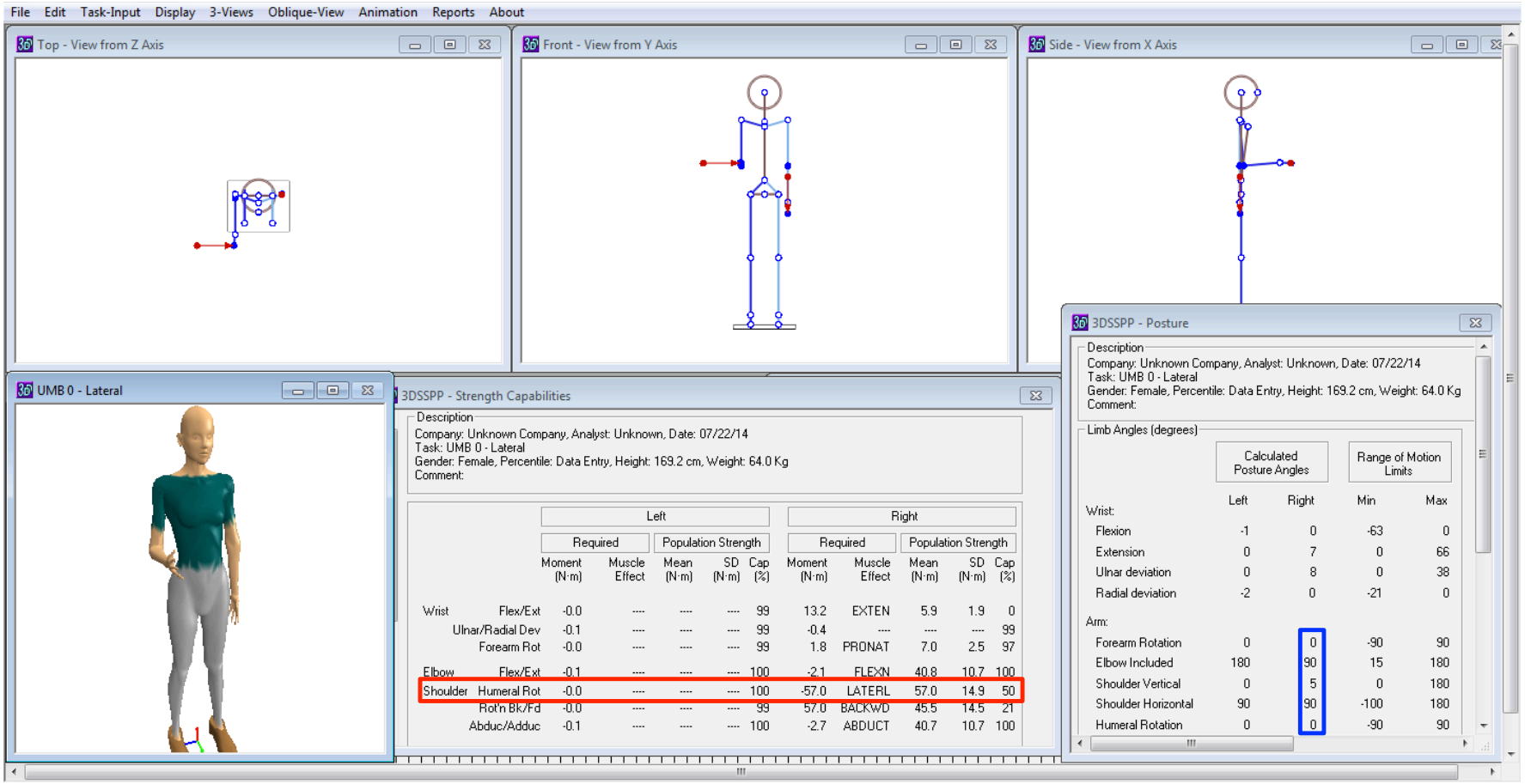

Figure 5.2: The programing error within 3DSSPP for the lateral humeral rotation strength is shown. The manikin has be positioned into the correct Stobbe (1982) test posture for lateral humeral rotation, as indicated by the blue box. The red box highlights how the max strength for this posture is 57 Nm for the 50th percentile female. This lateral humeral rotation strength should be 19.9 Nm (Table 4.2), as measured by Stobbe (1982).

Another possible reason why 3DSSPP performed poorly is how its equations (Figures B.3-B.11 in the Appendix) predict strength. They use a variety of inputs including: 1) an anchor point strength (the Stobbe JAS value), and 2) 2-3 different joint angle inputs (Table B.1 in Appendix). The JAS (anchor point strengths) were only measured in one specifically defined posture for each of the eight strengths. This is a very important point, as this is one of the reasons that 3DSSPP (IAA model) has resulted in large inaccuracies in terms of hand force prediction. The joint angle corrections, that are present in each equation, modify the JAS anchor point strength (from Stobbe) by either subtracting or adding to the value. These joint angle corrections were developed by Schanne (1972), and were explained in section 2.1. Next, the IAA takes the resultant of the involved strengths, and the user then iterates the loads up until the maximum strength for one of the axes is reached. This load is then considered to be the manual arm strength. The problem with this approach is that the shoulder is a very complicated structure, and cannot be simplified effectively using the IAA (Figure 4.3).

It is interesting to note that, depending on the selected input values, certain strength equations within 3DSSPP can actually predict a negative strength value. For example, medial humeral rotation is dependent on the horizontal shoulder and humeral rotation angles (Table B.1 in the Appendix). If the horizontal shoulder angle is locked at the minimum range of motion (ROM) value of -100° (ROM = -100° to 180°), and then the humeral rotation is manipulated throughout its entire allowable ROM within 3DSSPP, the equation predicts a negative medial humeral rotation strength at all points (Figure B.4 in the Appendix). In 3DSSPP, the equation for lateral humeral rotation is also capable of predicting a strength that is close to zero using input joint angle values within the ROM limits within 3DSSPP (Figure B.4 & B.5 in the Appendix). These very low, or even negative, strength predictions, in combination with the aforementioned programming error, serve to contribute as additional issues with the 3DSSPP. These problems are additive to the issue surrounding the IAA method of modeling, specifically in regards to complex structures such as the shoulder. Taken together, these issues lead to the numerous inaccurate hand load predictions made by the model.

5.3.2 – Poor Performance of the WAA

In theory, based on previous evidence (Makhsous et al. 1999; Holzbaur et al. 2005) that was adapted by Hodder & Potvin (2014), the WAA was hypothesized to be a physiological valid new approach to predicting strength, such that it could potentially replace the IAA currently present in several proactive ergonomics tools. However, in my study, the predictions made by the WAA were not much more accurate that those made by the IAA. In fact, there was a significant difference between the MAS and that predicted with the WAA, for 17 of 24 conditions; two more means than the IAA vs. MAS. Additionally, both models (IAA & WAA) had similar correlations and large RMSEs when compared to the empirical MAS values (Figures 4.3 & 4.4).

These results all suggest that simply changing the calculation approach from the IAA to the WAA, within 3DSSPP, will not solve the high strength prediction errors of 3DSSPP. A possible explanation for the WAA's poor performance is that the WAA is mathematically designed such that it can never predict a strength greater than the IAA. The overall mathematical process for both the IAA and WAA was outlined in full detail in Chapters 1 and 2 (Figures 1.3, 1.4, & 2.17). Previous literature (Chaffin & Erig, 1991; La Delfa 2011) noted that 3DSSPP (IAA) tends to over predict strength. As such, I assumed that the WAA would predict strengths closer to the MAS, since the WAA prediction is always less than that of the IAA. But, since the IAA tended to under predict strength by and average ~22% in my study, the WAA also tended to under predicted strength by even more (average of ~31%, Figure 4.12). As such, the WAA performed quite poorly, even though it was hypothesized to be more accurate than the IAA.

This issue ultimately relates back to the problem of the poor strength predictions for each individual axis. Since it became apparent, from my Results, that there is a major issue with the humeral rotation strength predictions within 3DSSPP, I decided to to perform a subsequent analysis to determine the correlation and RMSE between the prediction models and the MAS values for all trials that were not limited by either medial or lateral humeral rotation (n=175). When comparing the results of this analysis to the original, which included all trials (n=360), there was a slight improvement in the correlation values for both the IAA vs. MAS and WAA vs. MAS of 5.1% and 6.5%, respectively (Figure 4.13). Both models, however, still left over 77% of the variance

unexplained. However, when examining the RMSEs between each model and the MAS value, there was a 13.3% decrease in the RMSE for the WAA, while the IAA RMSE stayed almost the same as that with all 360 trials (Figure 4.3). This 13.3% decrease still resulted in a large RMSE of 63.6 N (~14.3 lbs), which is ~84% of the Ford one-armed effort limit of 17 lbs.

Ultimately, there are too many inaccurate predictions made by both 3DSSPP (IAA) and the WAA, as indicated by the large RMSEs and low explained variances. For an ergonomist to make an informed decision on whether or not a task is acceptable, they require a tool that is capable of providing them with an accurate answer that is within a reasonable error range. The fact that both the IAA and WAA still had RMSEs that were similar to the maximum force limit of 17 lbs set by Ford, even when trials limited by humeral rotation strength were removed, indicates that either model could both over or under predict strength by an unacceptable magnitude. Neither under predicting, nor over predicting, strength are acceptable practices in the field of ergonomics, as it will either cost the company a large amount of money in terms of decreased production or increased injury claims (and human suffering).

5.4 – Limitations

5.4.1 – Kinematics

A potential limitation of the study is the accuracy of the kinematics system that was used. For simplicity sake, the Fastrak electromagnetic system (Polhemus, Colchester, VT.) was used over an infrared motion capture system. This system allowed for an easier setup protocol to ensure that testing sessions lasted a reasonable length of time. This system was used to track the various joint centre locations of the shoulder, elbow, wrist, and hand. The sensors, that were placed on each of the joint centres (shoulder, elbow, wrist, and hand) are electromagnets, whose location could be traced relative to the electromagnetic source, which was placed in a fixed position posterior to the participant's right shoulder. The limitation in this system is that it is somewhat susceptible to interference by metal objects, as they affect the electromagnetic field. During all trials, a display of the markers location was provided in real time on a separate feedback screen was visible to myself. If I noticed any erratic behavior or dropout by the markers, the trial would be re-collected immediately. Although, sometimes it was difficult to monitor this

during each trial, as several different pieces of information were being displayed that required attention, such as the force output level and the direction of the exertion.

In addition, a potential limitation exists in regards to determining the joint centres using the Fastrak markers. Since each of the four markers had to be placed superficially on the skin, each of the four joint centres had to be estimated using a series of vectors, as described in section 3.4.1. Like any estimation, there is always some inherent error present, and this case was no different. It is very likely that there are slight errors for each joint centre location, which can affect the calculated joint angles and moment arms of the resultant hand force vector. It is unlikely, however, that these small errors would translate into major significant changes in the hand loads predicted by the IAA and WAA. Overall, I made my best effort to accurately estimate the joint centre location. Also, every trial (n=360) was visually examined during post processing, checking to see if the joint angles and overall arm posture looked reasonable for each condition. In total, the hand load outputs from only 7 of the 360 trials (~2%) were replaced due to what was deemed suspect kinematics. This was done using a standard data replacement technique.

5.4.2 – Eye 0° Hand Location

The four hand locations were chosen with the intent of populating a large reach envelope, such that a rigorous test of the IAA and WAA could be performed. Out of the four, the eye 0° hand location proved to be the most difficult in terms of setup, as it was in a somewhat awkward location relative to the participant. For this hand location, the vertically oriented handle was positioned such that it was as close to inline with the right shoulder as possible. This position, in combination with the high handle height, meant that the method of coupling the participant's wrist to the handle had to be varied for each exertion, in comparison to the other three hand locations. Section 3.2.2 contains a detailed description of the different coupling techniques. Since the hand had to be moved around when the coupling technique changed, during post processing, it was noticed that there was a larger variability in the eye 0° hand location then originally intended. As such, the hand location ranged from a shoulder 0° to overhead 0° hand location, instead of maintaining the eye 0° location. Additionally, because of the required position of the hand, this forced participants into an awkward posture, to allow them to complete the intended exertion. It is possible that the variability from trial-to-trial, and the induced

postures for the eye 0° hand location may have led to some awkward types of exertions that participants are not used to. As such, this may have resulted in them not giving their true 100% maximum effort. However, every attempt was made to ensure that participants were comfortable during each exertion. It is important to note the intended hand locations studied were not essential to predicting strength, as only the kinematic data and JAS were used in the IAA and WAA. As such, when participants did feel like their arm was awkwardly postured, slight corrections to their body position relative to the vertical handle were made. Often, this would take them out of the true "eye 0°" hand location, however, it allowed them to be in a more comfortable position, which hopefully reduced any awkwardness, and led to true maximum 100% exertions. In either case, the Fastrak would have captured the specific posture and hand location they used, so that a fair comparison could be made between the MAS and 3DSSPP.

5.4.3 – The Wrist

It was decided that, for simplicity sake, wrist strength would be excluded from this study, such that only shoulder and elbow strength were to be included in the models. 3DSSPP, however, does account for the wrist strength, and is able to incorporate this into the model to predict max hand loads and joint strength capabilities of the entire arm, including the wrist. It is probable that, if the wrist strength had been included in the IAA model, there would have been a variation in the strengths and hand loads that were measured and predicted. The accuracy of these predictions relative to the MAS values, however, probably would not have increased. In fact, by adding the three degrees of freedom at the wrist to the current four degrees of freedom (three shoulder, one elbow) within the IAA and WAA models, it is likely that the accuracy of the predictions would have decreased even further. This is due to the fact that 3DSSPP assumes the strength about one wrist axis would be unaffected by moment demands about the other two wrist axes. For example, it is assumed that wrist flexion and extension strengths are unaffected by pronation/supination torque demands at the forearm, or radial/ulnar deviation moment demands at the wrist. However, it has been shown that the flexion/extension strengths are at least affected by the pronation/supination angle (Langstaff et al. 2013). As such, any errors in terms of predicting wrist strength would only act to further decrease the accuracy of the IAA and WAA models..

Since I decided to test arm strength, while not including the wrist, a method of coupling the forearm (at a point just proximal to the wrist joint centre) to the vertical handle had to be developed for each direction. Two methods were developed: 1) the hand & wrist were placed inside the handle, using foam padding to align the point of force application on the wrist correctly, or 2) the wrist was coupled to the handle using a padded wrist cuff and a metal hook. Both of these have been outlined in section 3.2.2 of the methods. Similar to awkward arm postures, as previously discussed, applying force at a point just proximal to the wrist can also be awkward. Typically, humans are used to completing exertions while holding or pressing on something with their hand. As such, using the wrist as this point of application can be somewhat unnatural, and not a true representation of how an individual would complete a task. However, to allow us to test only the shoulder and elbow, the wrist had to be removed from the linked segment, and this was the best solution found. Additionally, the awkwardness of the wrist coupling techniques could have caused some unfamiliar exertions to occur, again not leading to true maximum exertions. However, if participants' strengths were not limited by any awkward exertions, it is possible that the MAS values would have been even higher than what were measured in the study. This would have lead to an even greater discrepancy between measured and predicted values, as the IAA and WAA would have under predicted strength to an even greater degree. Throughout testing, however, participants were asked to comment on their level of comfort, and in regards to the wrist, if they were uncomfortable, the positioning and tightness of the padding was modified.

5.4.4 – Direction of Force Exertion

For the MAS collection, the recorded maximum force was the force in the intended direction on the tri-axial load cell (in the X, Y, or Z direction). It was stated to the participants that, for a trial to be deemed valid, the force in the intended direction must be at least 90% of the total resultant. However, the resultant produced from an exertion is always greater than just the force in the intended direction along one axis. Therefore, it is possible that the resultant force could be quite a bit larger than the force in the intended direction, especially at high force levels (e.g. while completing a push exertion) and when the participant just made the 90% threshold. It could be valuable to conduct

the same analysis using the resultant force, instead of the force in the intended direction, to see how the results changed.

5.5 – Future Directions

It would be interesting to apply the strength prediction regression equation developed by La Delfa et al. (2014), to the data that were collected in this study. That equation (Figure 2.20) used only the H, V, and L hand location values as inputs into the equation. The results from that study showed that the equation performed very well (r^2 = 92.5% with an RMSE of 6.4 N) in terms of predicting 1D force exertions. I would hypothesize that the equation would perform just as well with the data from this study, and would yield much more accurate hand force predictions than the IAA or WAA models. It is important to note that the equation developed by La Delfa et al. (2014) accounts for all seven degrees of freedom (three at the shoulder, one at the elbow, & three at the wrist). The data I collected, however, only contains the four degrees of freedom, as it excluded the wrist. As such, it is likely that the predictions using these data may not be as accurate as in their study, however, it is still likely that the equation would vastly outperform the IAA and WAA.

In general, it is my opinion that the form of modeling presented by La Delfa et al. (2014), is the direction that upper extremity proactive ergonomic tools need to take. There are several advantages to using their all-encompassing regression modeling technique. First, as mentioned, it accounts for all seven degrees of freedom of the upper extremity, just like 3DSSPP. Unlike 3DSSPP, however, their regression model treats the whole arm as one functional unit, with the goal of producing a force at the hand. It is not concerned with how the individual strengths in each independent axis combine to produce one force at the hand. As such, it avoids the complication of correcting strengths based on arm posture. Also, by using simple inputs of the H, V, and L location of the hand, it is an easy approach for an ergonomist to manipulate when they are assessing a given task. La Delfa (2011) developed another equation that accounted for not only 1D exertions, but also 2D and 3D. Although, that equation did not perform as well as the 1D equation developed by La Delfa et al. (2014), it still explained 75.4% of the variance, with an RMSE of only 9.1 N. As such, it still greatly out-performs the IAA and WAA in terms of prediction accuracy. An additional advantage is that their model was based off 1D, 2D,

and 3D exertion directions, while the hand was in a variety of hand locations and arm postures, not just eight different ones, like 3DSSPP. A potential disadvantage is that, currently, the regression style model cannot predict which strengths are limiting a specific task. Ergonomists, however, typically are not concerned with what joint axis strength(s) are limiting a task and, instead, are only concerned with if a task is acceptable or not based on the overall required strength at the hand. Due to this, I believe that the regression form of modeling the arm is truly the next best step for upper extremity proactive ergonomics tools.

Chapter 6 – Conclusion

The main purpose of this thesis was to give 3DSSPP (IAA) the best opportunity to accurately make strength predictions by using subject-specific strength data, and to compare those predictions to the empirically measured manual arm strength (MAS). To this extent, the IAA performed quite poorly. The predicted values were shown to be significantly and substantially different than the measured MAS values. The IAA was found to only explain 17.9% of the variance, with an RMS error of 74.5 ± 68.2 N (maximum error = 266.1 N) between the IAA predictions and the measured MAS values. This result confirmed the first hypothesis, that the IAA values would be statistically different than the MAS values. This finding indicates that 3DSSPP (IAA) is not an accurate enough proactive strength prediction tool to be used by ergonomists. The secondary purpose of this thesis was to evaluate the weighted average approach (WAA), as it was hypothesized that it could be a potential replacement for the IAA. It was found, however, that the WAA predictions were also significantly different than the measured MAS values. The WAA was shown to only explain 19.1% of the variance, with an RMS error of 73.4 ± 60.6 N (maximum error = 260.0 N). These results were marginally better than the IAA, however, they definitely do not warrant the replacement of the IAA with the WAA, so I could not accept the second hypothesis.

The main issue with these approaches is that both work off the premise of predicting strength in each shoulder and elbow axis, and then combing the predicted strengths to determine the force that could be produced at the hand using the entire arm. When combining the strengths, either the resultant of the involved axes is taken (IAA) or the weighted average is calculated, using the direction cosines of the involved axes (WAA). Either method, however, first requires the prediction of strength about each individual axis. As such, regardless which method of strength prediction is chosen, both encounter this problem of trying to simply the shoulder and arm into a series of individual axes to predict manual arm strength.

The shoulder, and the arm in general, are simply too complex to allow for this form of simplification for the purposes of manual arm strength prediction. From a physiological standpoint, the shoulder uses a variety of muscles acting about multiple axes to generate force and complete exertions. Instead, the shoulder and elbow act as one functional unit to generate a force at the hand, allowing humans to complete a

required exertion for a task. As such, it is now my conclusion that the individual axis approaches to strength prediction (either the IAA or WAA) need to be disregarded as a viable method of strength prediction for proactive ergonomics tools. Instead, tools should be shifting towards methods that treat the arm as a singular functional unit (similar to La Delfa, 2011 and La Delfa et al. 2014), as ergonomists and engineers are generally only concerned with what the individual can do at the hand, and are less concerned with how the muscles contributed to producing the force, or what joints of the arm might be limiting strength.

References

Anton, D., Shibley, L., Fethke, N., Hess, J., Cook, T., & Rosecrance, J. (2001). The effect of overhead drilling position on shoulder moment and electromyography. *Ergonomics, 44* (5), 489-501.

A W M van der Windt, D., Thomas, E., Pope, D., F de Winter, A., Macfarlane, G., Bouter, L., & Silman, A. (2000). Occupational risk factors for shoulder pain: a systematic review. *Occupational & Environmental Medicine, 57*, 433-442.

Chaffin, D. & Erig, M. (1991). Three-dimensional biomechanical static strength prediction model sensitivity to postural and anthropometric inaccuracies. *IIE Transactions*, *23* (3), 215-227.

Chow, A., & Dickerson, C. (2009). Shoulder strength of females while sitting and standing as a function of hand location and force direction. *Applied Ergonomics, 40*, 303-308.

Clarke, H. (1966). Muscle Strength and Endurance in Man*. Englewood Cliffs, NJ: Prentice-Hall.*

Das, B., & Wang, Y. (2004). Isometric pull-push strengths in the workspace: 1. Strength profiles. *International Journal of Occupational Safety and Ergonomics, 10* (1), 43-58.

Garg, A., Hegmann, K., & Kapellusch, J. (2005). Maximum one-handed shoulder strength for overhead work as a function of shoulder posture in females. *Occupational Ergonomics, 5*, 131-140.

Grieve, J., & Dickerson, C. (2008). Overhead work: Identification of evidence-based exposure guidelines. *Occupational Ergonomics, 8*, 53-66.

Haslegrave, C., Tracy, M., & Corlett, E. (1997). Force exertion in awkward working postures-strength capability while twisting or working overhead. *Ergonomics, 40* (12), 1335-1362.

Hodder, J.N., & Potvin J.R. (2014). Examining Methods for Predicting Multidirectional Shoulder Strength. *The World Congress of Biomechanics, Boston, MA., July 6-11th, 2014.*

Holzbaur, K. R. S., Murray, W. M., & Delp, S. L. (2005). A Model of the Upper Extremity for Simulating Musculoskeletal Surgery and Analyzing Neuromuscular Control. Annals of Biomedical Engineering, 33(6), 829–840.

Hughes, R., Johnson, M., O'Driscoll, S., & An, K. (1999). Age-related changes in normal isometric shoulder strength. *The American Journal of Sports Medicine, 27* (5), 651-657.

La Delfa, N. (2011). *An evaluation of female arm strength predictions based on hand location, arm posture and force direction.* Hamilton, Ontario: M.Sc. Thesis, *McMaster University.*

La Delfa, N., Freeman, C., Petruzzi, C., & Potvin, J. (2014). Equations to predict female manual arm strength based on hand location relative to the shoulder. *Journal of Ergonomics, 57* (2), 254-261.

Langstaff, N., La Delfa, N., Hodder, J.N., & Potvin, J.R. (2013). The interacting effects of forearm rotation and exertion direction on wrist strength. *Association of Canadian Ergonomists Conference*, *Whistler, B.C., 2013.*

Makhsous, M., Hogfors, C., Siemien'ski, A., & Peterson, B. (1999). Total shoulder and relative muscle strength in the scapular plane. *Journal of Biomechanics, 32*, 1213-1220.

MacKinnon, S. (1998). Isometric pull forces in the sagittal plane. *Applied Ergonomics, 29* (5), 319-324.

Muggleton, J., Allen, R., & Chappell, P. (1999). Hand and arm injuries associated with repetitive manual work in industry: a review of disorders, risk factors and preventive measures, *Ergonomics*, *42* (5), 714-739.

Nussbaum, M., & Zhang, X. (2000). Heuristics for locating upper extremity joint centres from a reduced set of surface markers. *Human Movement Science, 19*, 797-816.

Peebles, L., & Norris, B. (2003). Filling 'gaps' in strength data for design. *Applied Ergonomics, 34*, 73-88.

Putz-Anderson, V., Bernard, B., Burt, S., Cole, L., Fairfield-Estill, C., Fine, L., Grant, K., Gjessing, C., Jenkins, L., Hurrell Jr., Nelson, N., J., Pfirman, D., Roberts, R., Stetson, D., Haring-Sweeney, M., & Tanaka, S. (1997). Musculoskeletal disorders and workplace factors. *National Institute for Occupational Safety and Health (NIOSH)*.

Roman-Liu, D., & Tokarski, T. (2005). Upper limb strength in relation to upper limb posture. *International Journal of Industrial Ergonomics, 35*, 19-31.

Schanne, F. (1972). A three-dimensional hand force capability model for the seated operator. PhD Dissertation. *University of Michigan* .

Stobbe, T. (1982). The development of a practical strength training program for industry. PhD Dissertation. *University of Michigan* .

The University of Michigan Center for Ergonomics. (2012). *3D Static Strength Predication Program Version 6.0.6 User's Manual*. Ann Arbor, Michigan

Warwick, D., Novack, G., Schultz, A., & Berkson, M. (1980). Maximum voluntary strengths of male adults in some lifting, pushing and pulling activities. *Ergonomics, 23,* 49-54.

Work In Progress Ergonomics. *Handpak Ergonomic Software: User's Manual.* Hamilton, Ontario.

WSIB of Ontario. (2012). 2012 WSIB statistical annaul report: Schedule 1. *Ontario Provincial Government*, 1-99.

WSIB of Ontario. (2012). 2012 WSIB statistical annaul report: Schedule 2. *Ontario Provincial Government*, 1-76.

Yassi, A. (2000). Work-related musculoskeletal disorders. *Current Opinion in Rheumatology*, *12*, 124-130.

Appendix A: Letter of Information and Consent

March 17th, 2014

Letter of Information and Consent

An Evaluation of the Approach Used by the 3-Dimensional Static Strength Prediction Program to Predict Arm Strength Using Specific Participant Elbow and Shoulder Strengths.

Investigators: Dr. James Potvin & Andrew Hall

Principal Investigator: Dr. James Potvin
Department of Kinesiology
McMaster University,
Hamilton, Ontario, Canada
(905) 525-9140 ext. 23004;

Student / Co-Investigator Andrew Hall
Department of Kinesiology
McMaster University,
Hamilton, Ontario, Canada
(905) 525-9140 ext. 21327
Cell: 905-531-5530

Research Sponsor: Automotive Partnership Canada

Purpose of the Study
The goal of this study will be to compare outputs from an ergonomics strength prediction program for a series of given arm postures and exertions directions, to recorded arm strengths for individual participants. The predictions by this program will be completed using strength inputs for the elbow and shoulder for each participant. The real world application of this program is to predict the strength requirements for a given work task (e.g. An auto assembly line worker fastening a part onto a car). It is hypothesized that when the program's outputs are produced using a participant specific elbow and shoulder strengths as inputs, these will not line up well with the collected participant specific arm strength data.

The direct applications and implications of this research include the improvement of ergonomic tools that are in use today. Currently, very important ergonomic decisions regarding shoulder strength are being made based on the somewhat inaccurate shoulder strength predictions by this ergonomics strength prediction program. This research will attempt to highlight the inaccuracies of the program, to ultimately pave the way for the implementation of an ergonomics tool that is capable of accurately predicting shoulder strength, thus lowering the incidence of work-related shoulder injuries.

Procedures involved in the Research
Participation in this study will involve two sessions in the McMaster Occupational Biomechanics Laboratory in the Ivor Wynne Centre, room A108. Before study commencement, physical characteristics such as height, weight, age, and arm length will have to be measured. This data will be kept confidential.

This study will consist of two separate strength measurements. One of these will consist of specific elbow and shoulder strength measurements, such as maximum elbow flexion strength. For this collection, you will sit in a chair parallel to a slotted rail setup. Your right arm will be secured at your elbow using a padded brace or arm strap, and then force will be measured at your elbow or at your wrist using a padded wrist strap. During the this protocol, you will be asked to apply as much force as possible on the padded arm or wrist attachments. You will complete 3 maximum strength trials in 8 different arm postures (24 total). These arm postures each test a different shoulder or elbow strength.

The other strength measurement will consist of measuring your arm strength in various hand locations and exertions directions at the hand. For this collection,

you will sit in a chair perpendicular to the slotted rail setup. You will be attached at the wrist to a vertical handle that is mounted to a force plate attached to the slotted rail apparatus. You will be asked to apply as much force as possible while your wrist is attached to a handle on the force plate that will be set in four randomized hand positions. The force plate will be used to measure the three dimensional forces that you are exerting on the handle. The hand positions are comprised of two heights (belly height & eye height) as well as at two angles (0° & 45°). For each of the four hand positions, there will 6 different exertion directions in 3D space that you must perform (24 total efforts). During these trials, a very intuitive computer program will aid you in making sure you are pulling or pushing in the appropriate direction, and will provide you feed back on the direction of your effort. For this arm strength collection, kinematic sensors will be used to determine the posture of your right arm, whie you are performing the exertions. Three kinematic sensors will be taped onto your arm and one taped onto your sternum, or chest bone. These kinematic sensors will allow us to track your arm in 3-D space by use of an electromagnetic source. This electromagnetic source is not felt at all and will put you at no risk whatsoever.

For both collections, you will have a waist strap, and a padded left shoulder strap that crosses your body and clips into the chair to help secure your body in the chair. Throughout both data collections, your left hand will be able to grasp the left armrest on the chair. For both protocols, each effort will last for 3-5 seconds. Overall, approximately 48 exertions will be completed during the study. In order to complete these exertions with adequate rest between trials, the two protocols will be completed in two separate 1-hour testing sessions, where you will complete 24 exertions in each one. Each exertion will be separated by approximately 90 seconds of rest. It is important that you give a complete maximal effort to every one of the exertions during each testing session. There will be at least two days of rest between subsequent testing days.

Potential Harms, Risks or Discomforts:
As this is a study that measures physical exertion and force production, there exists a possibility of localized muscle fatigue in the shoulder, upper arm, upper back and pectoral region. This would be due to the exertion of force and the recruitment of muscle to produce that force, similar to what may be felt after lifting weights at the gym. It should be noted that you will be in complete control of how much force is being applied or produced. Furthermore, you will be free to take a break or stop participating at any time if you feel uncomfortable or tired. You will be given ample rest between conditions and will be free to end a session if you feel it is necessary. It may be necessary for you to return for more than two sessions if you do not feel comfortable performing the current protocol as it is designed.

Potential Benefits

Although there will be no direct benefits to you, the study will have a lot of practical and theoretical applications. Benefits of participating in the study would be to experience first hand some of the methods and procedures used in conducting ergonomic research. As described above, benefits to the scientific community would be improvement of the ergonomic tools available to ergonomists in order to make more valid assessments that will hopefully reduce the incidence of work related shoulder injuries.

Payment or Reimbursement:
This study will pay participants $5 per testing session, in the form of a Tim Hortons gift card. The study protocol will require a total of 2 testing session per participant, therefore, each participant will receive $10 in gift cards for their participation at the end of the study.

Confidentiality:
You will be assigned a randomly generated subject code known only to the investigators and therefore your identity cannot be determined by anyone other than the investigators. Your personal information including name, age, and physical characteristics will be kept anonymous on all documents using the coding system. The information obtained in this study will be used for research purposes only and will be kept in a locked cabinet or stored on a password-protected computer for a maximum of 10 years.

Participation:
Your participation in this study is strictly voluntary. If you choose to volunteer, you have the right to withdraw from the study without any consequence at any time either before or during the testing sessions. If you choose to withdraw, all of your digital data will be permanently deleted from the computers and all paperwork will be shredded. If you choose to withdraw prior to completion will be pro-rated for your time based on the sessional rate of $5 per session. Should you have to return to the lab for a 3rd session, you will also be paid for your time at a rate of $5 per session.

Information about the Study Results:
You may obtain information about the results of the study by contacting one of the investigators or by leaving your email address on a confidential form to which the final results will be mailed.

Information about Participating as a Study Subject:
If you have questions or require more information about the study itself, please contact Andrew Hall.

This study has been reviewed and has received ethics clearance from the McMaster Research Ethics Board. If you have concerns or questions about your rights as a participant or about the way the study is conducted, you may contact:

McMaster Research Ethics Board Secretariat
Telephone: (905) 525-9140 ext. 23142
c/o Office of Research Services
E-mail: ethicsoffice@mcmaster.ca

CONSENT

I have read the information presented in the information letter about the study being conducted by Dr. Potvin and Andrew Hall at McMaster University. I have had the opportunity to ask questions about my involvement in this study, and to receive any additional details I wanted to know about the study. I understand that I may withdraw from the study at any time, if I choose to do so, and I agree to participate in this study. I have been given a copy of this form.

_____

Name of Participant

Appendix B: IAA Model Validation

B.1 – IAA Model Validation

Although the predicted hand load was the primary validation marker, the predicted joint angles and joint axis strengths were also validated. When examining the various predicted postural joint angles of the upper extremity for the average participant, the model also could explain 100% of the variance between the IAA predicted angles and those predicted by 3DSSPP, with a low RMS error of 0.28° (Figure B.1). Finally, the model explained 100% of the variance within the strength predictions in each axis for the average participant, again with a low RMS error of 0.08 Nm (Figure B.2).

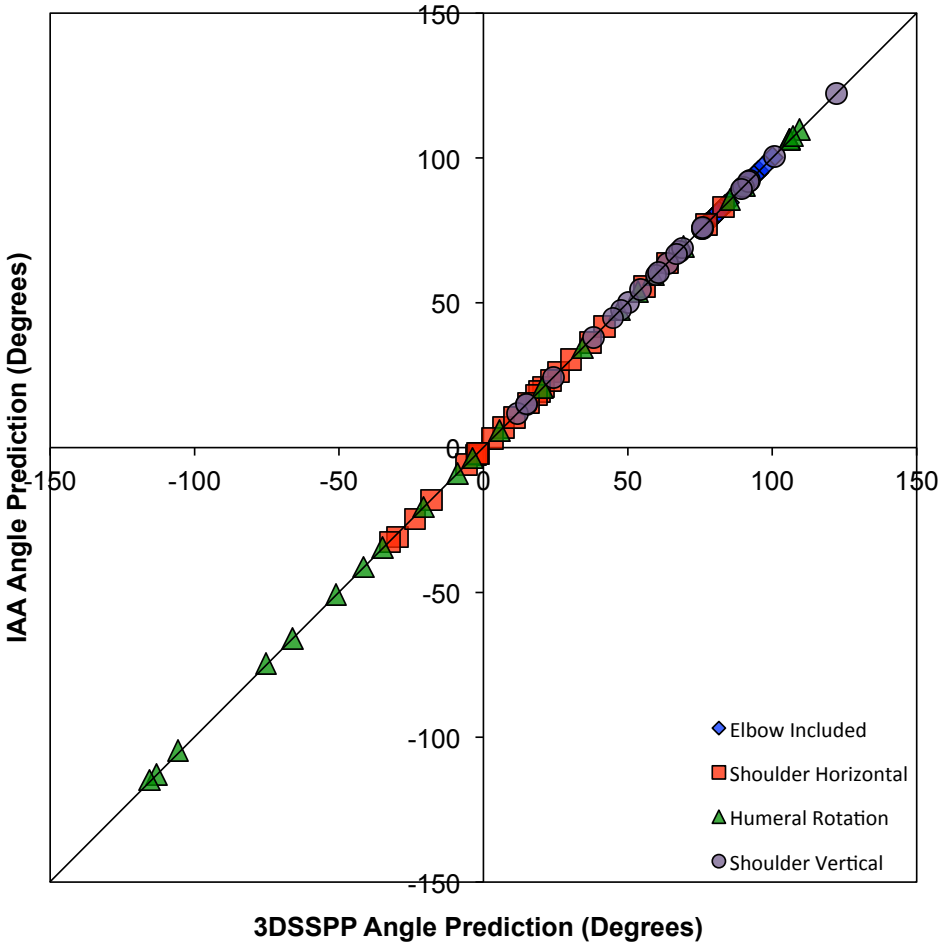

Figure B.1: IAA model validation for postural joint angles, comparing the predicted joint angles from the IAA model and 3DSSPP for the average participant (n=24 comparisons, 4 hand locations x 6 directions). The diagonal line represents a perfect prediction. The R-square was 1.000 and the RMS error was 0.28°.

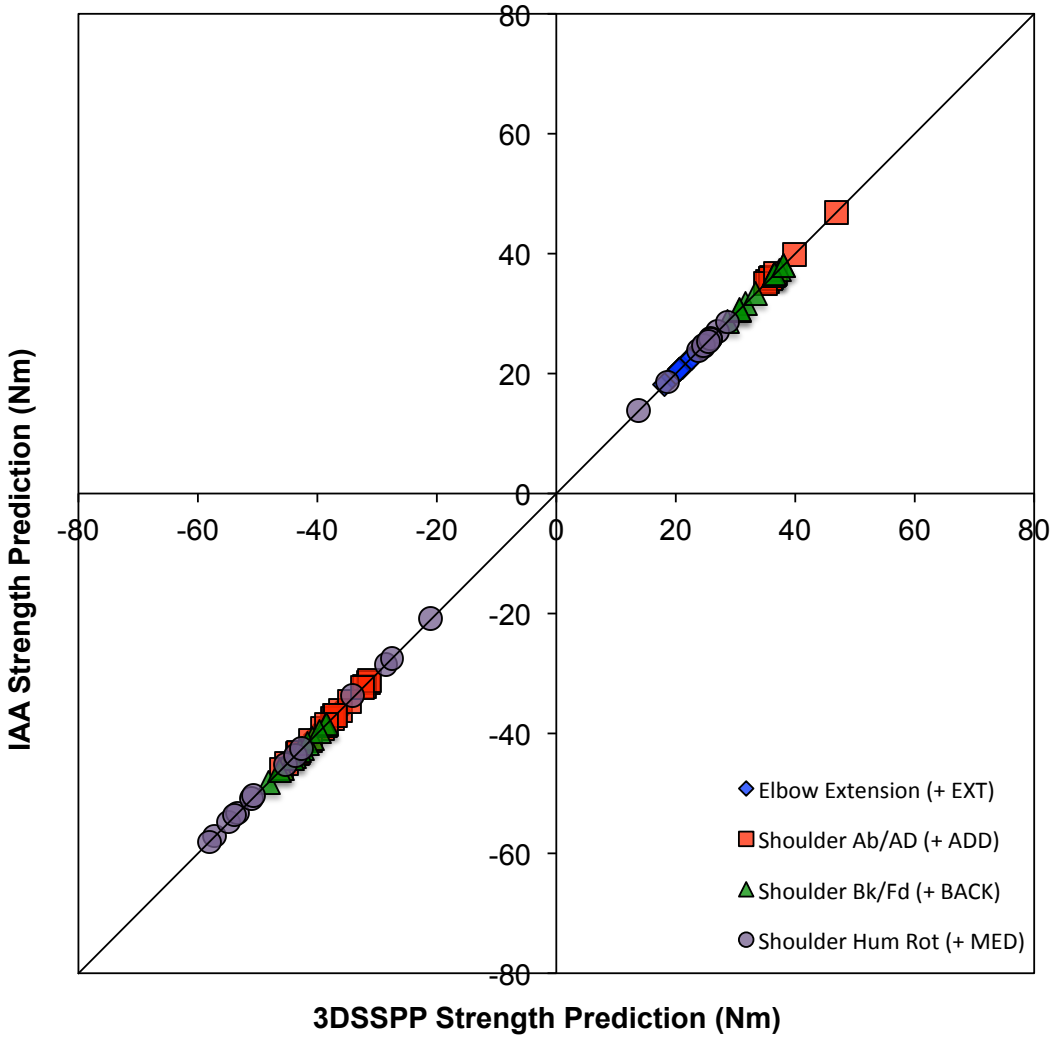

Figure B.2: IAA model validation for strength predictions in each of the three shoulder axes and one elbow axis, comparing the predicted strengths from the model and 3DSSPP for the average participant (n=24 comparisons, 4 hand locations x 6 directions). The diagonal line represents a perfect prediction. The R-square was 1.000 and the RMS error was 0.08 Nm.

B.1.1 – IAA Strength Prediction

There are several equations that are present within the 3DSSPP (IAA) software, that are used to predict joint strength (e.g. humeral rotation). These equations use inputs that include: 1) specific joint angles, and 2) baseline strengths from Stobbe's (1982) database. These equations create curves that depict how joint strength (Nm) changes with a change in a specific joint angle (e.g. humeral rotation angle) (Table B.1 & Figure B.3). As shown in Table B.1, each equation is dependent on a different set of angular inputs. For example, when looking at the curves representing the equations for medial

and lateral humeral rotation, strength is dependent on both the humeral rotation (Figure B.4) and the horizontal shoulder (Figure B.5) angles. Within 3DSSPP, joint angle limits have been set such that the inputs for these equations cannot exceed these limits. For each strength equation, the joint angle for one input (e.g. horizontal shoulder angle) was fixed at two points: 1) the minimum angle (e.g. -100°), and 2) the maximum angle (e.g. 180°). Next, the equations were displayed for each of the two fixed input points (min and max) by plotting the joint strength as a function of the change in another input joint angle within the equation (e.g. humeral rotation). This joint angle input was altered in 10° increments from the lower limit angle (e.g. humeral rotation: -90°) to the upper limit angle (e.g. humeral rotation: 90°). This same process was carried out for the adduction/abduction (Figure B.6 & B.7), forward/backward (Figure B.8 & B.9), and elbow flexion/extension (Figure B.10 & B.11) joint strengths. The adduction and abduction strengths are affected by a change in the vertical shoulder, horizontal shoulder, and humeral rotation angle. The forward and backward strengths are affected by both the vertical and horizontal shoulder angles. It is important to note that the elbow angle also affects the forward and abduction joint strengths, however, it was decided to only show how changes in the three different shoulder angles affected strength.

Table B.1: The inputs for the eight different strength equations within 3DSSSPP are shown. The first column contains the JAS as measured by Stobbe (1982), and the second column contains the JAS that is present in the each equation within 3DSSPP. The following seven columns are the seven different angular inputs (either linear or squared). These inputs either add (+) or subtract (-) from the Stobbe posture value.

		Stobbe Strength	Stobbe Posture	Elbow Ext	Elbow Ext^2	Shoulder Horiz	Shoulder Horiz^2	Shoulder Vert	Humeral	Humeral^2
Elbow	Extension	25.6	25.5	-				-		
	Flexion	29.5	29.5	+	-			-		
Shoulder	Forward	39.1	39.1	+		+		-		
	Backward	34.1	34.0			+		-		
	ABduction	36.9	36.9	+				-	-	
	ADduction	34.9	34.9			-	+	-		
	Lateral Humeral	19.9	57.0			+			-	
	Medial Humeral	21.4	21.4			+	-		+	-

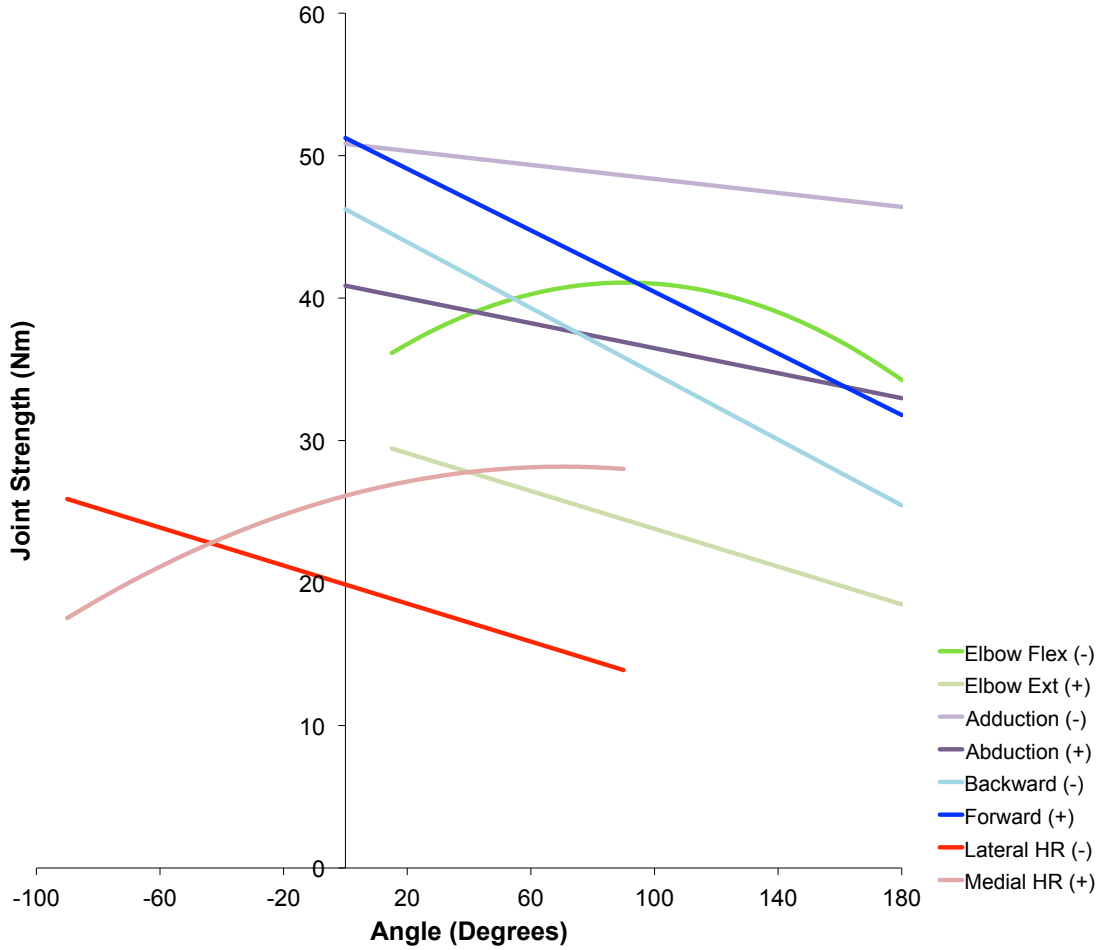

Figure B.3: The general curves created by the eight different equations (Table B.1) present in 3DSSPP are shown. For these curves, the angular inputs for these equations were locked in place, excluding the pertinent joint angle (e.g. the elbow angle for elbow flexion and extension). Each angular input has been presented in Table B.1. The angular inputs were locked as follows: elbow angle = 90°, shoulder vertical = 0°, shoulder horizontal = 90°, humeral rotation = 0°. This placed the arm in a 90° elbow flexed posture with the humerus vertically oriented beside the torso. This is the same posture that lateral humeral rotation was tested in (Figure 3.6). Next, for each equation, the strength predictions (Nm) (Y-axis) corresponding to the variation in the pertinent angle (X-axis) were plotted on the graph. These pertinent angles were as follows: 1) included elbow angle for elbow flexion/extension, 2) vertical shoulder angle for adduction/abduction, 3) vertical shoulder angle for forward/backward, and 4) humeral rotation for medial and lateral humeral rotation. The + and - signs in the legend indicate if that strength was a result of an increase (+) or decrease (-) in the pertinent angle.

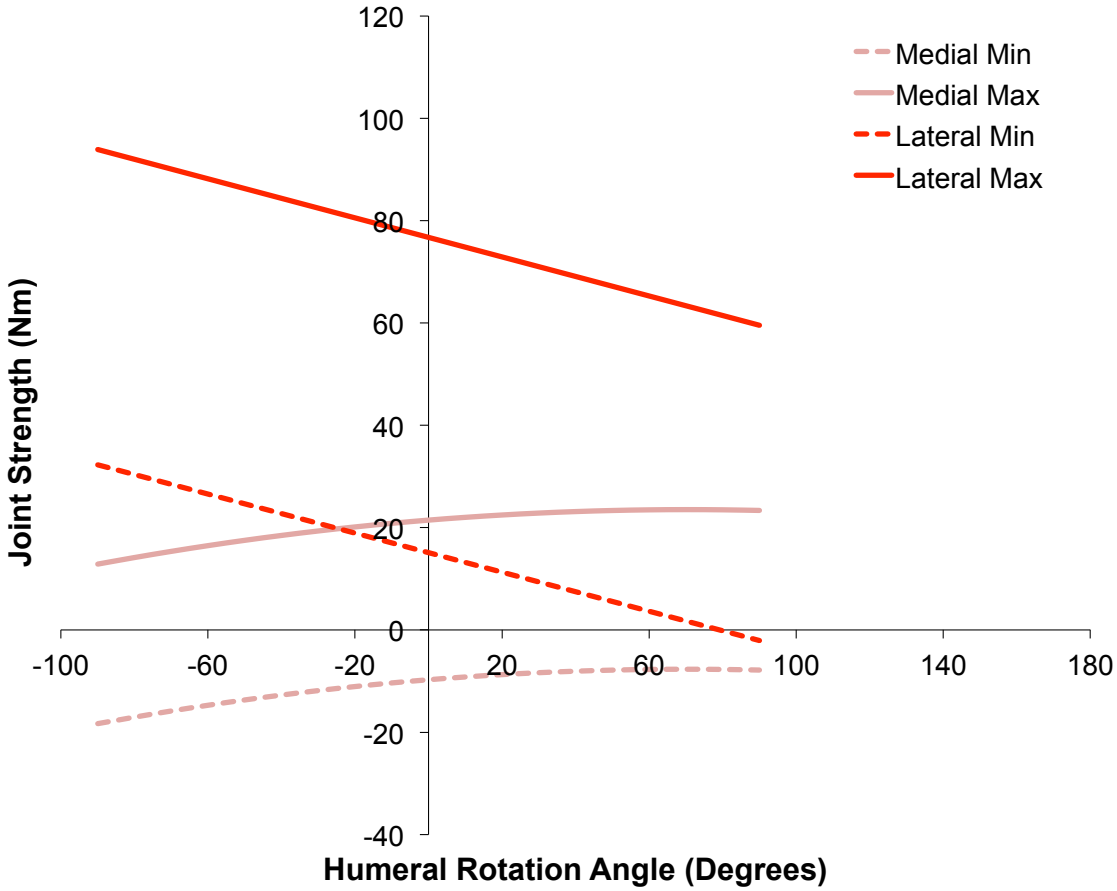

Figure B.4: The specific curves representing the strength prediction equations present in the 3DSSPP (IAA) model for medial and lateral humeral rotation strengths while the humeral rotation angle is varied. A separate equation exists for both medial and lateral humeral rotation, and each uses different inputs to model strength about a fixed anchor point based on Stobbe's (1982) database. This figure specifically, shows how joint strength (Nm) on the Y-axis changes, with a change in the humeral rotation angle (X-axis), while the horizontal shoulder angle is kept constant at the minimum (dotted lines) and maximum (solid lines) values.

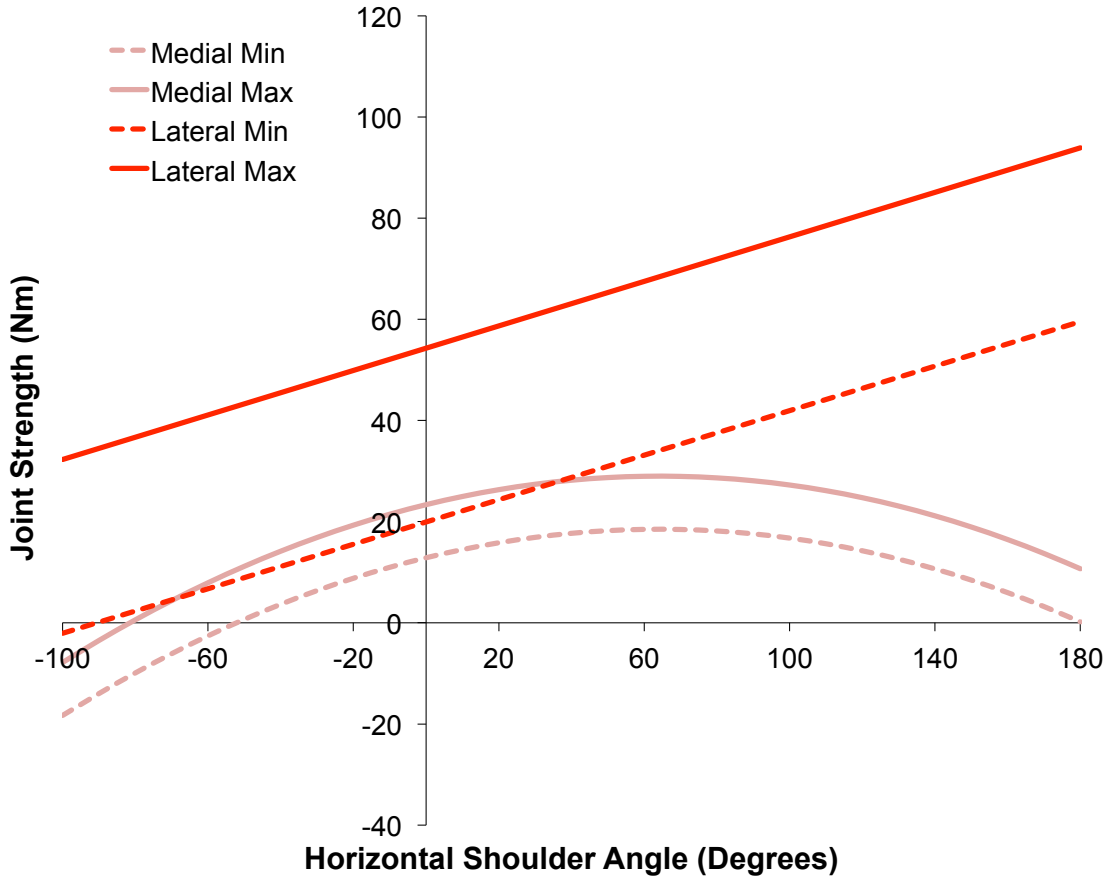

Figure B.5: The specific curves representing the strength prediction equations present in the 3DSSPP (IAA) model for medial and lateral humeral rotation strengths while the horizontal shoulder angle is varied. A separate equation exists for both medial and lateral humeral rotation, and each uses different inputs to model strength about a fixed anchor point based on Stobbe's (1982) database. This figure specifically, shows how joint strength (Nm) on the Y-axis changes, with a change in the horizontal shoulder angle (X-axis), while the humeral rotation angle is kept constant at the minimum (dotted lines) and maximum (solid lines) values.

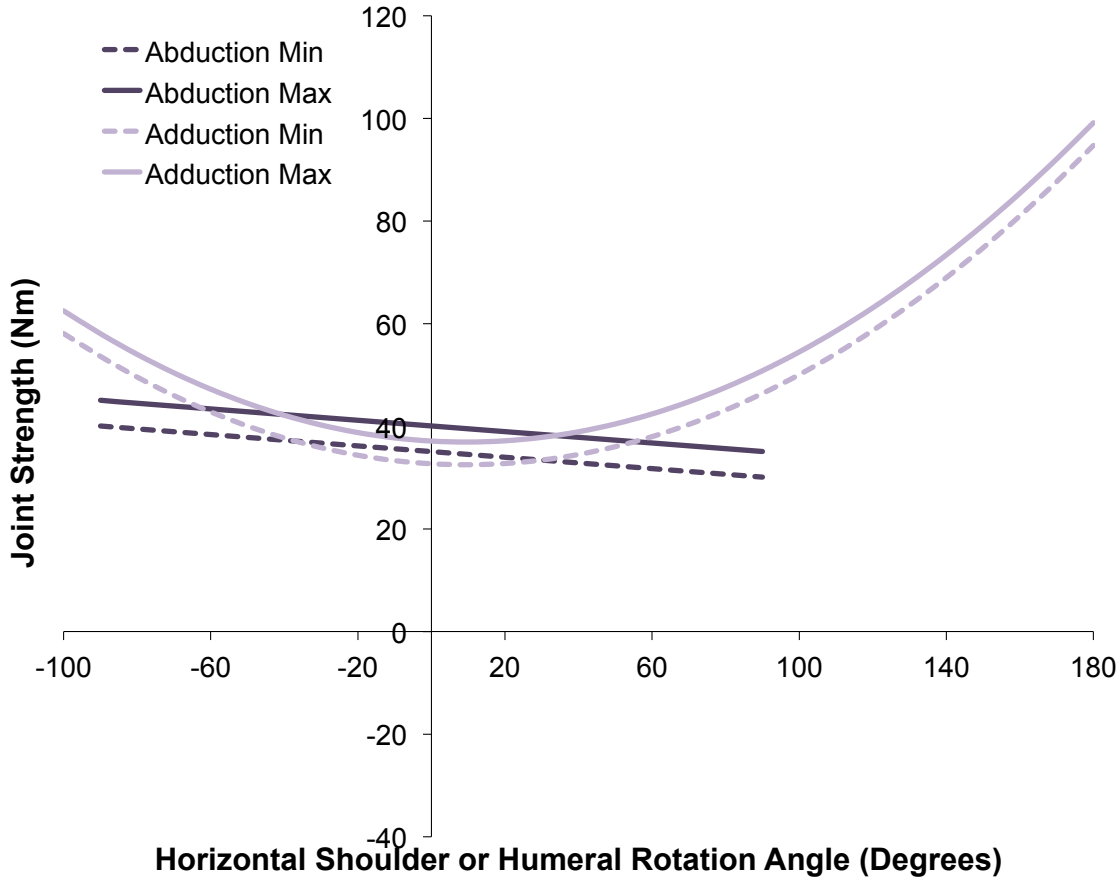

Figure B.6: The specific curves representing the strength prediction equations present in the 3DSSPP (IAA) model for abduction and adduction strengths while either the horizontal shoulder angle (adduction) or humeral rotation angle (abduction) is varied. A separate equation exists for both adduction and abduction, and each uses different inputs to model strength about a fixed anchor point based on Stobbe's (1982) database. This figure specifically, shows how joint strength (Nm) on the Y-axis changes, with a change in the horizontal shoulder or humeral rotation angles (X-axis), while the vertical shoulder angle is kept constant at the minimum (dotted lines) and maximum (solid lines) values.

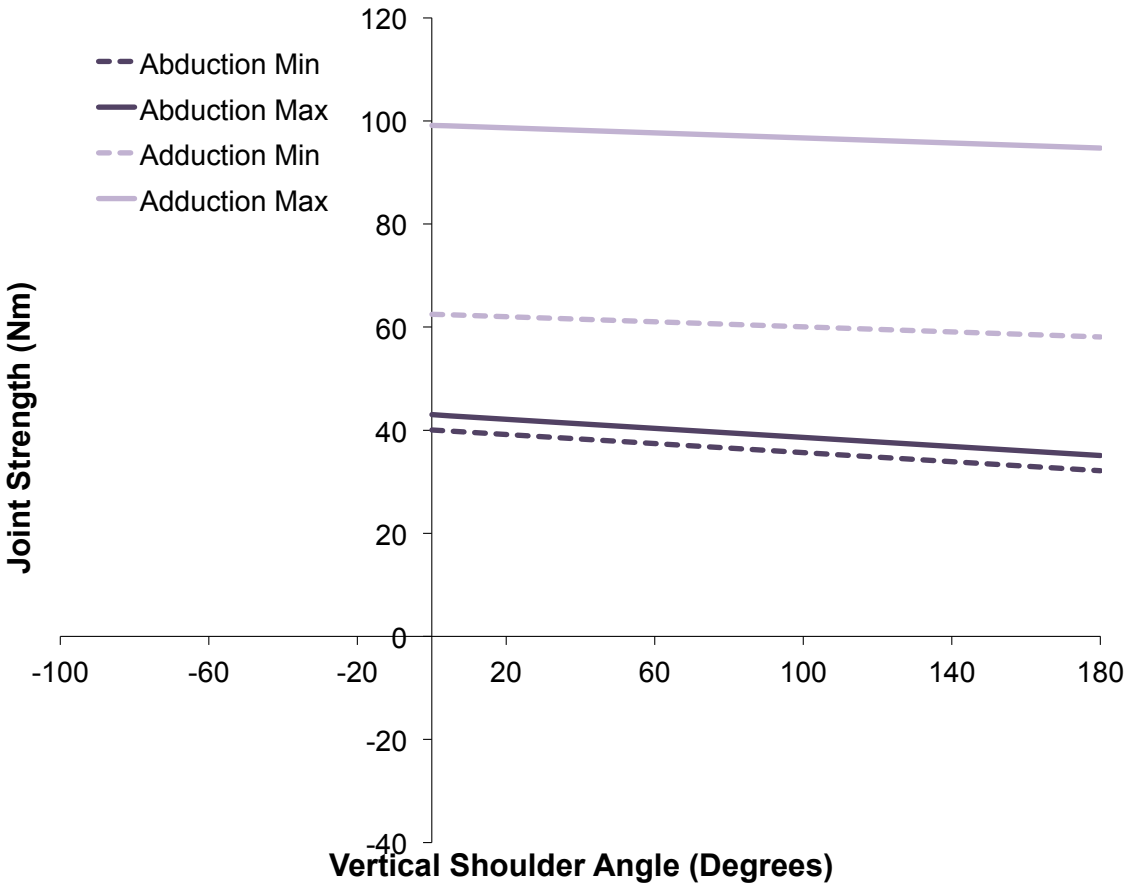

Figure B.7: The specific curves representing the strength prediction equations present in the 3DSSPP (IAA) model for abduction and adduction strengths while the vertical shoulder angle is varied. A separate equation exists for both adduction and abduction, and each uses different inputs to model strength about a fixed anchor point based on Stobbe's (1982) database. This figure specifically, shows how joint strength (Nm) on the Y-axis changes, with a change in the vertical shoulder angle (X-axis), while the horizontal shoulder and humeral rotation angle is kept constant at the minimum (dotted lines) and maximum (solid lines) values.

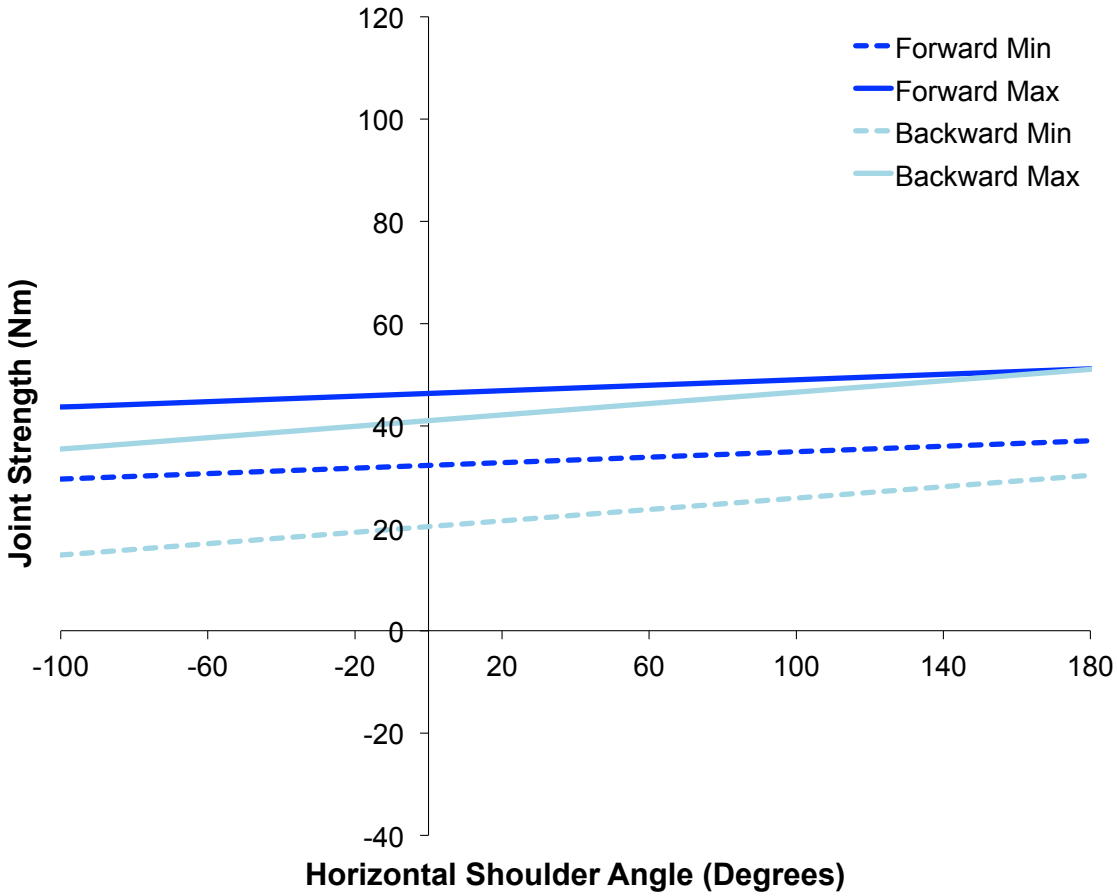

Figure B.8: The specific curves representing the strength prediction equations present in the 3DSSPP (IAA) model for forward and backward strengths while the horizontal shoulder angle is varied. A separate equation exists for both forward and backward, and each uses different inputs to model strength about a fixed anchor point based on Stobbe's (1982) database. This figure specifically, shows how joint strength (Nm) on the Y-axis changes, with a change in the horizontal shoulder angle (X-axis), while the vertical shoulder and elbow (for forward only) angles are kept constant at the minimum (dotted lines) and maximum (solid lines) values.

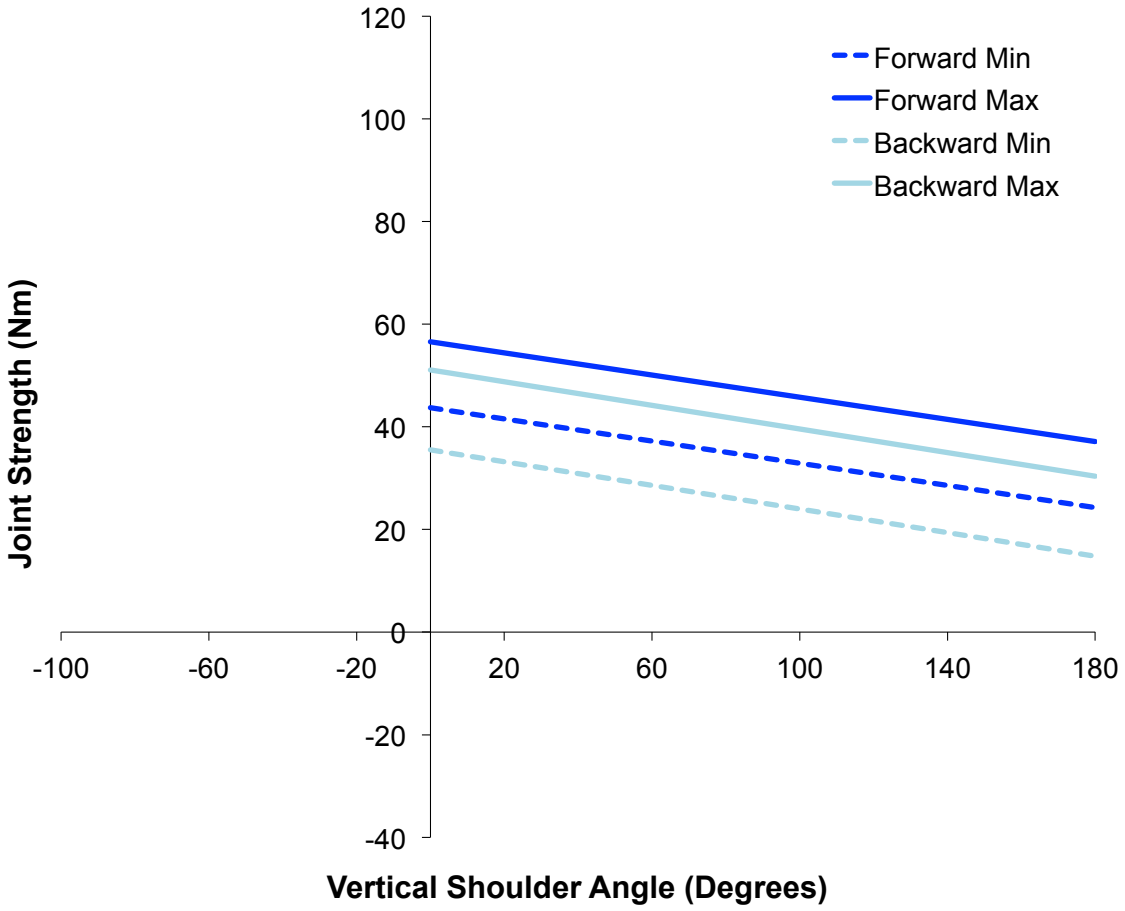

Figure B.9: The specific curves representing the strength prediction equations present in the 3DSSPP (IAA) model for forward and backward strengths while the vertical shoulder angle is varied. A separate equation exists for both forward and backward, and each uses different inputs to model strength about a fixed anchor point based on Stobbe's (1982) database. This figure specifically, shows how joint strength (Nm) on the Y-axis changes, with a change in the vertical shoulder angle (X-axis), while the horizontal shoulder and elbow (for forward only) angles are kept constant at the minimum (dotted lines) and maximum (solid lines) values.

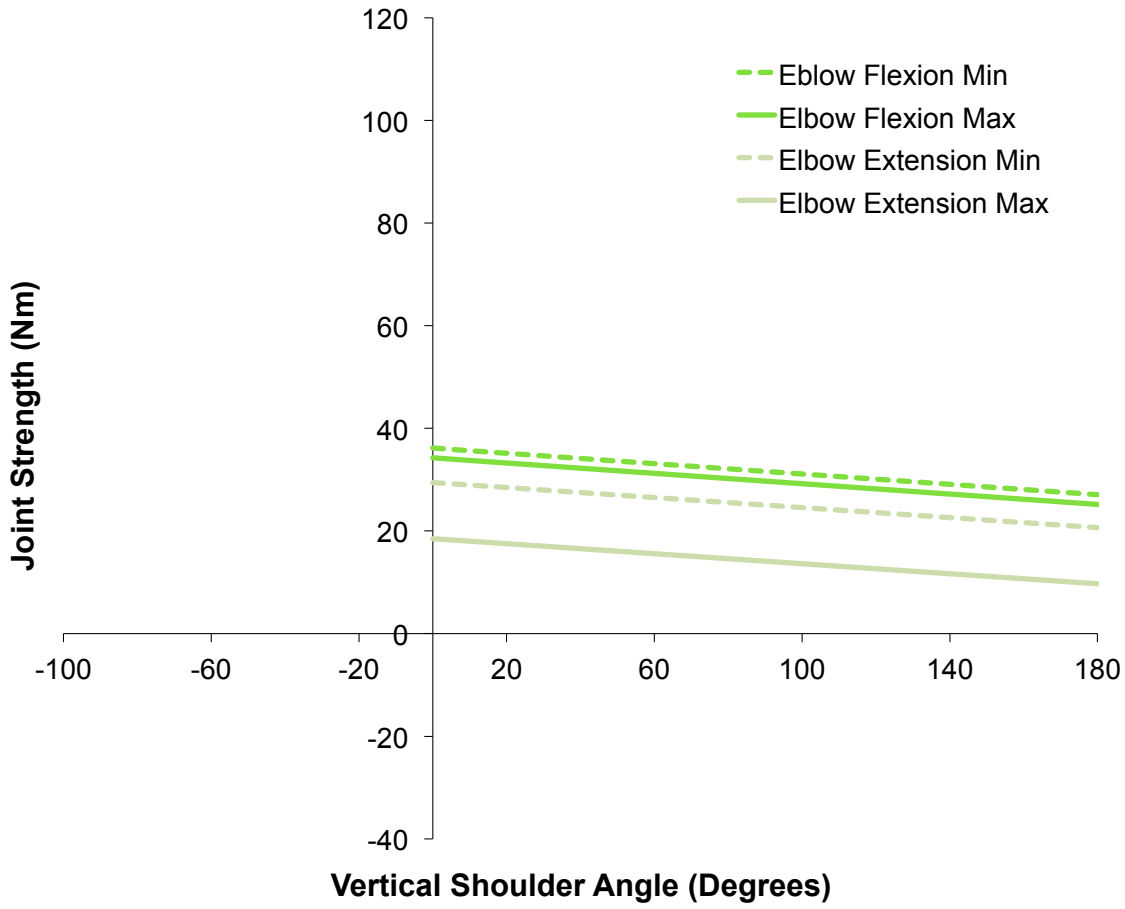

Figure B.10: The specific curves representing the strength prediction equations present in the 3DSSPP (IAA) model for elbow flexion and extension strengths while the vertical shoulder angle is varied. A separate equation exists for both flexion and extension, and each uses different inputs to model strength about a fixed anchor point based on Stobbe's (1982) database. This figure specifically, shows how joint strength (Nm) on the Y-axis changes, with a change in the vertical shoulder angle (X-axis), while the elbow angle is kept constant at the minimum (dotted lines) and maximum (solid lines) values.

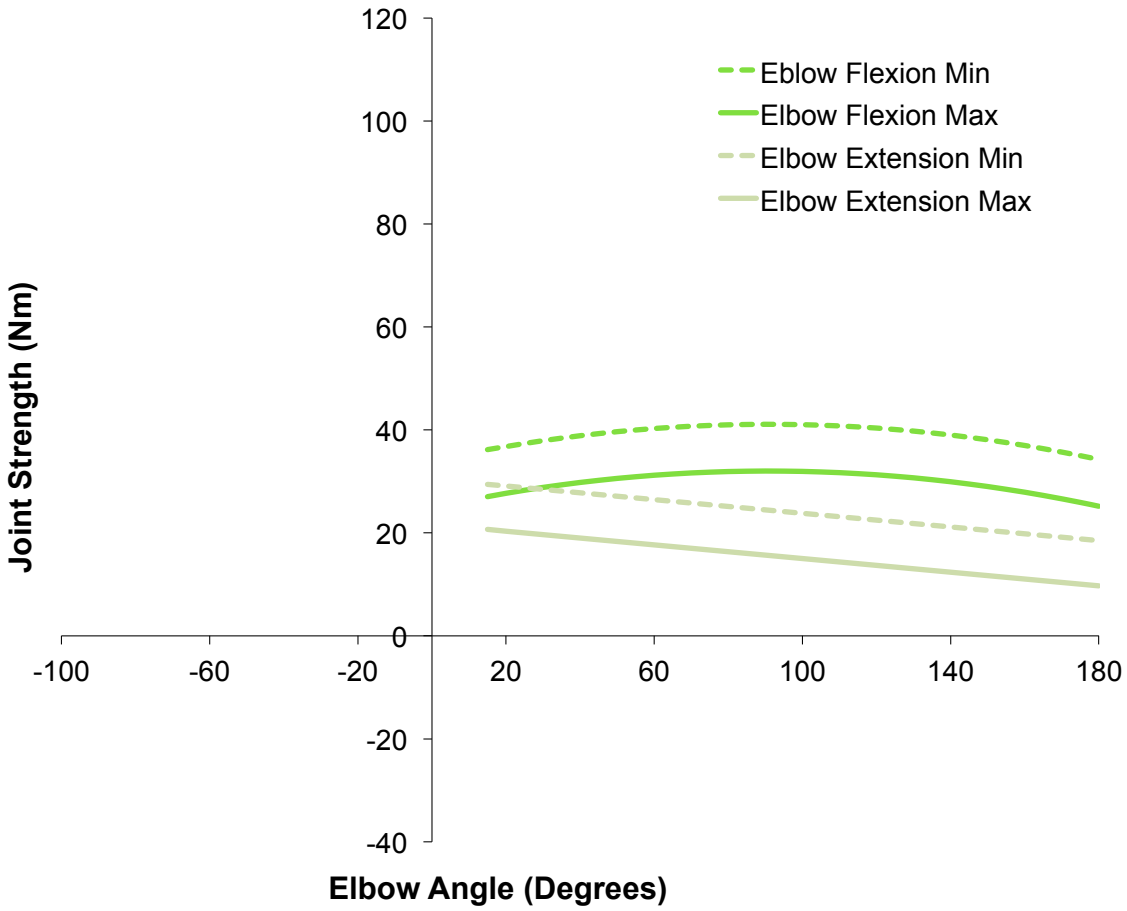

Figure B.11: The specific curves representing the strength prediction equations present in the 3DSSPP (IAA) model for elbow flexion and extension strengths while the elbow angle is varied. A separate equation exists for both flexion and extension, and each uses different inputs to model strength about a fixed anchor point based on Stobbe's (1982) database. This figure specifically, shows how joint strength (Nm) on the Y-axis changes, with a change in the elbow angle (X-axis), while the vertical shoulder angle is kept constant at the minimum (dotted lines) and maximum (solid lines) values.

Appendix C: Strength Estimation Summary Ignoring Humeral Rotation

Table C.1: A summary of the how the RMSE, correlation, explained variance (r-square), and unexplained variance changed for both the IAA and WAA with the removal of all trials that were limited by either medial or lateral humeral rotation (n = 175). For each of the IAA and WAA, three separate columns distinguish the results when humeral rotation strengths are included (HR), when they are not included (No HR), and the percentage change between the two. A green percentage change indicates an increase in the value, and a red percentage change indicates a decrease in the value.

	IAA			WAA		
	HR	No HR	% Change	HR	No HR	% Change
RMSE	74.5	71.6	-3.8%	73.4	63.6	-13.4%
r	0.423	0.452	6.9%	0.437	0.473	8.3%
r-square	0.179	0.205	14.3%	0.191	0.224	17.2%
Unexplained Variance	0.821	0.795	-3.1%	0.809	0.776	-4.1%